Energy & Environmental Science

REVIEW

View Article Online
View Journal | View Issue

Cite this: *Energy Environ. Sci.*, 2015, **8**, 2199

A review of developments in pilot-plant testing and modelling of calcium looping process for CO_2 capture from power generation systems

Dawid P. Hanak, Edward J. Anthony* and Vasilije Manovic

A nearly complete decarbonisation of the power sector is essential to meet the European Union target for greenhouse gas emissions reduction. Carbon capture and storage technologies have been identified as a key measure in reducing the carbon-intensity of the power sector. However, no cost-effective technology has yet been developed on a commercial scale, which is mostly due to high capital cost. Moreover, the mature technologies, such as amine scrubbing or oxy-combustion technologies, impose a high projected efficiency penalty (8–12.5% points) upon integration to the power plant. The calcium looping process, which is currently being tested experimentally in bench- and pilot-scale plants worldwide, is regarded as a promising alternative to the chemical solvent scrubbing approach, as it leads to the projected efficiency penalty of 6–8% points. The calcium looping concept has been developing rapidly due to the introduction of new test facilities, new correlations for process modelling, and process configurations for improved performance. The first part of this review provides an overview of the bench- and pilot-plant test facilities available worldwide. The focus is put on summarising the characteristics and operating conditions of the test facilities, as well as extracting the key experimental findings. Additionally, the experimental data suitable for validation or verification of the process models are presented. In the second part, the approaches to the carbonator and the calciner reactor modelling are summarised and classified in five model complexity levels. Moreover, the model limitations are assessed and the needs for modelling baselines for further process analyses are identified. Finally, in the third part the approaches for the integration of calcium looping to the power generation systems and for the improvement of the process performance are identified and evaluated. This review indicates that calcium looping integration resulted in the projected efficiency penalty of 2.6–7.9% points for the coal-fired power plants and 9.1–11.4% points for the combined-cycle power plants. Also, it was found that the calcium looping process can be used to develop a novel high-efficiency (46.7%$_{LHV}$) coal-fired power generation system, making this technology even more promising compared to the other CO_2 capture technologies.

Received 20th April 2015,
Accepted 3rd June 2015

DOI: 10.1039/c5ee01228g

www.rsc.org/ees

Broader context

Fossil fuels are expected to remain essential for the global power generation portfolio. As a result, carbon capture and storage technologies are expected to play a crucial role in greenhouse gas emissions reduction from the power generation sector. Mature technologies, such as amine scrubbing and oxy-combustion that are currently under demonstration at a commercial scale, are projected to reduce the net efficiency of electricity production by up to 12.5% points. For this reason, in order to minimise the efficiency penalty and the associated increase in the cost of electricity, novel CO_2 capture technologies are being developed. Calcium looping processes appears to be a promising technology that could reduce the efficiency penalty to 7% points. Development of this technology has advanced at a rapid rate over the past decade, especially since 2009. This review provides a comprehensive overview of bench- and pilot-plant testing, the available models to represent the process performance, alternative process configurations to reduce energy requirements and approaches for process integration for commercial-scale power generation systems. It is shown that further pilot-plant testing to generate data for process models validation could significantly minimise prediction uncertainty. Also, the requirement for baseline modelling assumptions and further development in sorbent performance are highlighted as key to future development.

1 Introduction

The European Union aims to reduce its greenhouse gas emissions relative to 1990 levels by 30% by 2020,[1] 40% by 2030,[2,3] and

Combustion and CCS Centre, Cranfield University, Bedford, Bedfordshire, MK43 0AL, UK. E-mail: b.j.anthony@cranfield.ac.uk

80–95% by 2050. To meet the 2050 target, a nearly complete decarbonisation of the power sector is required due to the high fossil fuel contribution in the energy mix.[4] Power generation accounted for more than one-third of the total greenhouse gas emissions in 2010.[5] For this reason, transformation of the power generation sector is key to limiting the average global temperature increase.[6]

One reason behind the high carbon intensity of the power generation sector is the major share (42%) of coal-fired power plants (CFPP) in the global supply of electricity,[7] the current average net thermal efficiency of which amounts to $33\%_{LHV}$ due to the high (75%) share of subcritical units in the global CFPP fleet.[6] Moreover, due to the recent emergence of shale gas in North America, American exports of coal have increased. As a result, the price of coal has fallen significantly in Europe and electricity generation from coal has increased at the expense of gas-based electricity generation.[6] If the current market trend continues, coal will continue to be used for power generation as predicted by the Energy Information Administration.[8] Hence, a complete decarbonisation of the power sector may be even more challenging in the future.

Carbon capture and storage (CCS) technologies are expected to play a crucial role in greenhouse gas emissions reduction from the power generation sector.[9] However, the first-of-a-kind large-scale CO_2 capture plant was only commissioned in 2014,[10] although the technology required for CCS deployment exists in other industries.[6,11] This is because no cost-effective technology for fossil fuel power plants has yet been fully demonstrated on a commercial scale. A relatively high capital cost, due to the size of equipment required to accommodate the flue gas volume, and the efficiency penalty associated with a significant increase in the cost of electricity,[12] make CCS infeasible at the moment. Nevertheless, the IEA 2 °C scenario predicts that 63% of the CFPPs will be equipped with CCS installations by 2050.[6] There are several mature CO_2 capture technologies that are close to market commercialisation in the power generation sector.[13,14]

The first full-scale capture project at Boundary Dam is based on a chemical absorption post-combustion capture plant using amine solvent,[10] with other post-combustion plants and oxy-combustion CFPPs under construction or in the planning stage.[9] Such technologies impose a significant projected efficiency penalty reaching up to 12.5% points, identified through analysis of the overall process performance using computational and modelling tools.[15–18] A reduction in the process efficiency, in turn, affects fuel economy and thus the cost of electricity. Moreover, these CO_2 capture technologies would require additional effort, and therefore cost, to mitigate the environmental, health and safety issues.[14] These are the main drivers for development of novel technologies that would affect electricity generation to a lesser degree, and would not be harmful to the environment or human health. A promising alternative to both oxy-combustion and chemical solvent absorption is a second generation CO_2 capture technology called calcium looping (CaL) that uses a calcium-based solid sorbent.

Development of the CaL process has advanced at a rapid rate over the past decade, especially since 2009. This is seen not only in the increased number of test facilities, but also in the

Table 1 A summary of the review studies related to calcium looping process

Source	Review scope
Stanmore and Gilot[19]	– Summary of the sintering, sulphation, particle fragmentation and attrition effect on the sorbent activity. – Detailed information on the correlations for mathematical modelling of carbonation, calcination, sulphation and sintering. – A brief overview of the models for prediction of the aerodynamics and trajectories of particles, as well as reaction rates in the circulating fluidised bed (CFB).
Harrison[20]	– Comparison of the standard steam-methane reforming process and the CaL process for H_2 production. Review of the thermodynamic analyses, sorbent durability and process configurations. – Review of the experimental studies on hydrogen production.
Florin and Harris[21]	– Review of process configurations for the enhanced hydrogen production from biomass gasification. – Summary of the sorbent regeneration measures. – A brief reference to the sorbent activity decay. – Review of the experimental trials on hydrogen production from carbonaceous fuels using calcium looping.
Blamey *et al.*[13]	– Detailed description of the carbonation, calcination, sintering and sorbent performance under repeated cycle operation. – Summary of sorbent deactivation and reactivation measures. – Review of the calcium looping process applications. – A brief summary of semi-empirical correlations allowing estimation of the sorbent conversion.
Dean *et al.*[14]	– Summary of the calcium looping cycle fundamentals, sorbent deactivation and sorbent performance. – Review of the calcium looping thermodynamic and economic performance, as well as its applicability in the cement industry and hydrogen production. – A brief reference to the sorbent activity decay. – Review of the pilot plant trials for calcium looping before 2011.
Anthony[22]	– Review of sorbents performance improvements and reactivation strategies for natural and synthetic sorbents. – Brief outline of calcium looping process applicability and experimental facilities.
Liu *et al.*[23]	– Review of sorbent performance enhancements. – Review of synthesis methods for sintering-resistant sorbents.
Kierzkowska *et al.*[24]	– Summary of the carbonation reaction fundamentals. – Review of recent developments in synthesis of CaO-based sorbents.
Romano *et al.*[25]	– Outline of CaL process simulations and notes on further modelling activities.
Boot-Handford *et al.*[15]	– Summary of the process performance, sorbent deactivation and regeneration. – A brief update on CaL pilot-plant trials.

increase in the development of process models. The CaL process has been widely investigated using thermodynamic and mathematical modelling, computational fluid dynamic (CFD) modelling and process modelling and integration into power generation systems. Analysis of mature technologies using process simulation and modelling tools has revealed that this approach allows a cost-effective investigation of concept feasibility and applicability, as well as development and optimisation of different process configurations. In addition, a whole process approach allows determination of the impact that integration of the CO_2 capture plant imposes on the power plant. However, a reliable assessment of the process performance requires the process models to be validated with experimental data.

Although pilot plant facilities and modelling approaches have been reviewed (Table 1), some critical aspects have not been analysed in detail. Moreover, the field of CaL has been developing rapidly due to the introduction of new test facilities, new correlations for process modelling, and CaL process configurations for improved performance. The aim of this paper is to review the available test facilities worldwide, the modelling approaches, and the integration studies that will guide the future development of the CaL process. The focus of the first part of this review will be on recent developments in CaL technology. The second part reviews the available approaches for prediction of the CaL process performance. Finally, the third part identifies and evaluates the approaches for CaL integration into power generation systems.

2 Calcium looping process for CO_2 capture

2.1 Process description

Use of calcium-based sorbents for CO_2 absorption was patented in 1933 and the research was primarily directed towards sorption-enhanced hydrogen production.[20,26] A configuration proposed by Hirama *et al.*[27] and Shimizu *et al.*,[28] which includes two interconnected CFBs operating under atmospheric pressure (Fig. 1), is the one most commonly referred to in the literature as appropriate for power generation systems. Application of such a configuration for the CaL process with appropriate design of the heat exchanger network (HEN) has been shown to have a thermal efficiency comparable to current combustion systems.[29]

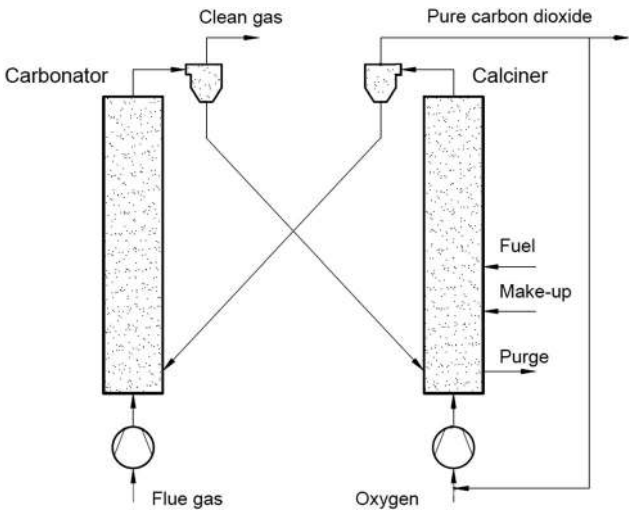

Fig. 1 Conceptual scheme of CaL process system for CO_2 capture.

In the CaL process the flue gas from fuel combustion in air, which usually contains between 4%$_{vol}$ and 15%$_{vol}$ CO_2 depending on the primary fuel used, is fed to the carbonator. In contrast to amine scrubbing, there is no requirement for flue gas precooling as absorption in the CaL process is conducted at a high temperature to assure high capture efficiency. Under such conditions, CO_2 reacts chemically with CaO through an exothermic solid-gas reaction.

CO_2 is removed from the flue gas in the form of solid $CaCO_3$ at a reasonably fast rate.[26,28,30,31] CO_2 removal efficiency decreases rapidly as the temperature increases and becomes zero at approximately 775 °C as the equilibrium partial pressure of CO_2 exceeds the partial pressure in flue gas containing 15%$_{vol}$ CO_2 above this temperature.[32] The optimal operating temperature of the carbonator ranges between 580 °C and 700 °C due to the trade-off between the reaction kinetics and the equilibrium driving forces.[33,34]

$CaCO_3$ is transferred to another fluidised-bed reactor, the so-called calciner, in which it is calcined and CO_2 is reclaimed.[26] Calcination is conducted at 850–950 °C to achieve rapid reaction without excessive sintering.[14,28,35] It needs to be highlighted that at 900 °C, the equilibrium CO_2 partial pressure is about 1 bar,[36] and hence a pure CO_2 stream can be theoretically achieved in the calciner operated at that temperature under atmospheric conditions. However, the higher calciner temperature is favourable and required in terms of reaction kinetics. On the other hand, a practical conversion rate can be achieved at temperatures below 900 °C if the gas atmosphere in calciner is diluted by steam, which can be easily separated by condensation from the CO_2 steam. Furthermore, since high-grade heat is available in the CaL process, which can be recovered to produce additional amounts of steam for the steam cycle, the higher carbonator and calciner temperatures are preferred in order to allow reaching desired steam parameters. Therefore, selection of the CaL operating temperatures can be seen as a design trilemma, in which the CO_2 capture level is restricted and process performance must be maximised, while the unit size minimised. As calcination is endothermic, additional fuel in the calciner is required. To produce a CO_2 stream of high purity, which can be directly transported for safe storage or use after the purification and compression stages, combustion takes place in an O_2/CO_2 environment.[28,37,38] Although this configuration has been demonstrated at the pilot-plant scale,[14] other configurations that use indirect heat sources may become available in future.[30,39] It is estimated that the calcination step consumes 35% to 50% of the overall heat input to the system.[40]

If it were not for sorbent sintering, attrition, and sulphation, the cyclic operation of carbonation and calcination would be performed without sorbent purge and make-up, and these processes would only be limited by thermodynamic equilibrium and the chemical reaction and diffusion rates. Manovic and Anthony[41] noted that the carbonator and the calciner should be operated within a particular temperature range in which the

minimum temperature is determined by the desired reaction rate while the maximum temperature is related to the desired CO_2 concentration. In general, the lower temperature limit is related to the desired partial pressure of CO_2, hence purity of the CO_2 stream, while the upper temperature is limited by the sorbent structural properties. Unfortunately, the conversion of the sorbent decreases with the number of carbonation and calcination cycles due to changes in particle structure,[42] especially due to enhanced sintering of CaO, which has been shown to be enhanced above 900 °C.[43] Regardless of having a negative impact on the sorbent performance, sulphur oxides would be efficiently captured due to the high Ca/S ratio in the calciner and the carbonator,[44] through indirect (1) and direct sulphation (2).[45]

$$CaO + SO_2 + 0.5O_2 \rightarrow CaSO_4 \quad (1)$$

$$CaCO_3 + SO_2 + 0.5O_2 \rightarrow CaSO_4 + CO_2 \quad (2)$$

2.2 Calcium looping as a novel CO_2 capture technology

CO_2 capture technologies commonly referred to in literature are: absorption-based separation using physical or chemical solvents; adsorption-based separation using solid sorbents; membrane separation; cryogenic separation techniques and oxy-fuel combustion; and biological systems using microbes or algae (Fig. 2).[46–49] However, due to the relatively low concentration of CO_2 in the flue gas (4–15%$_{vol}$), large volumes of flue gas need to be processed, and such technologies still have not been commercially deployed in the power industry due to a considerable drop in the net thermal efficiency of the integrated system, and also due to high equipment capital cost. As a result, the cost of electricity in the CFPPs and natural gas-fired combined cycle power plants retrofitted with CCS is expected to increase by 60–125% and 30–55%, respectively.[50–52] Although this is the key reason why development of new technologies needs to be pursued, there are also other issues which must be considered, such as environmental impact and operational safety.

Application of amines for CO_2 separation, such as monoethanolamine (MEA), has been first proposed for fuel gas or combustion gas by Bottoms in 1930.[54] This technology has been widely applied for sour gas sweetening and is used to remove CO_2 from natural gas or other industrial gases for ammonia and methanol production, as well as to produce CO_2 for enhanced oil recovery.[53,55,56] Using MEA or different amine-based solvents, such as piperazine (PZ) or methyldiethanolamine (MDEA), is currently the most likely technology to be applied to reduce the environmental impact of fossil fuel power plants.[13,15,57] Although several amine scrubbing processes have been operated in other industries,[58,59] the first full-scale demonstration plant using

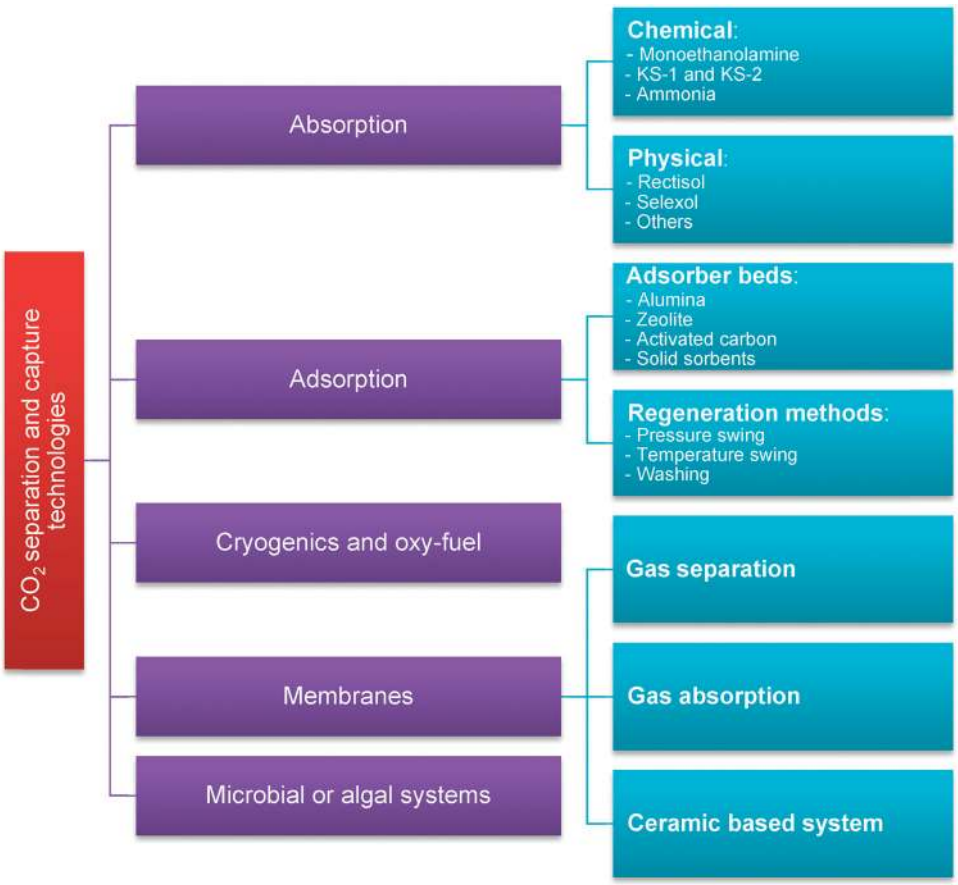

Fig. 2 Classification of the CO_2 separation and capture technologies (adapted with permission from Rao and Rubin.[53] Copyright 2015 American Chemical Society).

amine scrubbing technology from the power sector, which is Cansolv's integrated SO_2/CO_2 process fitted to Unit 3 of the Boundary Dam CFPP, and was only commissioned in 2014.[10] The following problems need to be resolved before amine scrubbing can be widely deployed in power generation:

- Solvent regeneration uses steam from the power plant steam cycle creating a projected efficiency penalty of 9.5–12.5% points when reference MEA solvent is employed.[16–18,60] Yet, recent studies identify that the projected efficiency penalty can be reduced to 8.5% points using amine-blends, such as MDEA/PZ,[61] or to 7.0% points using PZ solvent.[61,62]
- Amine solvents are prone to degradation due to reaction with O_2 and O_2-containing components in the flue gas, such as NO_x and SO_x, resulting in heat stable salts.[63]
- Solvent concentration is limited to 30% (MEA) to prevent plant equipment corrosion.[64]
- Inappropriate handling and disposal of degradation products may cause environmental and health issues.[14,64–66]

Using ammonia for CO_2 capture, which imposes a lower efficiency penalty, is proposed as an alternative to amine scrubbing.[67] Development of ammonia-based CO_2 capture processes reached the pilot-plant stage in a relatively short period of time. However, some projects were cancelled due to cost and schedule overruns.[68–70] The main advantages of ammonia over amine-based solvents are:

- It is commercially available at a lower price than MEA.
- It has higher CO_2 absorption capacity compared to an MEA solution of the same concentration.
- There is lower heat of reaction resulting in lower heat requirement for solvent regeneration. This is reflected in a projected efficiency penalty of 4.1 to 7% points[71–73] although this has not been substantiated experimentally.[59]
- There is no solvent degradation on contact with the flue gas components.
- The stripper can be operated at elevated pressure, hence temperature, leading to reduced compression work.
- Ammonia is not as corrosive as amines and can be used as a multicomponent (CO_2, SO_2, NO_x, HCl and HF) capture solvent.[74–76]

Unfortunately, although substitution of amines with ammonia may bring some reduction in the energy intensity of the capture process, it does not improve the process safety as ammonia is both a toxic substance and highly flammable. Moreover, a major drawback of ammonia is its high volatility leading to ammonia slip during the CO_2 absorption process.[63] To comply with environmental requirements, the ammonia slip can be controlled either by adding an additional ammonia water wash or by operating the absorber below 20 °C. Unfortunately, in both cases the resulting capital and operating costs increase and thus, as was expected,[59,74,77] only a slight reduction of the average cost of CO_2 avoided from \$61/t-CO_2 to \$53/t-CO_2 was reported.[78]

Another technology that is relatively close to market commercialisation is oxy-fuel combustion, in which the fuel is combusted in an O_2-rich atmosphere. Although there are neither commercial nor full-scale demonstration plants operating at the moment,[59] some projects are in the planning stage.[97] However, a recent suspension of funding at an advanced stage of the FutureGen project[79,80] shows that completion of such projects is highly dependent upon financial incentives and political climate. The primary advantage of oxy-combustion technology is that it produces a nearly pure CO_2 stream after the flue gas has been through SO_x and NO_x emission control systems and ash separation units. This CO_2 then only needs to be conditioned and dehydrated prior to compression and transport. The main challenges of this technology, which are likely to slow its wide implementation, are:

- The net efficiency of the oxy-fuel power plant is reduced by 8–12% points[15] because of the cryogenic air separation unit (ASU) for O_2 production.[13]
- High safety standards are required to prevent oxygen leakage.[13]
- The combustion temperature must be controlled to avoid hot spots in the combustion zone that would enhance NO_x production in the boiler.[15]
- Air leakage into the boiler must be minimised to maintain desired purity of the CO_2 stream and to minimise the power requirement of the CO_2 compression and purification unit.[81,82]

If the direct combustion of fuel is considered as a means for satisfying the heat requirement in the calciner, the CaL process can be seen as a merging of the post-combustion CO_2 capture and the oxy-combustion technologies, where only some portion of fuel is burned in an O_2-rich environment. Currently, CaL concepts are being tested experimentally at bench- and pilot-scale plants worldwide. The main advantages of the CaL system over the solvent-based CO_2 capture technologies are:

- Heat can be recovered and used to generate an additional amount of high-pressure steam through the exothermic carbonation of lime at 650–700 °C and utilisation of heat available in the process streams.[83]
- The predicted efficiency penalty is 7% to 8% points,[84] with the CO_2 capture stage accounting for 2% to 3%, which is mainly due to the oxygen requirement.[39] This is comparable to the efficiency penalty of a flue gas desulphurisation unit (FGD) (0.5–4%).[85]
- The technology uses fluidised bed reactors, which have been commercially proven for coal combustion systems.
- Compared to an oxy-fuel power plant, 30–50% less O_2 is required for oxy-combustion of fuel in the calciner, leading to smaller ASU size.[28,39]
- Natural limestone or dolomite, the source for CaO, is globally available and inexpensive[31] and CaO is characterised by high CO_2 absorption capacity.
- The average cost of CO_2 avoided is estimated to be \$29–50/t-CO_2 which is more than 50% less than for amine scrubbing.[78,86–89]
- Compared to solvents, $CaCO_3$ and CaO are much less hazardous to the operators' health and the environment.[14]

Reduction in the sorbent CO_2 carrying activity on cycling operation as a result of sintering, attrition and sulphation appears to be the major challenge of this technology. Although this results in a considerable amount of spent sorbent to be replaced, some part of the sorbent can be reused for cement production, increasing the profitability of both the power and cement industries.[14]

3 Review of calcium looping bench- and pilot-scale testing

Insight into system behaviour under various operating conditions is required to optimise process parameters and to assess feasibility, before commercial-scale installations are designed and built. Although the CaL process has only been considered for CO_2 capture from fossil-fuel power systems since 1999, a number of test facilities have already been built (Table 2), with rapid progress after 2009. The review by Dean *et al.*[14] devoted to the CaL process has described bench-scale tests using the 10 kW_{th} unit at IFK (University of Stuggart), 30 kW_{th} unit at the INCAR-CSIC, 75 kW_{th} unit at CANMET Energy and 120 kW_{th} unit at the Ohio State University. However, this review mostly focused on the attrition and material performance during the bench-scale tests. Moreover, the developments in the pilot-plant testing by 2010 and 2013 have been outlined by Anthony[22] and Boot-Handford *et al.*,[15] respectively. This section focuses on the progress in CaL process testing at a bench- and pilot-scale from 2010, with the aim of gathering the valuable design and operational data for development and validation of process models.

3.1 Industrial Technology Research Institute

3.1.1 Experimental facility description

3.1.1.1 Bench-scale unit. The Industrial Technology Research Institute (ITRI) in Taiwan has developed a 1 kW_{th} bench-scale unit, which can be operated in either batch or continuous mode. The unit comprises a bubbling fluidised bed (BFB) carbonator (gas velocity of 0.2–0.4 m s^{-1}), with a gas distributor located at the entrance, and a moving bed (MB) calciner. The solids are transported between the carbonator and the calciner through a 2.5-cm solid circulation pipe of 0.5 m length.[90]

The unit was modified by substituting the MB calciner with an air-fired rotary kiln calciner (RK) (Fig. 3). This increased the capacity to 3 kW_{th}. The calciner was designed to have a length-to-diameter ratio of 18.5 and an inclination angle of 5°, based on operating experience from the cement industry. Such design corresponds to a residence time of approximately 30 min at a speed of 1 rpm. Furthermore, liquefied petroleum gas is directly fired in the calciner using the 58 kW_{th} burner. The gas enters the BFB carbonator through the perforated plate distributor composed of 96 holes of 1.5 mm in diameter. Although the carbonation reaction is exothermic, the carbonator was heated using an external heating system to balance the heat losses to the environment.[91]

3.1.1.2 Pilot-scale facility. Design of the 1.9 MW_{th} pilot plant, which removes a tonne of CO_2 per hour from the Hualien cement plant flue gas containing 20–25% of CO_2,[92] was based on experience with the 3 kW_{th} unit. The perforated plate gas distributor was selected due to higher attainable velocities, based on cold model tests. The design consists of a double-layered perforated plate with 6 mm holes and an open-area ratio of 1.56%. As a means of temperature control thirty-six 2 m water-cooled double steel jackets were suspended at the top of the carbonator. The system is designed to operate with an

Table 2 Review of design and operating conditions of bench- and pilot-scale calcium looping facilities

	Carbonator					Calciner						
Research institute	Size (kW_{th})	Type[a]	Diameter (m)	Height (m)	Temperature (°C)	Type[a]	Diameter (m)	Height (m)	Temperature (°C)	Inlet CO_2 content ($\%_{vol}$)	Max. CO_2 capture level (%)	CO_2 purity ($\%_{vol}$)
Industrial Technology Research Institute	1	BFB	0.1	2.5	600–700	MB	0.05	0.9	800–900	12.5	99	N/A
	3	BFB	0.1	2.5	600–700	RK	0.27	5	500–1000	12.5	99	N/A
	1900	BFB	3.3	4.2	650	RK	0.9	5	500–1000	12.1–14.5	N/A	N/A
Consejo Superior de Investigaciones Científicas	30	CFB	0.1	6.5	568–722	CFB	0.1	6	800–1000	15–16	90	27
	1700	CFB	0.65	15	600–715	CFB	0.75	15	820–950	12.5	90	85
Darmstadt University of Technology	1000	CFB	0.59	8.66	650–670	CFB	0.4	11.35	<1000	12–12.6	92	N/A
IFK at University of Stuttgart	10	BFB	0.114	3.5	630–700	CFB	0.071	12.4	850–900	15	97	20–55
	200	CFB	0.023	10	650	CFB	0.021	10	875–930	15	N/A	N/A
	200	CFB	0.033	6	600–680	CFB	0.021	10	875–930	15–16	93	N/A
Ohio State University	120	EB	N/A	N/A	450–650	RK	N/A	N/A	850–1300	3–25	>90	N/A
Vienna University of Technology	100	BFB	0.28[b]	2	650	CFB	0.08[b]	5	850	N/A	N/A	N/A
CANMET Energy	75	BFB/MB	0.1	2–5	580–720	CFB	0.1	4.5–5	850–950	8	97	N/A
Cranfield University	25	EB	0.1	4.3	600–650	BFB	0.165	1.2	900–950	15	80	N/A
Tsinghua University	10	BFB	0.149	1	630	BFB	0.117	1	850	15	95	22.5

[a] BFB – bubbling fluidized bed; CFB – circulating fluidised bed; MB – moving bed; EB – entrained bed; RK – rotary kiln. [b] Equivalent diameter based on cross-section area.

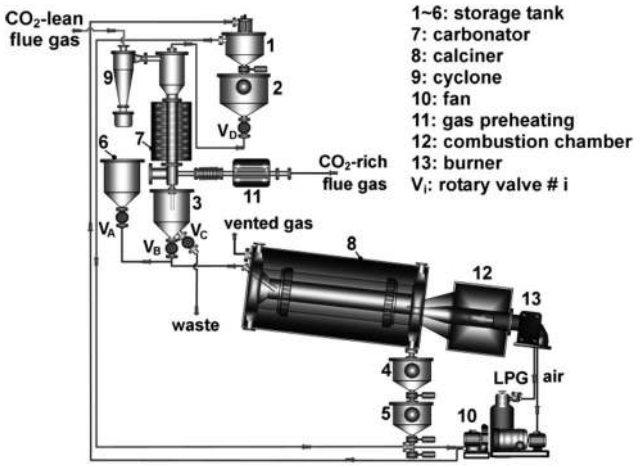

Fig. 3 3 kW_{th} bench-scale unit at ITRI (reprinted with permission from Chang *et al.*[91] Copyright 2015 Wiley).

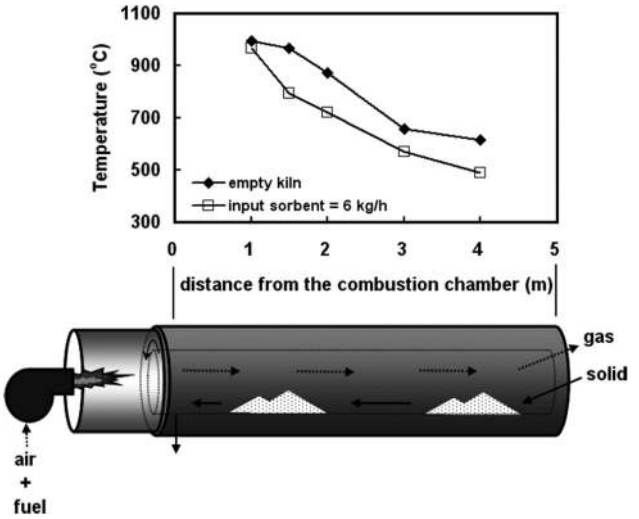

Fig. 4 Temperature distribution in the rotary kiln calciner in the first test (reprinted with permission from Chang *et al.*[91] Copyright 2015 Wiley).

average conversion of 20–40% and CO_2 capture levels of 80–95%. Heat for calcination is provided through direct oxy-combustion of diesel in the RK calciner which requires flue gas recirculation for temperature control. A key benefit of this configuration is more uniform temperature distribution in the calciner and thus, increased usable length for calcination.

3.1.2 Test campaign using 1 kW_{th} bench-scale unit. Tests were performed to assess CO_2 capture efficiency using a fluidising medium in the carbonator composed of 85%$_{vol}$ air and 15%$_{vol}$ CO_2. Prior to performing the experiments, the industrial grade limestone was calcined at a temperature of 850 °C.[90]

During 57 h of continuous operation 0.1 kg h^{-1} of fresh limestone was supplied to the calciner. The experiment revealed that the CO_2 capture level in the carbonator was maintained at above 99% over the entire time. Although preliminary results indicated the practicability of such a configuration, the MB carbonator was difficult to operate.[91]

3.1.3 Test campaign using 3 kW_{th} bench-scale unit. As in the previous case, the flue gas entering the carbonator contained approximately 15%$_{vol}$ CO_2, representative of values found in CFPPs. The flue gas was first preheated to 230 °C and then fed from the feed tank to the carbonator at a controlled rate of 47 dm^3 min^{-1}. To account for the sorbent deactivation, fresh limestone was fed to the calciner, while some of the solids circulating in the system, which comprises both inactive and active sorbent, was purged from the system.

The first test performed using the modified 3 kW_{th} unit was a batch test to evaluate operation of the RK calciner. It demonstrated that if the calciner is fed with fresh limestone at the rate of 6 kg h^{-1}, the useable length for the calcination reaction is approximately 1.5 m, corresponding to a sorbent residence time of 9 minutes. This arises because a temperature of 1000 °C was observed 1 m from the combustion chamber and thus excessive sintering would occur in this region (Fig. 4). On the other hand, a temperature of 721 °C was observed 2 m from the combustion chamber causing operating conditions downstream of the calciner to be unsuitable for the endothermic calcination reaction. Nevertheless, the calcination efficiency was found to be higher than 96%, while the carbonation conversion was 63.7%, proving low sorbent sintering rates.[91]

The 3 kW_{th} pilot plant was then used to run a 100 h campaign, the main objective of which was to keep the CO_2 capture level above 85%. This campaign showed that selection of the appropriate fresh sorbent make-up rate and spent sorbent purge rate is not only critical for reaching the desired CO_2 capture level, but also for ensuring stable and efficient operation of the system; if the make-up rate was lower than the purge rate, the total solid inventory in the system was reduced and excessive degradation of the sorbent activity was observed. On the other hand, increasing the solid inventory through an increased make-up rate improved the CO_2 capture level to above 99%. However, this would increase the operating cost of the process as it would require more heat input to the calciner. It needs to be highlighted that such a high level of inventory in the calciner had not been expected at the design stage, and thus, its efficiency dropped to 39% because insufficient heat was supplied through liquid petroleum gas combustion to sustain the endothermic calcination reaction.

When the inventory in the carbonator, which was operated at approximately 650 °C, fluctuated around the desired value the CO_2 capture level varied between 80% and 100%. The average residence time of solids in the carbonator was 2 h, with an average conversion of solids in the carbonator of 30% and a calcination efficiency of 75%. This campaign also revealed that particle attrition is an important phenomenon in the CaL system as the mean particle size decreased from 248 μm to 188 μm over this period.[91]

3.1.4 Data for process modelling. An unconventional process configuration developed at the ITRI, which includes the RK calciner, is beneficial in investigating integration opportunities between the power and cement industries. Since the equipment sizes and the key operating conditions have been disclosed,[90,91] the data available should be sufficient to, at least, verify the model behaviour in terms of solids inventory or operating temperatures

under varying operating conditions. Moreover, a simple verification could be performed for the carbonator and calciner performance. It will be of benefit to benchmark the model with the performance of the 1.9 MW_{th} pilot plant, provided that detailed experimental data become available.

3.2 Consejo Superior de Investigaciones Científicas

3.2.1 Experimental facility description

3.2.1.1 Bench-scale unit. The Instituto Nacional del Carbón – Consejo Superior de Investigaciones Científicas (INCAR-CSIC) has developed a 30 kW_{th} unit which consists of two interconnected CFB reactors. The carbonator is 6 m high and 0.1 m in internal diameter. It is fluidised using a synthetic flue gas containing 3–25%$_{vol}$ of CO_2 and is operated at 568–722 °C.[93] The heating system in the carbonator is only used during system start-up. Coal is combusted in 2–6% excess air to maintain the desired temperature in the calciner.[93] The calciner is 6.5 m high and the same internal diameter and is operated at 800–900 °C. Each reactor is equipped with a high-efficiency cyclone, from which the solids are directed through a vertical standpipe to the BFB loop seal.[94]

3.2.1.2 Pilot-scale facility. By combining the experience gained through running the 30 kW_{th} unit and the industrial experience for large-scale CFB combustors, INCAR-CSIC in agreement with ENDESA, Foster Wheeler and HUNOSA, with substantial R&D support from University of Stuttgart (IFK), Lappeenranta University, Imperial College and the University of Ottawa and CanmetENERGY, developed a 1.7 MW_{th} pilot plant designed to process approximately 1% of the flue gas produced in the 50 MW_{el} La Pereda CFPP in Asturias, Spain (Table 4). This project, called CaOling, was part-funded by the European Union 7th Framework Programme. The pilot plant comprises two interconnected CFB reactors 15 m in height with an internal diameter of 0.75 m in the calciner and 0.65 m in the carbonator (Fig. 5) operating with gas velocities of 3–5 m s^{-1} which are similar to those encountered in industrial CFBs.[95]

The typical operating temperatures for the carbonator and calciner are 600–715 °C and 820–950 °C, respectively. The temperature in the carbonator can be controlled through removable bayonet tubes. The calciner is directly fired with coal, either in an oxy-combustion or air-combustion environment. Fresh limestone is continuously fed to the calciner to maintain the desired average conversion of sorbent of 0.1–0.7 (Table 3). In both CFB reactors the solids leaving the risers are separated from the gas stream in the high-efficiency cyclones, and then directed to the double BFB loop seals by gravity. This design allows control of the solid looping rates between, and thus the solid inventories in, the CFB reactors.[96]

3.2.2 Test campaign using 30 kW_{th} bench-scale unit. The preliminary experiments conducted by Alonso *et al.*[94] revealed operating issues with the unit. A main concern was insufficiently high separation efficiency of the cyclones (92–97%) that led to loss of solids inventory. This resulted in unstable operation of the system as the solid looping rates and the solids inventory could only be kept constant for a short time. Nevertheless, this study showed that the carbonator was operated in nearly isothermal conditions (±20 °C) and that the actual CO_2 capture levels were close to equilibrium values at a particular carbonator temperature, provided that the amount of solid bed inventory and the solid looping rate were satisfactory.

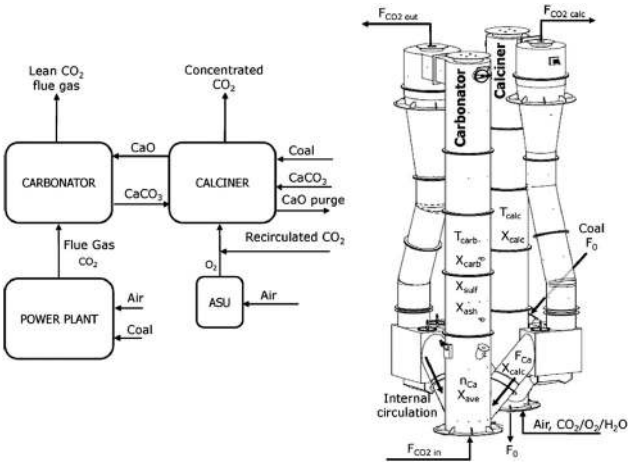

Fig. 5 Design of the 1.7 MW_{th} pilot plant at INCAR-CSIC (adapted with permission from Arias *et al.*[96] Copyright 2015 Elsevier).

On extension of the risers' heights and reconstruction of the high-efficiency cyclones, the system stability was improved. The modified system operated with CO_2 capture levels of 70–90%, which were close to the equilibrium value at 650 °C, depending on the gas velocity (2.0–2.1 m s^{-1}) and the solids circulation rates (0.8–2.3 kg m^{-2} s^{-1}). However, for the highly cycled particles, which can attain an average conversion close to the residual conversion of 0.07–0.12, the CO_2 capture level dropped to 65–75% for a solids circulation rate of 1.0–1.8 kg m^{-2} s^{-1}.[94]

In tests carried out by Rodríguez *et al.*,[93] the 30 kW_{th} unit was used to treat flue gas containing 20%$_{vol}$ CO_2. Initially 20 kg of limestone was loaded into the system that was operated at 800–850 °C for the calciner and 630–700 °C for the carbonator, with gas velocities of 3 m s^{-1}. The analysis revealed that the purity of the CO_2 stream released from the calciner was approximately 27%$_{vol}$ and the concentration of CO_2 in the clean gas was approximately 7%$_{vol}$. This corresponded to an actual CO_2 capture level of approximately 70%, which was lower than the equilibrium CO_2 capture level within this temperature range. It was found that under realistic operating conditions an actual CO_2 capture level of 70–90% was achievable for bed inventories of 400 kg m^{-2} for solid looping rates of 0.5–2.2 kg m^{-2} s^{-1}.

3.2.3 Test campaign using 1.7 MW_{th} pilot plant. Arias *et al.*[96] reports that the 1.7 MW_{th} pilot plant was operated for more than 1800 h, with 380 h in CO_2 capture mode with a CO_2 capture level of 40–95%. Stable operation under oxy-combustion in the calciner (excess O_2 of more than 5%$_{vol}$) has been maintained for 170 h.

Representative results from the experimental trials were reported for the first time by Sánchez-Biezma *et al.*[97] (Fig. 6). These results confirm the findings from previous studies that if the process is operated with proper solid inventory and sorbent activity, the actual CO_2 capture in the carbonator is close to the equilibrium value at given temperature (above 90% at 660 °C). Moreover, a SO_2 capture level of more than 95% was achieved.

Table 3 Operating conditions of the 1.7 MW_{th} pilot plant at INCAR-CSIC[a] [95,96]

Input from power plant	Value	Pilot plant operating conditions	Value
Flue gas flow rate (kg h^{-1})	680–2300	Maximum coal flow (kg h^{-1})	325
CO_2 concentration ($\%_{vol}$)	12.6	Maximum fresh sorbent flow (kg h^{-1})	300
O_2 concentration ($\%_{vol}$)	5.5	O_2 flow to calciner (kg h^{-1})	300–600
H_2O concentration ($\%_{vol}$)	7.0	CO_2 flow to calciner (kg h^{-1})	700–2250
SO_2 concentration ($\%_{vol}$)	0.07	Air flow to calciner (kg h^{-1})	600–2500
N_2 concentration* ($\%_{vol}$)	74.83	Inventory in carbonator (kg m^{-2})	100–1000

[a] Nitrogen concentration calculated to balance the remaining constituents.

Table 4 Operating conditions of the 75 kW_{th} CanmetENERGY pilot plant

Parameter	Minimum	Maximum
CFB calciner		
Initial sorbent inventory (kg)	4.5	5.0
Sorbent make-up batch (kg)	0.3	0.5
Biomass consumption rate (kg h^{-1})	4.0	7.6
Coal consumption rate (kg h^{-1})	2.6	5.8
Air flow rate (air-firing mode) (kg h^{-1})	8.0	14.4
O_2 flow rate (oxy-firing mode) (kg h^{-1})	5.2	7.7
Moving or bubbling FB carbonator		
Air flow rate (slpm)	40	100
CO_2 flow rate (slpm)	7.5	19.0
CO_2 concentration at inlet ($\%_{vol}$)	15.0	16.5
Air flow for solid conveying (slpm)	35	55

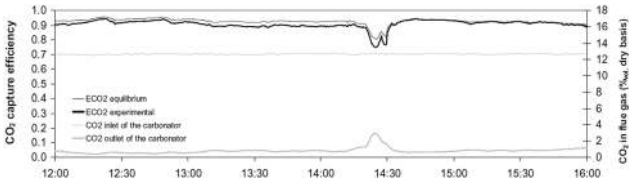

Fig. 6 Representative steady state results captured during testing of the 1.7 MW_{th} pilot plant at INCAR-CSIC (reprinted with permission from Sánchez-Biezma *et al.*[97] Copyright 2015 Elsevier).

As no fresh limestone was added to the system, the conversion of the CaO to $CaCO_3$ decreased towards the residual value of 0.1. Also, there were several issues with maintaining proper solid inventories when the oxy-firing mode was tested. Although CO_2 purity in the gas leaving the calciner reached 85% when the calciner temperature was 950 °C, low solid inventory and sorbent activity caused the CO_2 capture level to drop below the equilibrium level, to around 75%. Nevertheless, the authors claim that high CO_2 capture levels can be achieved even if highly deactivated sorbent is used with high sulphate conversions, provided the system is operated with the proper solid inventory.

Arias *et al.*[96] reported and thoroughly investigated the steady state operation of the 1.7 MW_{th} pilot plant at INCAR-CSIC. In the initial phase of the experimental trials, a CO_2 capture level of less than 40% was reached due to the high content of non-calcined limestone in the solid inventory because the calciner was operated below 920 °C. Moreover, the conversion dropped to 0.067 after more than 5 h of continuous operation without fresh limestone make-up. The same conclusion was drawn as in the study by Sánchez-Biezma *et al.*[97] that a CO_2 capture level of more than 80% can be reached, even when the sorbent has reached its residual conversion and there is a high SO_2 capture level (95%), provided enough solid inventory is available. These results confirm trends determined using the 30 kW_{th} unit and prove that the solid inventory and the sorbent conversion are the most relevant operating parameters in the carbonator reactor.

3.2.4 Data for process modelling. Information available in the literature, which includes detailed descriptions of the bench- and the pilot-scale facilities, provides essential input into model development. Most of the operating conditions, such as temperatures, solid looping rates, oxygen consumption rates and CO_2 contents in off-gases from the calciner and the carbonator have been disclosed. This allows for a local validation of model predictions. Moreover, global performance of the carbonator and the calciner can be validated.

Tests conducted using both facilities revealed that the carbonator operates at nearly isothermal conditions, which allows the assumption of isothermal conditions in modelling the FB reactors. Moreover, the actual CO_2 capture level was found to be close to that determined by equilibrium at a given temperature. Such assumption is, however, only valid for relatively active sorbent, as the experimental trials showed a reduction in CO_2 capture level for highly cycled particles.

3.3 Institute of Energy Systems and Technology at Darmstadt University of Technology

3.3.1 Experimental facility description. The 1 MW_{th} pilot plant erected and commissioned at Darmstadt University of Technology comprises two interconnected CFB reactors that are refractory lined to minimise heat loss (Fig. 7). The carbonator, which is 8.66 m high and 0.59 m in internal diameter, is equipped with internal cooling tubes to control the temperature. Moreover, in contrast to other pilot plants, fresh limestone is fed to the carbonator, where it is heated to 650 °C utilising the exothermal carbonation reaction. Such configuration is claimed to reduce fuel and O_2 consumption in the calciner.[98] In addition, synthetic flue gas, which can be heated up to 350 °C using auxiliary electric heaters, is used as a fluidising medium in the carbonator. O_2-enriched air preheated up to 450 °C is used to fluidise the calciner that is 11.35 m high and 0.4 m in internal diameter. To maintain the calcination reaction, the pilot plant is designed to combust either gaseous fuel, using a gas burner or a bed lance, or solid fuel, which is introduced by a gravimetric dosing system.

Unlike other pilot plants, the solids between the loop seals of the CFBs are transferred by screw conveyors. These can be equipped with heat transfer jackets, allowing for accurate control

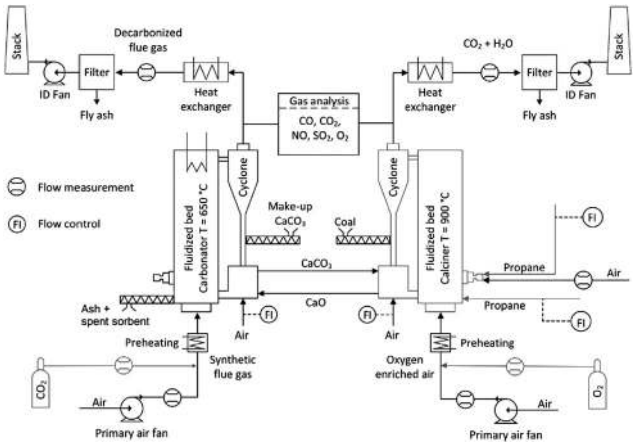

Fig. 7 Process flow diagram of the 1 MW_{th} pilot plant at Darmstadt University of Technology (reprinted with permission from Ströhle *et al.*[98] Copyright 2015 Elsevier).

of solids circulation rate and are capable of flexible operation under various loads. However, in a commercial-scale unit, large volumes of solids will be transferred between the reactors and the solid loads will vary due to changes in the power plant load, making the screw conveyors mechanically inefficient.[99] The flue gas and the CO_2 stream are subsequently cooled down in the heat exchangers, and then cleaned from fly ash in the fabric filters.

3.3.2 Test campaign. The first tests using the 1 MW_{th} pilot plant were conducted in July 2011. Since then, the facility has been operated for around 400 h to analyse CO_2 capture using the CaL process. In the first campaign, lasting 72 h, a continuous separation of CO_2 from the 1300 N m^3 h^{-1} synthetic gas comprising 10–12%$_{vol}$ CO_2 was analysed.[98] Throughout the campaign, the make-up flow was maintained at 70–150 kg h^{-1} and the solid looping rate between 1500 and 3000 kg h^{-1}. The study revealed that lower CO_2 capture levels are obtained if CaO, which has been calcined at 1000 °C before the test, is fed to the carbonator rather than fresh limestone. This is because a large fraction of older sorbent was present in the bed and caused a drop in the fraction of active sorbent. An increase in CO_2 capture level was observed when fresh limestone was fed to the carbonator. Despite the poor performance of the calciner cyclone and the low CO_2 concentration in the CO_2 stream caused by limited firing power in the calciner, the total CO_2 capture level was greater than 90%.

After increasing the power of the burners and the lances and improving the cyclone performance, a second test campaign using propane firing in the calciner was carried out. These changes led to a significant reduction in the make-up rate. Moreover, the fluidisation air was enriched with 50% O_2 to maintain a desirable gas velocity in the calciner and to ensure nearly complete combustion of propane. Again, the carbonator was operated at 660 °C and was fed with synthetic flue gas containing 12%$_{vol}$ CO_2. To maintain a desired average CO_2 capture level in the carbonator, the solid looping rate was kept at 2000 kg h^{-1}, which corresponded to an average Ca : C molar ratio of 11.6. The maximum CO_2 capture level in the carbonator was found to be 85%, increasing to 92% when oxy-combustion of propane in the calciner is considered.

In the third campaign, the calciner was fired with pulverised coal and the fluidisation air was enriched by 45–50% O_2. The temperature in the carbonator reached 670 °C. The same amount of synthetic flue gas was used as in the second campaign. To reach the same CO_2 capture level in the carbonator (85%), the solid looping ratio needed to be increased to approximately 2800 kg h^{-1} (Ca : C = 17.2). The CO_2 concentration in the clean gas was close to the equilibrium CO_2 concentration at that operating temperature. Therefore, the reaction was limited by chemical equilibrium leading to stable operating conditions. The CO_2 capture level dropped to approximately 60% when the temperature in the carbonator dropped to 610 °C.[98]

3.3.3 Data for process modelling. The description of the facility by Ströhle *et al.*[98] provides the information on equipment dimensions required for detailed process modelling. The data gathered from the three campaigns allow validation of the performance of a model overall and in respect of the carbonator CO_2 capture level. Some information on local parameters, such as fluidising air temperature, CO_2 flow rate at the inlet to the carbonator and the solid looping rates is available and would increase the quality of model validation. In addition, an operating range for some parameters, such as the fresh sorbent make-up rate and solid looping rate, was disclosed and would allow validation of a model at different operating points.

3.4 Institute of Combustion and Power Plant Technology at University of Stuttgart

3.4.1 Experimental facility description

3.4.1.1 10 kW_{th} bench-scale dual fluidised bed unit. The Institute of Combustion and Power Plant Technology (Institut für Feuerungs-und Kraftwerkstechnik, IFK) at the University of Stuttgart has developed a CaL bench-scale unit based on a 10 kW_{th} dual fluidised bed (DFB) that can be operated in continuous mode.[100] The practicability and stability of the DFB system was first analysed using a down-scaled cold model.[101,102]

In the 10 kW_{th} IFK unit, the CFB (gas velocity of 4–6 m s^{-1}) and the BFB (gas velocity less than 1.2 m s^{-1}) can each be operated either as the carbonator or calciner. A benefit of operating the BFB as the carbonator and the CFB as the calciner is ease in process control. The novel configuration of this DFB system results in control of the calcium circulation rate between the beds by varying the cone valve opening and the BFB absolute pressure. Due to heat losses to the environment, the CFB, the BFB and the solid circulation system are electrically heated.[103] The temperature in the calciner can be raised by direct natural gas combustion in O_2-enriched air (40%$_{vol}$ O_2), if the electric heating system capacity is insufficient.[100]

3.4.1.2 200 kW_{th} pilot-scale dual fluidised bed facility. To investigate the long-term performance of the process under real combustion conditions, a 200 kW_{th} pilot plant was built at the IFK. The pilot plant design includes a CFB calciner operating in a fast-fluidisation regime and a reconfigurable CFB carbonator that can operate either under a turbulent or fast-fluidised fluidisation

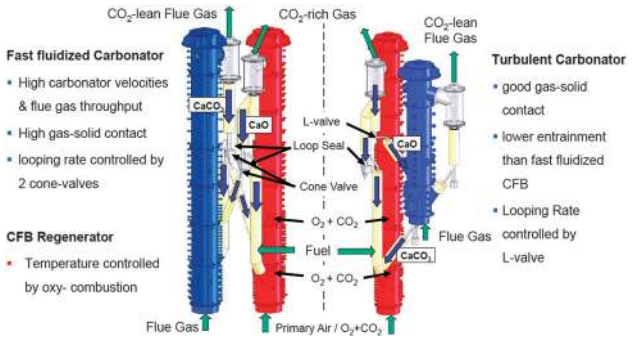

Fig. 8 Comparison of 200 kW_{th} DFB pilot plant configurations at IFK.[106]

regime (Fig. 8).[104,105] A design involving two symmetric CFBs, which operate in a fast-fluidised regime, required redesign of the solid circulation system and implementation of two cone valves for controlling the looping ratios in both CFBs independently.[105] Conversely, for the configuration with the carbonator operating in the turbulent regime, the solid circulation rate is controlled through the L-valve which is directly fed from the CFB calciner.[104]

The fast-fluidised CFB calciner, 10 m in height and 0.021 m in internal diameter, is equipped with a staged oxidant supply for oxy-combustion of solid fuel (coal, wood pellets, wood chips). Although the firing system is designed to handle up to 70%$_{vol}$ O_2 to meet the energy demand in the calciner, flue gas recirculation is implemented to achieve realistic operating conditions. In the turbulent fluidised bed carbonator (6 m in height and 0.033 m in internal diameter), the heat is removed using the FB heat exchanger. It is also designed to operate under lower fluidisation velocities and with lower residence time than the CFB carbonator.[104] The fast-fluidised CFB carbonator, 10 m high and 0.023 m in internal diameter,[102] is fluidised with the flue gas, and the heat released due to the exothermal reaction is removed *via* a water-cooled heat exchanger in the dense bed region and bayonet cooler in the lean bed region. The facility has a 400 kW_{th} gas burner to generate hot gas and heat up the system during start-up. To minimise the heat loss in the system, the reactors are lined with insulating concrete and refractory material resistant to abrasion.[105]

3.4.2 Test campaign using a 10 kW_{th} DFB unit. The tests were conducted using German limestone from Swabian Alb that was used to clean synthetic flue gas having 15%$_{vol}$ CO_2 to simulate CFPP conditions. It was relatively straightforward to achieve steady state operation with a minor make-up of fresh sorbent to account for attrition losses. When the carbonator was operated at 660 °C, the achievable CO_2 capture level exceeded 90%. The maximum level of 97% was observed in the periods when fresh sorbent was added to the carbonator, causing its temperature to drop to around 625 °C.

The effect of the carbonator operating temperature and the CO_2 capture level was then analysed and compared with the equilibrium data. The CO_2 capture level was reported to be close to that determined by chemical equilibrium at the given temperature, which was assured by maintaining a Ca : C ratio higher than 14.[103] A recent study by Varela *et al.*[107] identified that the CO_2 capture level of 90% is achievable at Ca : C ratio of 8, provided that steam is present in the carbonator and the calciner. Such behaviour is explained by likely enhancement of sorbent morphology in the presence of steam, favouring sorption and desorption of CO_2. Moreover, the increase of the CO_2 concentration in the calciner, which can be associated with CO_2 recycle to lower O_2 concentration in the fluidising gas, was found to significantly affect the reactor efficiency.

3.4.3 Test campaign using the 200 kW_{th} DFB facility. Dieter *et al.*[104] reported that more than 600 h of successful operation has been recorded and the facility was found to be hydrodynamically stable. The tests performed mainly aimed at reaching steady state conditions under variable temperature with synthetic flue gas containing 14%$_{vol}$ CO_2.

Although O_2 concentrations reached 50%$_{vol}$ during wood pellet combustion, no hot spots were observed and the temperature profile in the calciner was uniform (875–930 °C). This indicates the key benefit of staged oxidant supply. However, the desired temperature of 650 °C was observed only in the dense region of the turbulent FB carbonator, while the temperature was reduced in the upper region. Nevertheless, the CO_2 capture level was maintained above 90% indicating that most of the reaction takes place in the dense region. Fluctuations in the carbonator temperature (620–650 °C) have a minor effect on the carbonator efficiency. Furthermore, higher CO_2 capture levels are obtained if wet flue gas, such as from the desulphurisation unit, is fed to the carbonator. These results were found to closely follow the trend determined by the equilibrium calculations revealing good gas-solid contact in the carbonator (Fig. 9). This means that lower looping ratios would be required to reach the desired CO_2 capture level, leading to energy saving in the regenerator.[104]

3.4.4 Data for process modelling. The literature provides a detailed description of the equipment sizes and configurations, allowing for development of a model. Nevertheless, the limited information available on the equipment operating conditions and efficiencies and the lack of detailed stream data will restrict model validation, especially in terms of the conversion rates

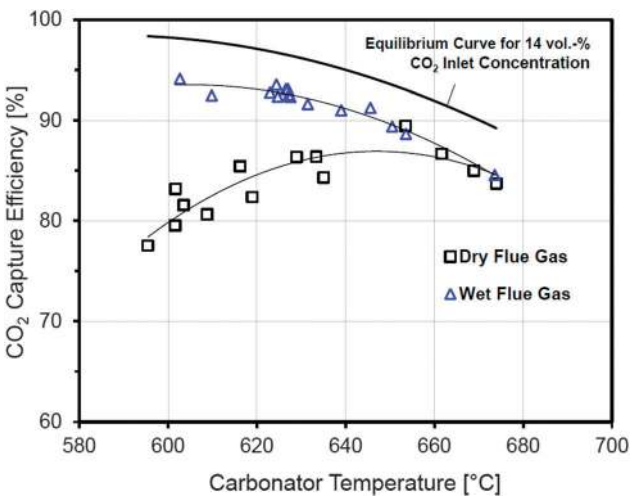

Fig. 9 Effect of the carbonator temperature on the CO_2 capture level data from the 200 kW_{th} DFB at IFK.[106]

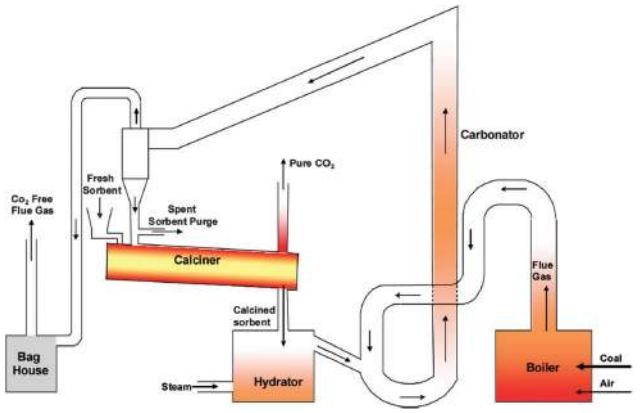

Fig. 10 Process flow diagram of the Ohio State University sub-pilot plant (reprinted with permission from Wang *et al.*[112] Copyright 2015 American Chemical Society).

and the solid looping rates. However, the results from both campaigns clearly indicate that the carbonator performance can be reasonably well represented using equilibrium models, provided an appropriate solid inventory, sorbent conversion and looping rate of Ca : C > 14 are assumed.

3.5 Ohio State University

3.5.1 Experimental facility description. The researchers at Ohio State University have pioneered the concept of simultaneous CO_2 and SO_2 capture using the Carbonation-Calcination Reaction process (CCR). The process was proposed as a merger of the Ohio State Carbonation Ash Reactivation (OSCAR) process[108–110] and the Calcium-based Reaction Separation for CO_2 (CaRS-CO_2) process,[111] two processes developed and patented by Ohio State University.

In the 120 kW_{th} sub-pilot plant (Fig. 10) the CaO or $Ca(OH)_2$ can be fed to the carbonator, which is the entrained bed (EB) reactor operated at 450–650 °C to allow for CO_2 and SO_2 capture. Sorbent regeneration is conducted in the electrically-heated RK calciner. Calcined sorbent is then hydrated using steam to improve the sorbent conversion over multiple cycles.[112] Some of the deactivated sorbent (2–10%) is purged and the fresh sorbent is fed directly to the calciner.

3.5.2 Test campaign. The CCR sub-pilot plant was used to purify flue gas produced in air-combustion of coal and natural gas in the stoker and containing 12.5%$_{vol}$ CO_2 and 1450 ppm$_v$ of SO_2. Prior to being fed to the carbonator the flue gas temperature was maintained at 650 °C using natural gas.

In the once-through test, Wang *et al.*[112] showed that the presence of fly ash in the carbonator does not affect the CO_2 and SO_2 capture levels. In addition, the amount of fly ash entering the carbonator needs to be considered when deciding on the purge fraction to maintain the proper amount of active sorbent in the system.

The study clearly indicated that application of $Ca(OH)_2$ with the mass median diameter (D_{50}) of 3 μm results in CO_2 capture levels between 40 and 100% for Ca : C ratios between 0.5 and 1.7. This performance was superior to traditional lime, as CO_2 capture levels of 9% were found for ground lime (D_{50} = 600 μm) and pulverised ground lime (D_{50} = 18 μm) at the same Ca : C ratio. Nevertheless, as pointed out by Dean *et al.*,[14] separation and fluidisation of such small particles from the gas stream in industrial-scale reactors would be extremely challenging and, therefore, the process feasibility and practicability is somewhat questionable.

3.5.3 Data for process modelling. Information on design characteristics of the CCR process available in the papers and patents is limited and does not reveal the equipment sizes. This would not allow for detailed model development. Nevertheless, simplified models, which consider only thermodynamic performance, could be developed.

The results of the test campaign are detailed enough to validate the global performance of a model. Unfortunately, no detailed information is provided on the local data, such as the solid looping rates or limestone make-up.

3.6 CANMET Energy Technology Centre

3.6.1 Experimental facility description. CanmetENERGY has developed a 75 kW_{th} pilot-scale DFB system which operates in semi-continuous mode to demonstrate the process feasibility. The system was first designed and analysed using process simulation by Hughes *et al.*[29] The pilot plant comprises a CFB calciner and a carbonator operated under either moving or bubbling bed conditions (Fig. 11).

Depending on the application the calciner is 4.5–5 m in height and 0.1 m in internal diameter and can be operated under air, O_2-enriched air or oxy-firing with flue gas recycle. The carbonator was divided into two stages to distinguish the combustion/sulphation and carbonation processes. Therefore, depending on the test performed it is 2–5 m in height and 0.1 m in internal diameter. Such configuration allows air or a mixture of air and superheated steam to fluidise both stages. To minimise the heat losses in the system, the reactors are lined with refractory and insulation materials. Moreover, each reactor is equipped with three 4.5–5 kW_{el} electric heaters that are used during start-up and sometimes to control the reactor temperature.[33,113] The CANMET Energy pilot plant has a novel

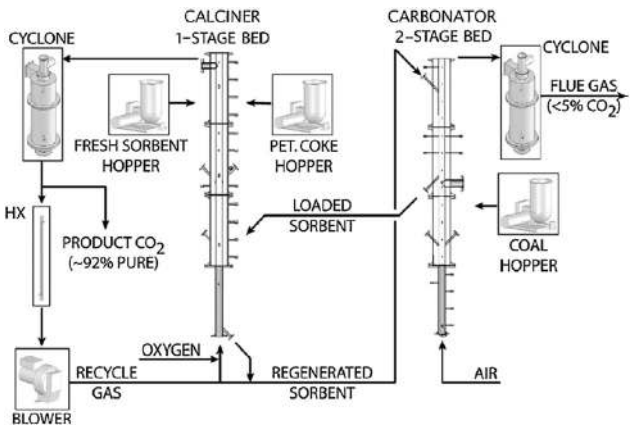

Fig. 11 Schematic of the 75 kW_{th} pilot plant developed at CANMET Energy (reprinted with permission from Hughes *et al.*[29] Copyright 2015 Elsevier).

solid transport system for sorbent looping that includes a 45° "T" that collects solids from the calciner-pierced distributor. The solids rate through the conveying line to the carbonator is controlled using a solenoid valve. The calcined sorbent enters the carbonator through the L-valve. Similarly, the 45° "T" line allows the carbonated sorbent to be directed to the calciner or to the second stage of the carbonator for SO_2 capture.

3.6.2 Test campaign using a 75 kW_{th} pilot plant. The 75 kW_{th} pilot plant has been operated under continuous mode for more than 50 hours (Table 4). During the tests, the carbonator was fed with a synthesised mixture of air and CO_2, to achieve CO_2 concentrations of 15–16%$_{vol}$. The fluidising air was preheated to 250 °C prior to being fed to the carbonator. The calciner was operated under three heating modes: electric heating, biomass combustion in air, and oxy-combustion of biomass and bituminous coal with flue gas recycle.

The tests performed by Lu *et al.*[33] confirmed that the CaL system can operate with a CO_2 capture level of 97% within the first several cycles. As the superficial gas velocity was increased, the CO_2 capture level decreased, which can be associated with lower residence time of gas in the carbonator. A considerable drop in the CO_2 capture level to approximately 72% was observed after 25 cycles. This confirms the impact of sorbent deactivation on process performance and implies the need for fresh sorbent make-up. The highest CO_2 capture level (98%) was reached within the temperature window of 580–600 °C for fresh sorbent and approximately 700 °C after 20 cycles. When the temperature dropped below 500 °C, the reaction rate slowed significantly. This was reflected in the off-gas CO_2 concentration of approximately 9–10%$_{vol}$ CO_2, hence in a drop of CO_2 capture level.

Finally, testing oxy-combustion of fuel in the calciner has proven this approach to be appropriate for providing heat for sorbent regeneration. There were no hot spots in the calciner, in spite of the high O_2 concentration in the primary gas of 40–50%$_{vol}$ balanced with the recycled flue gas. The maximum concentration of CO_2 was 85%$_{vol}$.

3.6.3 Data for process modelling. Information available in papers by Lu *et al.*[33] and Symonds *et al.*[113] include detailed descriptions of the process configuration and equipment dimensions which can be used to set up a model. Analysis of the CO_2 capture level under various operating conditions allows validation of the global performance of a model. Again, their study confirmed that the actual CO_2 capture levels could be close to the equilibrium values in practice. Their study also revealed that the carbonator temperature can be used as a means to maintain the desired CO_2 capture level, even with highly cycled sorbent. Although no information on the solid looping ratios and rates was provided, several operating limits were included in the paper by Lu *et al.*[33] that can form a basis for local validation of a model.

3.7 Cranfield University

3.7.1 Experimental facility description. A 25 kW_{th} bench-scale CaL rig developed at Cranfield University consists of an EB carbonator, 4.3 m high and 0.1 m in internal diameter, and a BFB calciner, 1.2 m high and 0.165 m in internal diameter.

Table 5 Optimal gas composition in 25 kW_{th} Cranfield University pilot plant[114]

Fluidising gas	Carbonator	Calciner
CO_2 volumetric flow rate (L min^{-1})	—	40
O_2 volumetric flow rate (L min^{-1})	—	16
Air volumetric flow rate (L min^{-1})	150	—
CH_4 volumetric flow rate (L min^{-1})	22.5	11

The desired operating temperature in the carbonator (600 °C) and the calciner (900–950 °C) is maintained using electric heating elements.[114]

The calciner is directly heated through oxy-combustion of natural gas. The resulting flue gas is used as the fluidising medium. The flue gas generated in the air-combustion of natural gas, which contains 8%$_{vol}$ CO_2, is used as the fluidising medium in the carbonator. The optimal operating gas input rates are presented in Table 5. Solid input to the calciner is achieved using a screw feeder with a maximum feeding rate of 1.6 kg h^{-1}. This proves the practical applicability of the screw conveyors for solid fuel and sorbent handling in the CaL units, as explained in Section 3.3.1. The solid looping rates are controlled *via* two fluidised loop seals, at the top and bottom of the calciner.[115] The unit has two cyclones at the top of the carbonator to ensure that the sorbent lost with the flue gas is kept to a minimum.[114]

3.7.2 Test campaign. A primary objective of the test campaign was maximisation of CO_2 capture level through modification of the process configuration and the operating conditions. CO_2 capture levels of 50% and 70% were reached with carbonator temperature windows of 650–700 °C and 600–650 °C, respectively. This improvement in efficiency at lower temperatures is attributed to its effects on chemical equilibrium, as reducing the temperature reduces the equilibrium CO_2 content and in turn increases the equilibrium CO_2 capture level.

Moreover, in batch runs the optimum CO_2 capture level, which was close to 90%, occurred for particle sizes between 125–250 μm. This was in agreement with results from another study carried out in the same group by Kavosh.[116] This behaviour was explained by an increase in the surface-to-volume ratio as the particle size was reduced. However, it was found that below 125 μm, the CO_2 capture level dropped below 50%. It appears that such small particles were Geldart's group C, and thus were difficult to fluidise leading to bed agglomeration.[117]

The maximum CO_2 capture level of 80% in the carbonator was reached after rig modifications resulting from the cold model, temperature and particle size distribution optimisation, and implementation of air shakers and heating elements to the loop seals to enhance solids transfer and temperature.[115]

3.7.3 Data for process modelling. The 25 kW_{th} unit has been described in detail in the analysed sources. As the description includes information on the equipment characteristics and operating conditions, it can be used for model development. The reliability of the CO_2 capture level prediction can be validated for various carbonator temperatures and particle size distributions. Unfortunately, the local level validation will be limited to flue gas and fuel oxy-firing in the calciner as no data on the solid circulating rates and solid inventory were disclosed.

3.8 Tsinghua University

3.8.1 Experimental facility description. The DFB system developed at Tsinghua University consists of two interconnected BFBs. The internal diameters of the carbonator and the calciner are 0.149 m and 0.117 m, respectively, and the height of each bed is 1 m. In this system, solids are transferred between the beds through the cyclones and the downcomers. In addition, solid injection nozzles are used to transport solids from the bed to the riser in each BFB. To compensate for the heat losses and to maintain the desired temperature in the carbonator and the calciner, each reactor was equipped with four 2.5 kW_{th} electric heaters. Additional electric heaters are used for heating the flue gas, the risers, the cyclones and the downcomers.[118]

3.8.2 Test campaign. In the test campaign, dolomite (D_{50} = 0.5 mm) was used as a source of natural sorbent to clean synthetic flue gas containing 12.1–14.5%$_{vol}$ CO_2. The solid looping rate was maintained at 30–36 kg h^{-1} which corresponded to an inventory height of 0.3 m in the two BFBs. When the desired temperatures in the carbonator (630 °C) and the calciner (850 °C) were achieved, the CO_2 fraction in the clean gas was 1.2%$_{vol}$, which corresponds to a CO_2 capture level of 89.2% in the carbonator. When the operating temperature of the carbonator was increased to 680 °C, the CO_2 fraction increased to 10%$_{vol}$ due to chemical equilibrium limitations.

In continuous CO_2 capture from synthetic flue gas, the calciner was operated at 810 °C, which led to maximum purity of 22.5%$_{vol}$ CO_2. On the other hand, the carbonator was operated at 640 °C reducing the CO_2 fraction in the clean gas to 0.7%$_{vol}$, which corresponds to a CO_2 capture level of 95%. Under such operating conditions the average conversion in the carbonator reached 70.4%. Due to incomplete calcination, the average conversion of particles leaving the carbonator was 16.2%. Finally, Fang *et al.*[118] have noted that after 7 h of continuous operation, the mean size of the particles was reduced to 0.16 mm and 0.42 mm in the calciner and the carbonator, respectively.

3.8.3 Data for process modelling. The bench-scale unit can serve as a basis for model development as its equipment sizes and operating conditions are or can be determined from other data provided by Fang *et al.*[118] A model can be validated at a global level as data are available for the carbonator CO_2 capture level under different operating conditions. Also, as the inlet gas flow rates to BFBs, the solid looping rates, and the CO_2 fraction in the gas streams from the carbonator and the calciner are available, local validation of the process streams can be conducted.

3.9 Vienna University of Technology

3.9.1 Experimental facility description. Researchers at the Vienna University of Technology have been testing a sorption-enhanced reforming (SER) process for biomass gasification in the 100 kW_{th} DFB gasifier facility (Fig. 12), another possible application of the CaL process.[119,120] Such process has a potential of improving the performance and reliability of the integrated-gasification combined cycle (IGCC) power plants. Other processes that utilise the sorption-enhanced reactions, such as a sorption-enhanced steam methane reforming (SE-SME), can yield high-purity H_2 (>95%$_{vol}$).[121,122] However, this process is more likely to be applied to meet increasing demands for H_2 in industrial processes, such as ammonia synthesis and fossil fuels processing,[123] rather than for large-scale power generation.

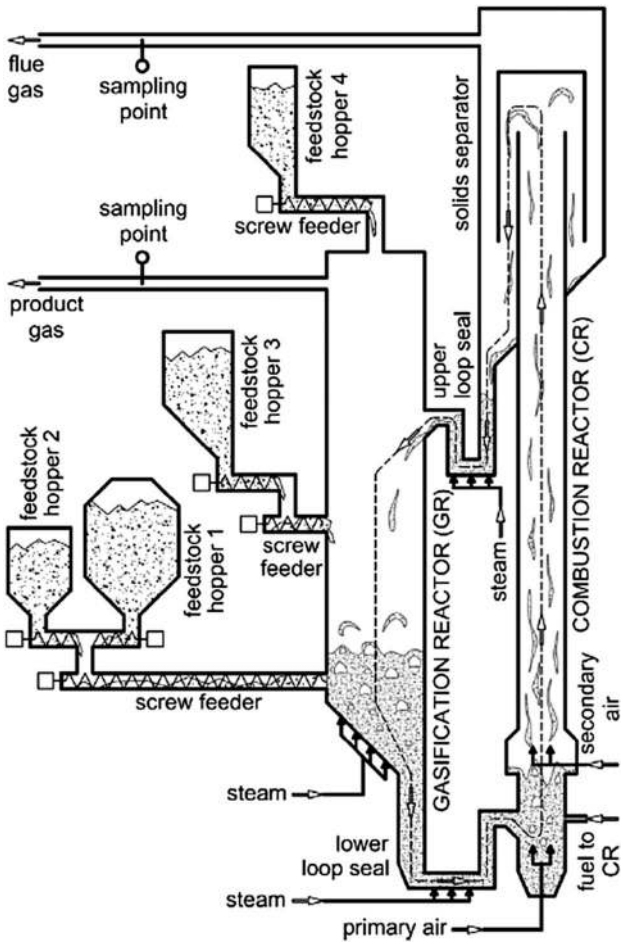

Fig. 12 Process flow diagram of the 100 kW_{th} bench-scale plant at Vienna University of Technology (reprinted with permission from Kirnbauer *et al.*[126] Copyright 2015 Elsevier).

In the conventional solid feedstock gasification process the BFB gasifier reactor operates at 850–900 °C, while air-combustion of fuel in the CFB combustor takes place at 920 °C. For this system, olivine was a suitable bed material with satisfactory resistance to attrition and moderate tar cracking activity.[120] The solids are transported between the reactors *via* two loop seals which are fluidised with steam. The concept was then successfully used for development of the biomass-fired 8 MW_{th} combined heat and power plant in Guessing, Austria that delivers 1.8 MW_{el} of electricity and 4.5 MW_{th} of heat to the local community.[124]

3.9.2 Test campaigns. The 100 kW_{th} unit has been modified to operate under SER process conditions with *in situ* CO_2 capture using limestone (Fig. 13). To assure proper conditions for the carbonation reaction, the BFB reactor temperature was reduced to approximately 700 °C[120] by reducing the solid looping rates between the reactors.[125]

The analysis by Pfeifer *et al.*[120] has revealed that compared to the conventional process, up to 70%$_{vol}$ higher H_2 yields are achievable.

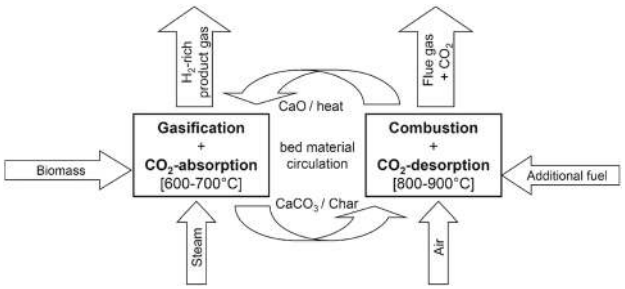

Fig. 13 Schematic representation of the sorption-enhanced reforming process with *in situ* CO_2 capture using calcium looping process (reprinted with permission from Koppatz *et al.*[125] Copyright 2015 Elsevier).

This is largely the result of an equilibrium shift in the water-gas shift reaction caused by CO_2 removal from the gasifier (Fig. 14). Moreover, a simultaneous reduction of the tar content from 4–8 g N^{-1} m^{-3} to 0.3–0.9 g N^{-1} m^{-3} was observed.

A first test campaign using the 8 MW_{el} Guessing CHP operating in SER mode was reported by Koppatz *et al.*[125] A temperature difference was required between the BFB gasifier and the CFB combustors to allow for efficient carbonation–calcination reactions. Therefore, the gasification temperature was reduced from 850–900 °C to 650–750 °C, while the combustion temperature was reduced from 950 °C to 850 °C. This was achieved through low solid looping rates. Moreover, olivine was substituted with limestone as the bed material. The content of H_2 and CH_4 in the syngas, hence its quality, decreases with increase of the gasification temperature. This could be explained by reduction of the driving force for the carbonation reaction, as the equilibrium partial pressure of CO_2 increases with temperature. The quality of the syngas produced in SER operating mode was higher than in the conventional process.

3.9.3 Data for process modelling. A detailed description of the experimental facility, which includes both the equipment dimensions and operating conditions, gives an opportunity for comprehensive equipment modelling. However, as the key objective of the test campaign was to improve syngas quality, no information was provided on the CO_2 capture level. Nevertheless, the available results allow validation of the syngas composition and comparison with the one reached in the conventional process. Although this kind of information does not provide a clear indicator of the CaL process performance in terms of the CO_2 capture level, it can still be used to validate the process performance.

3.10 Summary

In most of the studies, the key parameter describing performance of the CaL process is the CO_2 capture level. If a system is operated with appropriate solid inventory and sorbent conversion, the actual CO_2 capture level is close to the value determined by chemical equilibrium. This allows validation of the global performance of a model, which could be either equilibrium- or kinetics-based. Furthermore, unconventional configurations developed at ITRI and Ohio State University, which include the RK calciner, would be beneficial for validating a model when the power and cement integration is investigated.

The testing campaigns provide valuable insight in understanding process performance under varying operating conditions. Some information on local parameters, such as fluidising air temperature, flue gas composition and flow rate, CO_2 concentration in the gases leaving the CaL system, solid inventories or looping rates were disclosed. However, no complete data were available for any of the reviewed experimental campaigns. Further tests and more detailed data are required

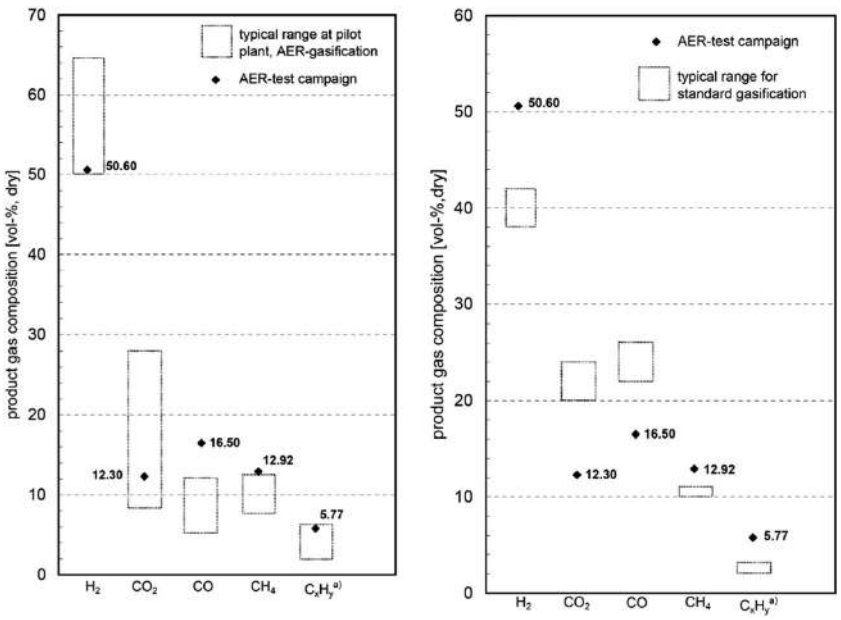

Fig. 14 Comparison of the syngas composition in conventional and SER gasification processes and the typical range at the pilot plant (adapted with permission from Koppatz *et al.*[125] Copyright 2015 Elsevier).

to allow validation of a model at the local level, and thus increase the quality of its prediction.

4 Models for the calcium looping processes

Development of novel power generation technologies needs to employ a range of analysis tools to evaluate various technology aspects. Therefore, experimental trials using bench- and pilot-scale facilities should be supported with analyses utilising mathematical and computational models that can be treated as a complementary source of information on process performance. Moreover, such models allow analysing the process scaling-up, and thus, expected net efficiency penalties, as well as operating and capital costs. Since the models vary in complexity and hence in computational requirements they can be applied at different stages of concept development to optimise the operating parameters of a process, to evaluate its performance under different operating conditions, or even to reliably size the equipment in the most time-efficient manner.

The current literature offers a selection of models for the key units, the carbonator and the calciner. They range from models based purely on thermodynamic equilibrium, usually defined by Gibbs' free energy minimisation,[26,32,127–131] through models considering sorbent degradation using semi-empirical correlations derived to fit experimental results,[11,16,34,39,42,84,86,132–146] to semi-predictive[28,30,31,37,93,135,147–149] and predictive models[150] that account for FB hydrodynamics and reaction kinetics. As the complexity of the models increases, the accuracy of their predictions increases as well. It needs to be stressed, however, that models of different complexity are suitable at different stages of process development; for example, thermodynamic or semi-empirical models would be more suitable for conceptual design studies, while predictive models would be appropriate at an advanced project stage, such as front-end engineering design. The CaL models available in the literature are reviewed in this section and their limitations are identified.

4.1 Modelling of the sorbent average conversion

The greatest challenge of using solid sorbents to capture CO_2 is the loss of their conversion with the number of carbonation–calcination cycles.[145] Thus far, the decay in sorbent maximum conversion, which is defined as the ratio of the actual and the theoretical mass of CaO that could have been converted to $CaCO_3$ for fully carbonated sorbent, has been represented using semi-empirical correlations. Since such representation includes fitting parameters, it would predict the activity decay well only for sorbent for which the values of fitting parameters were determined experimentally.

Dean *et al.*[14] have noted that the primary cause for sorbent deactivation is sintering of CaO during calcination at temperatures higher than 900 °C,[151] and high CO_2 and steam partial pressures.[43] High affinity of sorbent to SO_2 and H_2S, which are often present in the flue gas generated in a power plant, especially in units without FGD plants, would further affect the process performance due to increase in the solid looping rate. Although the once-through test performed by Sun *et al.*[152] in presence of SO_2 revealed no difference in the CO_2 capture in the chemically-controlled region of the carbonation, the calcination rate, and thus the sorbent conversion deteriorated as a result of $CaSO_4$ accumulation. Such observation was also made by Grasa *et al.*[153] The experimental trials showed that due to high Ca:S ratios in the system, the SO_2 and H_2S capture efficiencies could reach 100%.[112] As the regeneration process of sulphated sorbent is possible only at very high temperatures or in reducing conditions,[154,155] this would enhance sorbent sintering causing a further reduction in the activity. Moreover, attrition leading to excessive elutriation of sorbent and ash fouling could occur under such conditions.[13,14]

Sorbent performance is usually represented as a drop in the maximum sorbent particle conversion with the number of carbonation–calcination cycles (N). Since 2002, many semi-empirical correlations were developed to characterise the drop in the sorbent performance, for which the fitting parameters are often determined from the thermogravimetric analysis (TGA).[28,156–160] Such correlations were developed for non-pretreated sorbents,[42,139–145] and thermally pretreated sorbents[34,138] that experience self-reactivation.[34,161] Most of the semi-empirical correlations have been reviewed by Dean *et al.*,[14] and only the most important ones, required to understand the more complex models, are presented here.

A first semi-empirical model for the maximum sorbent conversion was developed by Abanades[145] based on the assumption that decay in the maximum carbonation conversion in the chemically-controlled stage depends only on the number of calcination–carbonation cycles.

$$X_N = k^{N+1} + X_r \tag{3}$$

There was a high degree of correlation between the maximum sorbent conversion predicted by the model and the experimental data (98.2%)[28,156,158–160] for a deactivation constant (k) and a residual carbonation conversion (X_r) of 0.782 and 0.174, respectively.

A study by Grasa and Abanades[143] has confirmed that the sorbent conversion decreases asymptotically to residual conversion that amounts to 0.075–0.08 and is constant when the number of calcination–carbonation cycles is higher than 50. Based on the proportionality between conversion and the surface area of highly cycled particles through the product layer thickness ($X = S/S_0$), Grasa and Abanades[143] have proposed a semi-empirical correlation for decay of the sorbent maximum conversion which is formulated similarly to typical catalyst deactivation correlations.

$$X_N = \frac{1}{\frac{1}{1 - X_r} + kN} + X_r \tag{4}$$

With a deactivation constant (k) of 0.52 and residual conversion (X_r) of 0.075, the prediction of the semi-empirical model presented in eqn (4) was accurate for a wide range of limestones, particle sizes and CO_2 partial pressures.

Li and Cai[139] have adopted a five-parameter correlation, with a similar structure to the one proposed by Abanades.[145]

$$X_N = a_1 f_1^{N+1} + a_2 f_2^{N+1} + X_r \quad (5)$$

Although the constants in eqn (5) were determined for a particular sorbent, no particular reference to their physical meaning was made. This semi-empirical model was found to successfully predict the decay in conversion of different sorbents (limestone, dolomite, $CaO/Ca_{12}Al_{14}O_{33}$), provided the fitting parameters were known.

4.1.1 Maximum average conversion of non-pretreated sorbent. The aforementioned semi-empirical models allow determination of the maximum carbonation conversion of sorbent particles that have undergone a given number of carbonation–calcination cycles. In real systems, however, the population of particles would comprise particles that have undergone different numbers of carbonation and calcination cycles. Based on the assumption that the solids are well mixed in the reactor, Abanades[145] proposed calculating the maximum average conversion in the carbonator as:

$$X_{ave,max} = \sum_{N=1}^{N=\infty} r_N X_N \quad (6)$$

The mass fraction of the particles that has undergone N carbonation–calcination cycles (r_N) is directly related to the solid looping rate (F_R) and fresh limestone makeup rate (F_0) as shown in eqn (7).

$$r_N = \frac{F_0 F_R^{N-1}}{(F_0 + F_R)^N} \quad (7)$$

Using the definition of the maximum carbonation conversion presented in eqn (3), Abanades *et al.*[39] have indicated that for a FB calciner (perfectly stirred reactor), the average conversion of sorbent entering the carbonator can be expressed using eqn (8) as a function of the process parameters: solid looping rate and fresh limestone make-up rate.

$$X_{ave,max} = \frac{k(1 - X_r)F_0}{F_0 + F_R(1 - X_r)} + X_r \quad (8)$$

Assuming that all sulphur present in the fuel reacts with the active sorbent to form $CaSO_4$, eqn (8) can be modified to account for sorbent deactivation caused by $CaSO_4$ formation.

$$X_{ave,max} = \frac{k(1 - X_r)F_0}{F_0 + F_R(1 - X_r)} + X_r - \frac{F_{CO_2}}{F_0 r_{C/S} y_{comb}} \quad (9)$$

As eqn (3) does not account for the residual conversion of sorbent, eqn (4) proposed by Grasa and Abanades[143] appears to be the most commonly applied in the literature. However, Li and Cai[139] have claimed that it is difficult to determine an explicit solution for an infinite sum in eqn (6) when the maximum conversion of the sorbent is formulated similarly to eqn (4). Therefore, they have derived a correlation for the average conversion by incorporating eqn (5) into eqn (6) and calculating the limit of the infinite sum of the geometric series. For $f_2 = 0$ the proposed correlation reduces to eqn (8) derived by Abanades *et al.*[39]

$$X_{ave,max} = \frac{a_1 f_1 F_0}{F_0 + F_R(1 - f_1)} + \frac{a_2 f_2 F_0}{F_0 + F_R(1 - f_2)} + X_r \quad (10)$$

Rodríguez *et al.*[11] have considered the impact of the reactor performance indicators, which define the extent of calcination (f_{calc}) or carbonation (f_{carb}) in each reactor, as well as the impact of the uncalcined sorbent (r_0) on the maximum average conversion.

$$f_{calc} = \frac{X_{carb} - X_{calc}}{X_{carb}} \quad (11)$$

$$f_{carb} = \frac{X_{carb} - X_{calc}}{X_{ave,max} - X_{calc}} \quad (12)$$

$$r_0 = \frac{F_0(1 - f_{calc})}{F_0 + F_R f_{calc}} \quad (13)$$

Having incorporated eqn (11)–(13) into eqn (6), and utilising the maximum conversion model proposed by Li and Cai,[139] Rodríguez *et al.*[11] derived a semi-empirical correlation for maximum average conversion.

$$X_{ave,max} = (F_0 + F_R r_0) f_{calc} \times \left[\frac{a_1 {f_1}^2}{F_0 + F_R f_{carb} f_{calc}(1 - f_1)} + \frac{a_2 {f_2}^2}{F_0 + F_R f_{carb} f_{calc}(1 - f_2)} + \frac{X_r}{F_0}\right] \quad (14)$$

Eqn (14) reduces to an equation similar to the one derived by Li and Cai[139] for $f_{calc} = 1$ and $f_{carb} = 1$, with the only difference being the squared f_1 and f_2 fitting parameters. However, it allows estimation of the maximum average sorbent conversion that can be reached in the carbonator. Mantripragada and Rubin[162] stated that the actual conversion depends on the carbonation and calcination degree; hence the actual conversion in the carbonator and the calciner, which can be seen as equivalent to rich- and lean-loading in the solvent scrubbing technologies, are corrected based on the carbonator and the calciner performance, using the following expressions:

$$X_{carb} = \frac{f_{carb}}{1 - (1 - f_{carb})(1 - f_{calc})} X_{ave,max} \quad (15)$$

$$X_{calc} = (1 - f_{calc}) X_{carb} \quad (16)$$

4.1.2 Maximum average conversion of hydrated sorbent. Partial hydration is an option for sorbent reactivation that yields higher average sorbent conversions compared to unhydrated sorbent.[163–167] Hence, the system can operate at lower solid looping and make-up rates leading to a reduced heat requirement for the calciner.[40] In this concept (Fig. 15) some of the solids leaving the calciner (F_H) are diverted to the hydrator, while the remaining ($F_R - F_H$) circulate to the carbonator as usual. Therefore, the average conversion models reviewed in Section 4.1.1 are not applicable.

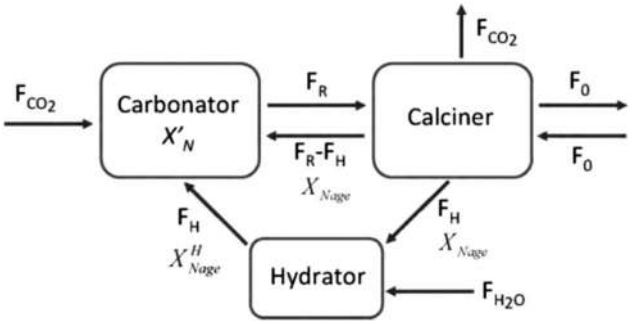

Fig. 15 Calcium looping process with sorbent reactivation through hydration (reprinted with permission from Arias *et al.*[137] Copyright 2015 Elsevier).

Arias *et al.*[137] have proposed a conversion model that can be used to predict the performance of a CaL plant with a hydrator operating in a continuous mode. As such a configuration does not produce any change in the number of carbonation–calcination cycles that each particle has undergone, the fraction of particles that has undergone N carbonation–calcination cycles can be still estimated using eqn (7). Moreover, since different fractions of sorbent having different maximum conversions are fed to the carbonator, the maximum conversion for a given calcination–carbonation cycle number N can be represented as:

$$X_N{}' = X_{N_{\text{age}}}\frac{F_{\text{R}} - F_{\text{H}}}{F_{\text{R}}} + X^{\text{H}}_{N_{\text{age}}}\frac{F_{\text{H}}}{F_{\text{R}}} \tag{17}$$

To estimate the maximum conversion $X_N{}'$, the particle age N_{age}, with conversion capacity in the previous cycle $N-1$, needs to be determined. For known value of $X_{N-1}{}'$, which was taken by Arias *et al.*[137] as approximately 0.7, the particle age before its Nth calcination is estimated using eqn (4) in reverse.

$$N_{\text{age}-1} = \left(\frac{1}{k}\right)\left(\frac{1}{X_{N-1}{}' - X_{\text{r}}} - \frac{1}{1 - X_{\text{r}}}\right) \tag{18}$$

The corresponding maximum conversions for the hydrated ($X^{\text{H}}_{N_{\text{age}}}$) or non-pretreated ($X_{N_{\text{age}}}$) sorbent can then be estimated using eqn (4). The decay constant (k^{H}) and the residual conversion (X^{H}_{r}) for the regenerated sorbent depend on the degree of hydration, and were estimated to be 0.63 and 0.15, respectively for 20% hydration, and 1.39 and 0.36, respectively for 60% hydration based on experimental data from Grasa *et al.*[166] (Fig. 16).

Stable maximum conversions were reached for a relatively small number of cycles. This is a result of a balance between the increase in sorbent conversion due to hydration and the loss in each carbonation–calcination cycle due to sintering.[137] Finally, the maximum average conversion of the sorbent can be determined as:

$$X_{\text{ave,max}} = \sum_{N=1}^{N=\infty} r_N X_N{}' \tag{19}$$

4.2 Modelling of carbonation and calcination kinetic rates

4.2.1 Apparent kinetics model for carbonation. Lee[168] has developed a kinetic model for CaO carbonation conversion that is reportedly simple to implement during process design and modelling. In this model, the CaO conversion rate is expressed as a function of the kinetic rate constant (k_{r}) and the actual and maximum conversion.

$$\frac{\mathrm{d}X}{\mathrm{d}t} = k_{\text{r}}\left(1 - \frac{X}{X_{\max}}\right)^n \tag{20}$$

When $n = 2$, the model prediction is close to the experimental data presented by Bhatia and Perlmutter,[169] as well as Gupta and Fan.[170] This was reflected in a lowest correlation coefficient of 95%.

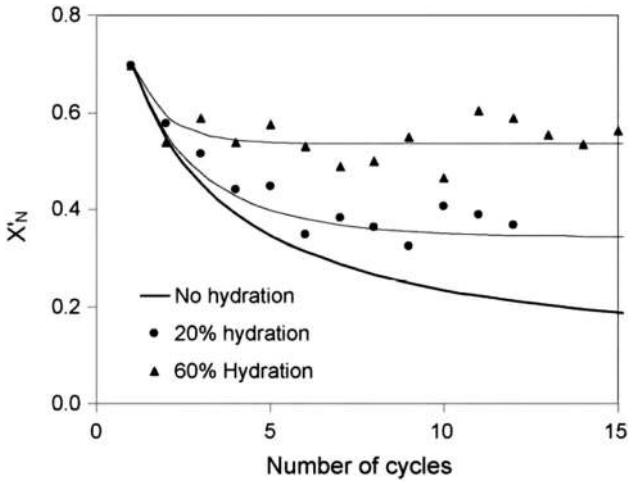

Fig. 16 Comparison of the experimental data in Grasa *et al.*[166] and the model prediction with $F_{\text{H}}/F_{\text{R}} = 1$ (reprinted with permission from Arias *et al.*[137] Copyright 2015 Elsevier).

Eqn (20) was formulated in such a way that it could be used to describe both chemical- and diffusion-controlled regions of the carbonation reaction. Having estimated the values for activation energies and pre-exponential factors using data from both sources, Lee[168] identified that the type of limestone does not have a great impact on the chemical-controlled regime parameters, while it does for the diffusion-controlled ones (Table 6). This was explained by the strong impact of the CaO morphology on the reaction rate in the diffusion-controlled region.

4.2.2 Carbonation kinetic model for highly cycled particles. Grasa *et al.*[171] have proposed a model for sorbent conversion that utilises a rate expression consistent with a grain model for the carbonation reaction. The expression is similar to the one determined by Abanades *et al.*[136]

$$\frac{\mathrm{d}X}{\mathrm{d}t} = k_{\text{s}} S_N (1 - X)^{\frac{2}{3}}\left(C_{\text{CO}_2} - C_{\text{CO}_2,\text{eq}}\right) \tag{21}$$

The model assumes that the active surface area of the particle that has undergone N calcination–carbonation cycles decreases proportionally with the maximum conversion of the particles at the end of the fast carbonation period. It also assumes that the $CaCO_3$ layer thickness (h) reaches a maximum of 50 nm in this period.

$$S_N = \frac{V_{\text{MCaCO}_3}\rho_{\text{CaO}}}{M_{\text{CaO}}h} X_N \tag{22}$$

Table 6 Characteristic parameters for the rate constant k[168]

	Bhatia and Perlmutter[169]		Gupta and Fan[170]	
Controlling mechanism	Activation energy (kJ mol^{-1})	Pre-exponential factor (s^{-1})	Activation energy (kJ mol^{-1})	Pre-exponential factor (s^{-1})
Chemical reaction	72.2	171.67	72.7	193.33
Mass transfer	189.3	2.62×10^{8}	102.5	3.88×10^{3}

Using eqn (4) to determine the maximum conversion at given cycle N, the active surfaces were determined to be between 1×10^{6} and 2×10^{6} m^2 m^{-3} for highly cycled particles, while the rate constant k_s was estimated to be 3.2×10^{-10} to 8.9×10^{-10} m^4 mol^{-1} s^{-1}. Similar values were yielded (3.1×10^{-10} to 8.7×10^{-10} m^4 mol^{-1} s^{-1}) when the pore model described in eqn (23) was applied with the pore structural parameter defined as $\Psi_N = 4\pi L_N/S_N^2$.

$$\frac{dX}{dt} = k_s S_N \left(C_{CO_2} - C_{CO_2,eq}\right)(1-X)\sqrt{1-\Psi \ln(1-X)} \quad (23)$$

Moreover, Grasa *et al.*[171] have pointed out that the central value of the estimated rate constant is remarkably close to the value of 6.05×10^{-10} m^4 mol^{-1} s^{-1} estimated using the pore model by Bhatia and Perlmutter.[169]

4.2.3 Changing grain size carbonation and calcination models. Recently, Yu *et al.*[172] have developed a kinetic model to represent the carbonation process through modification of the existing changing grain size model that was previously used to represent the reaction between CaO and SO_2.[173] This model assumes that carbonation is an unsteady-state process with the CO_2 concentration inside the particle represented in the radial coordinate system as the sum of the diffusion and chemical reaction terms.

$$\frac{dC_{CO_2}}{dt} = r_{CO_2} + \frac{1}{R^2}\frac{\partial}{\partial R}\left(D_e R^2 \frac{\partial C_{CO_2}}{\partial R}\right) \quad (24)$$

The first term in eqn (24) accounts for the reversible carbonation reaction for which the reaction rate per unit volume of the particle includes both carbonation and calcination reaction rates.

$$r_{CO_2} = -\left[k_{carb} S_0 \left(\frac{r_i}{r_0}\right)^2 V_R C_{CO_2} - k_{calc} S_0 \left(\frac{r_i}{r_0}\right)^2\right] \quad (25)$$

In the model, the carbonation rate constant is represented using eqn (26) proposed by Sun *et al.*,[174] while eqn (27) used for the calcination rate constant is taken from Borgwardt.[175]

$$k_{carb} = \begin{cases} 1.67 \times 10^{-4} \exp\left(-\dfrac{24\,000}{R_g T}\right)\left(P_{CO_2} - P_{CO_2,eq}\right) & \text{if } P_{CO_2} - P_{CO_2,eq} < 10 \text{ kPa} \\ 1.67 \times 10^{-3} \exp\left(-\dfrac{24\,000}{R_g T}\right) & \text{if } P_{CO_2} - P_{CO_2,eq} > 10 \text{ kPa} \end{cases} \quad (26)$$

$$k_{calc} = 3 \times 10^{-2} \exp\left(-\frac{205\,000}{R_g T}\right) \quad (27)$$

The equilibrium partial pressure ($P_{CO_2,eq}$) was calculated as a function of the reactor temperature,[36] and the initial surface area of CaO was determined based on the initial particle porosity (ε_0), initial grain radius (r_0) and molar volume of CaO and $CaCO_3$.

$$P_{CO_2,eq} = 10^{\left(7.079 - \frac{8808}{T}\right)} \quad (28)$$

$$S_0 = \frac{3(1-\varepsilon_0)}{r_0}\frac{V_{m,CaO}}{V_{m,CaCO_3}} \quad (29)$$

According to the changing grain size model, the change in the un-reacted radius of the CaO grain is dependent on the carbonation and calcination rate constants.

$$\frac{dr_i}{dt} = -\left(k_{carb} V_R V_R C_{CO_2} - k_{calc} V_R\right) \quad (30)$$

The local and average conversions of CaO were expressed as:

$$X = 1 - \left(\frac{r_i}{r_0}\right)^3 \quad (31)$$

$$X(t) = \frac{1}{\frac{4}{3}\pi {R_0}^3}\int_0^{R_0} 4\pi R^2 X \, dR \quad (32)$$

The second term in eqn (24) accounts for the effective diffusivity of CO_2 through the sorbent particle. It accounts for the product layer diffusivity (D_p), molecular diffusivity of CO_2 in N_2 (D_{m,CO_2}), the Knudsen diffusivity (D_K) and the porosity changes inside the particle during the reaction (ε).

$$D_e = \left[(1-X)\left(\frac{1}{D_{m,CO_2}} + \frac{1}{D_K}\right)^{-1} + X D_p\right]\varepsilon^2 \quad (33)$$

Yu *et al.*[172] have validated the model with the experimental result for the CGMG75 sorbent, which was composed of 75%$_{wt}$ CaO and 25%$_{wt}$ MgO, and 15%$_{vol}$ CO_2 in the synthetic flue gas. As shown in Fig. 17, the model prediction accurately reproduces the experimental data in both chemical-controlled and diffusion-controlled regions of the carbonation process.

García-Labiano *et al.*[176] proposed incorporating the Langmuir–Hinshelwood mechanism into the changing grain size model to describe the calcination process. The model is based on the similar mass balance to the one presented in eqn (24), but with the negative sign for the CO_2 source term, and accounts for both the diffusion and the reaction of the gas

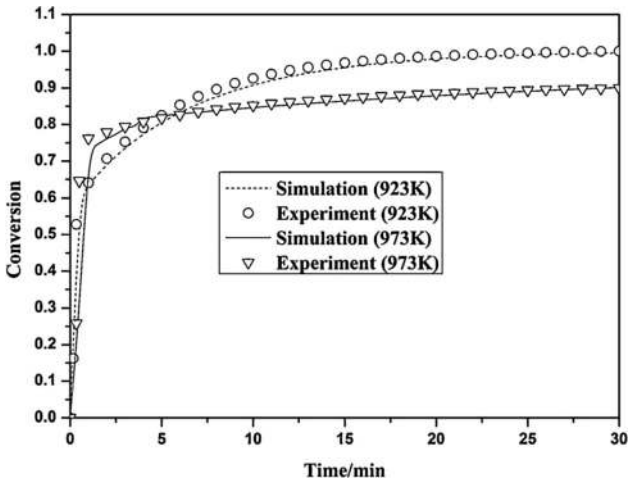

Fig. 17 Validation of the Yu *et al.*[172] model with the experimental data (reprinted with permisson from Yu *et al.*[172] Copyright 2015 Elsevier).

in a differential volume of the particle.

$$\frac{\partial C_{CO_2}}{\partial t} = -r_{CO_2} + \frac{1}{R^2}\frac{\partial}{\partial R}\left(D_e R^2 \frac{\partial C_{CO_2}}{\partial R}\right) \quad (34)$$

However, in contrast to the model by Yu *et al.*,[172] the calcination reaction is described using the two-stage Langmuir–Hinshelwood mechanism. In the first stage, considering that one CO_2 molecule can be chemisorbed on n out of L active sites, $CaCO_3$ is decomposed to CaO and adsorbed CO_2. CO_2 is then desorbed from the active site in the second step.

$$CaCO_3 + nL \underset{k_1}{\overset{k_2}{\rightleftharpoons}} CaO + nL(CO_2) \qquad K_1 = \frac{k_1}{k_2} \quad (35)$$

$$nL(CO_2) \underset{k_D}{\overset{k_A}{\rightleftharpoons}} CO_2 + nL \qquad K_A = \frac{k_A}{k_D} \quad (36)$$

The kinetic rate of calcination per unit of particle volume was then described as:

$$r_{CO_2} = k_{calc} S_e (1-\theta)\left(1 - \frac{P_{CO_2}}{P_{CO_2,eq}}\right) \quad (37)$$

The fraction of the active sites (θ) was found to be well represented by the Freundlich isotherm, for which the adsorption constant was represented using the Arrhenius expression.

$$\theta = c_0 \exp\left(-\frac{E}{R_g T}\right) P_{CO_2}^{\frac{1}{2}} \quad (38)$$

According to the changing grain size model, the reaction surface is dependent on the particle radius that, in turn, changes as the reaction proceeds.

$$S_e = S_0 \left(\frac{r_1}{r_0}\right)^2 \quad (39)$$

$$r_0 = \frac{3(1-\varepsilon_0)}{S_0} \quad (40)$$

$$r_1 = k_{calc} V_{M,CaCO_3}\left(1 - \frac{P_{CO_2}}{P_{CO_2,eq}}\right) \quad (41)$$

The effective diffusion was represented as a combination of the molecular and Knudsen diffusions, as well as the particle porosity.

$$D_e = \left(\frac{1}{D_{m,CO_2}} + \frac{1}{D_K}\right)^{-1} \varepsilon^2 \quad (42)$$

$$\varepsilon = \varepsilon_0 - \frac{\rho_{CaCO_3}\left(V_{M,CaO} - V_{M,CaCO_3}\right)}{M_{CaCO_3}}(1-\varepsilon_0)X(R,t) \quad (43)$$

The variation in the porosity inside the particle was determined from the initial porosity, the stoichiometric volume ratio of solid product to reactant product, and the local conversion of $CaCO_3$ given by eqn (43). The average conversion at a given time is represented using the same form as in eqn (32).

García-Labiano *et al.*[176] have validated the prediction of the model at different CO_2 partial and equilibrium pressures using different limestone compositions and found good agreement between the model prediction and the experimental data (Fig. 18). The changing grain size models, which were adapted to the carbonation and calcination processes, were found to closely represent the particle conversion at given temperature. Although these did not account for sorbent sulphation and ash accumulation, such models would provide a valuable tool in calciner modelling, provided they are coupled with reactor hydrodynamics.

4.3 Carbonator reactor modelling

4.3.1 Semi-predictive model with simple hydrodynamics. Alonso *et al.*[30] have developed a model for the carbonator that combines simple hydrodynamics correlations with the average conversion of the sorbent and residence time distribution functions. They have introduced a definition of the active fraction (f_a) of the particles that is dependent only on the actual residence time (t^*) and the average residence time (τ) in the carbonator.

$$f_a = 1 - \exp\left(-\frac{t^*}{\tau}\right) \quad (44)$$

$$\tau = \frac{N_{Ca}}{F_R} = \frac{W_{CaO}}{M_{CaO} F_R} \quad (45)$$

This definition of the active fraction of the particles in the carbonator, along with the definition for the average maximum conversion given by eqn (6), led to the following expression for the actual average sorbent conversion at the exit of the carbonator (46) and the CO_2 capture level in the carbonator (47).

$$X = X_{ave,max}\frac{\tau}{t^*}\left[1 - \exp\left(-\frac{t^*}{\tau}\right)\right] = X_{ave,max}\frac{f_a}{\ln\left[\frac{1}{1-f_a}\right]} \quad (46)$$

$$E_{carb} = \frac{F_R}{F_{CO_2}} X_{ave,max}\frac{f_a}{\ln\left[\frac{1}{1-f_a}\right]} \quad (47)$$

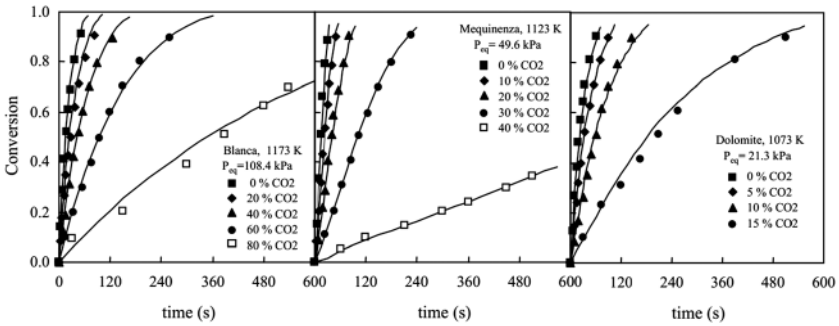

Fig. 18 Validation of the García-Labiano *et al.*[176] model with the experimental data (reprinted with permission from García-Labiano *et al.*[176] Copyright 2015 Elsevier).

Based on the carbon balance in the carbonator reactor, the same amount of CO_2 disappears from the gas phase and reacts with CaO to form $CaCO_3$.

$$F_{CO_2}E_{carb} = F_R X = N_{Ca} f_a \frac{dX_{ave,max}}{dt} \quad (48)$$

Only one value for the active fraction exists for a given operating point of the system that is characterised by the sorbent looping rate (F_R), fresh sorbent make-up rate (F_0), CO_2 rate to the carbonator (F_{CO_2}) and solids inventory (W_{CaO}). Therefore, the value for the active fraction at which the system is in balance is calculated iteratively.

The average reaction rate expression shown in eqn (49) proposed by Alonso *et al.*[30] does not consider the characteristic term for the grain models $(1 - X)^{2/3}$. Although this change makes it slightly different from the expressions proposed by Abanades *et al.*[136] and Grasa *et al.*,[171] the authors claim that this will not have a significant effect on prediction accuracy, as the conversion is low despite the relatively fresh sorbent and thus this term would be close to unity.

$$\frac{dX_{ave,max}}{dt} = k_s S_{ave,max}\left(C_{CO_2} - C_{CO_2,eq}\right) \quad (49)$$

Alonso *et al.*[30] assumed a conservative value for the carbonation rate constant of 4×10^{-10} m^4 mol^{-1} s^{-1} that falls within the lower part of the range 3.2×10^{-10}–8.9×10^{-10} m^4 mol^{-1} s^{-1} identified by Grasa *et al.*[171] In contrast to the previous study by Abanades *et al.*,[136] the average surface available for the carbonation reaction is calculated as a function of the average conversion, using an expression proposed by Grasa *et al.*[171]

$$S_{ave,max} = \frac{\frac{\rho_{CaO}}{M_{CaO}}}{h\frac{\rho_{CaCO_3}}{M_{CaCO_3}}} X_{ave,max} \quad (50)$$

Finally, the CO_2 capture level in the carbonator can be estimated from the carbon balance in the gas phase which can be formulated as a differential equation assuming a plug flow of the gas phase and perfect mixing of the solids.

$$F_{CO_2}\frac{dE_{carb}}{dz} = A f_a \frac{\rho_{CaO}}{M_{CaO}} r_{ave} = A f_a \frac{\rho_{CaO}}{M_{CaO}} k_s S_{ave,max}\rho_{M,g} \times \left[\frac{\left(f_{CO_2,0} - f_{CO_2,eq}\right) + \left(f_{CO_2,0}f_{CO_2,eq} - f_{CO_2,0}\right)E_{carb}}{1 - f_{CO_2,0}E_{carb}}\right] \quad (51)$$

Rodríguez *et al.*[93] and Charitos *et al.*[149] have developed a kinetic expression for the carbonation process based on the experimental studies using the 30 kW_{th} unit at INCAR-CSIC and the 10 kW_{th} unit at IFK. Their model is based on a CO_2 mass balance for a system operating at steady state, which is similar to the one formulated by Alonso *et al.*,[30] and is related to the amount of CO_2 captured in the bed.

$$F_{CO_2}E_{carb} = \frac{W_{CaO}}{M_{CaO}}\frac{dX}{dt} \quad (52)$$

Assuming that only a fraction of the CaO reacts with the CO_2 in the carbonator (X_{ave}), the first-order expression for the carbonation kinetic rate is:

$$\frac{dX}{dt} = \varphi_e k_{carb} X_{ave,max}\left(\overline{v_{CO_2}} - v_{CO_2,eq}\right) \quad (53)$$

Rodríguez *et al.*[93] found that for two limestones investigated at the INCAR-CSIC unit the carbonation rate constant (k_{carb}) was 0.37 s^{-1}. The investigation revealed that the reaction rate constant depends on the test unit as it was equal to 0.26 s^{-1} for the IFK unit and 0.33 s^{-1} for the INCAR-CSIC unit. The authors claim that this is in agreement with previous publications[169,177] reporting that temperature has little effect on carbonation rates. Moreover, the proposed model includes an effectivity factor (φ_e) that accounts for all physical resistances to the carbonation process and ideally it should be equal to unity for a stationary system. In reality, analysis of the experimental data revealed that the carbonator effectivity factor varies between 0.8 and 1.3. Such a high deviation from unity was probably a result of measurement uncertainty, as estimation of the solid circulation rates and average carbonation conversion is associated with an error reaching ±20%.[93,149]

Finally, using the definition for the active fraction of sorbent (f_a) proposed by Alonso *et al.*,[30] an expression for the CO_2 capture level, which links the average conversion of sorbent and the residence time distribution in the bed, was proposed.

$$E_{carb} = \varphi_e k_{carb} X_{ave,max} f_a \tau\left(\overline{v_{CO_2}} - v_{CO_2,eq}\right) \quad (54)$$

In the carbonator models proposed by Alonso *et al.*,[30] Rodríguez *et al.*[93] and Charitos *et al.*[149] only simple hydrodynamics and the average sorbent conversion were considered in estimating the carbonator CO_2 capture level. In the model by Alonso *et al.*,[30] the effect of the decay in sorbent conversion on the kinetic reaction rate is considered through estimation of the average surface area

that is available for the carbonation reaction. Conversely, the model by Rodríguez *et al.*[93] and Charitos *et al.*[149] assumes a fixed value for the carbonation rate constant, which was found to be similar for different limestones. Nevertheless, these models do not consider either sorbent sulphation or ash accumulation. However, the average sorbent conversion correlation used in each model can be easily adapted to account for sorbent sulphation, leading to more accurate prediction of the solid looping rates, and thus the heat requirement in the calciner.

4.3.2 Semi-predictive model with two-zone K–L hydrodynamics. Shimizu *et al.*[28] have carried out a study using a quartz fixed bed reactor with an inner diameter of 20 mm, and identified that the change in CO_2 concentration did not affect the kinetic constant (k_r = 0.025 $m^3\ mol^{-1}\ s^{-1}$) and the maximum conversion at which the reaction rate approaches zero (X_{max} = 0.3). As the reaction was found to be first order with respect to the CO_2 concentration, the following kinetic expression was proposed:

$$\frac{dX}{dt} = k_r C_{CO_2}(X_{max} - X) = k_r C_{CO_2} X_{max} \exp\left(-kC_{CO_2} t\right) \quad (55)$$

Assuming perfect mixing of solids and determining their average solid residence time in the reactor, Shimizu *et al.*[28] determined the average reaction rate as:

$$\tau = \frac{AH_D(1-\varepsilon_f)}{F_R} \quad (56)$$

$$\overline{\frac{dX}{dt}} = \int_0^\infty k_r C_{CO_2} X_{max} \exp\left(-k_r C_{CO_2} t\right)\frac{1}{\tau}\exp\left(-\frac{t}{\tau}\right)dt = \frac{k_r C_{CO_2} X_{max}}{k_r C_{CO_2}\tau + 1} \quad (57)$$

To account for BFB reactor hydrodynamics in estimating the CO_2 capture level, a two-zone model for an intermediate-sized particle by Kunii and Levenspiel (K–L)[178] was employed. The model assumes that the fluidised bed consists of bubble and emulsion regions in which the CO_2 concentration changes with height.

$$-\delta u_b{}^* \frac{dC_{CO_2,b}}{dz} = \delta K_{be}\left(C_{CO_2,b} - C_{CO_2,e}\right) + \frac{\gamma_b k_r C_{CO_2,b} X_{max}\rho_s}{M\left(k_r C_{CO_2,b}\tau + 1\right)} \quad (58)$$

$$-(1-\delta)u_{mf}\frac{dC_{CO_2,e}}{dz} = -\delta K_{be}\left(C_{CO_2,b} - C_{CO_2,e}\right) + \frac{(1-\delta)(1-\varepsilon_{mf})k_r C_{CO_2,e} X_{max}\rho_s}{M\left(k_r C_{CO_2}\tau + 1\right)} \quad (59)$$

Eqn (58) and (59) can be solved with the initial condition that $C_b = C_e = C_{in}$ at $z = 0$. The superficial gas velocity at the minimum fluidising conditions (u_{mf}) can be expressed as:

$$u_{mf} = \frac{d_p{}^2\left(\rho_s - \rho_g\right)g\varepsilon_{mf}{}^3\Phi_s{}^2}{150\mu(1-\varepsilon_{mf})} \quad (60)$$

Assuming a bubble diameter (d_b), the bubble and emulsion interchange coefficient (K_{be}) is defined as:

$$K_{be} = 4.5\left(\frac{u_{mf}}{d_b}\right) \quad (61)$$

Furthermore, the velocity of the rising bubble gas (u_b*) is determined from the bubble rise velocity (u_b), the minimum fluidisation velocity (u_{mf}) and the superficial gas velocity (u_0).

$$u_b{}^* = u_b + 3u_{mf} \quad (62)$$

$$u_b = u_0 - u_{mf} + 0.711(gd_b)^{0.5} \quad (63)$$

The last parameter required to compute CO_2 concentrations is the volume of bubbles per unit bed volume (δ) defined as:

$$\delta = \frac{u_0 - u_{mf}}{u_b + 2u_{mf}} \quad (64)$$

Finally, the average CO_2 concentration at a given bed height is represented by considering both the emulsion and the bubble zones:

$$C_{CO_2,ave,z} = \frac{\delta u_b{}^* C_{CO_2,b} + (1-\delta)u_{mf}C_{CO_2,e}}{u_0} \quad (65)$$

Using a similar approach to Shimizu *et al.*,[28] Abanades *et al.*[136] have proposed a carbonator model based on the two-zone K–L formulations for CO_2 mass balance in the emulsion and the bubble phases. However, in their model the bubble fraction is estimated as proportional to the extremes for fine and large particles defined by Kunii and Levenspiel.[179]

$$\delta = \frac{u_0 - u_{mf}}{u_b + \frac{5u_{mf} - u_b\varepsilon_{mf}}{4}} \quad (66)$$

Furthermore, the velocity of the rising bubble gas was defined based on the gas balance in the bed cross-section as:

$$u_b{}^* = \frac{u_0 - (1-\delta)u_{mf}}{\delta} \quad (67)$$

Having assumed that there were no solids in the bubble phase (γ_b = 0), and that only an active fraction of CaO (f_a), defined as the difference between the maximum carbonation conversion (X_N) and the actual conversion of CaO to $CaCO_3$ (X), reacted in the fast reaction regime, the following K–L formulations for the CO_2 mass balance in the bubble and emulsion phases were derived:

$$-\delta u_b{}^* \frac{dC_{CO_2,b}}{dz} = \delta K_{be}\left(C_{CO_2,b} - C_{CO_2,e}\right) \quad (68)$$

$$-(1-\delta)u_{mf}\frac{dC_{CO_2,e}}{dz} = -\delta K_{be}\left(C_{CO_2,b} - C_{CO_2,e}\right) + (1-\delta)(1-\varepsilon_{mf})f_a k_r C_{CO_2,e} \quad (69)$$

Similarly to Shimizu *et al.*,[28] Abanades *et al.*[136] have used eqn (61) to estimate the gas-interchange coefficient (K_{be}). Conversely, the overall reaction rate constant (k_r) was determined by considering both the kinetic- and diffusion-controlled regions of the carbonation reaction.

$$k_r = \frac{1}{\frac{d_p}{6k_g} + \frac{1}{K_{ri}}} \quad (70)$$

The mass transfer coefficient (k_g) is estimated using the Turnbull and Davidson[180] correlation for the Sherwood number (Sh)

that considers the effective CO_2 diffusivity in air, Reynolds number at minimum fluidisation conditions (Re_{mf}) and Schmidt number (Sc).

$$Sh = \frac{D_{CO_2}}{d_p k_g} = 2\varepsilon_{mf} + 0.95 Re_{mf}^{0.5} Sc^{0.3} \quad (71)$$

The carbonation rate is considered to be first order with respect to CO_2 and the mass transfer of CO_2 toward the CaO particle. It is expressed using semi-empirical eqn (72) similar to the one proposed by Bhatia and Perlmutter[169] with correction for decreasing conversion of the sorbent with number of cycles, which is calculated using eqn (4). In addition, the kinetic rate constant is a function of the conversion and is rewritten to have suitable units for the K–L model as presented in eqn (73).

$$\frac{dX}{dt} = \frac{k_s S_0}{1 - e_0} X_N (1 - X)^{\frac{2}{3}} \left(C_{CO_2} - C_{CO_2,eq}\right) \quad (72)$$

$$K_{ri} = k_s \frac{X_N S_0 \rho_{CaO}}{M_{CaO}} (1 - X)^{\frac{2}{3}} \quad (73)$$

In eqn (72) and (73), the intrinsic reaction rate constant (k_s) of 5.95×10^{-10} m^4 mol^{-1} s^{-1} was found to be independent of temperature between 400 °C and 725 °C for the CO_2 volume fraction range of 0.1–0.42. The initial surface area of fresh CaO (S_0) was 40×10^6 m^2 m^{-3} with initial porosity (e_0) of 0.5. Additionally, it was assumed that if the maximum carbonation conversion is reached, the chemical reaction rate becomes zero.

Using TGA, Li *et al.*[181] have identified that the carbonation rate was independent of temperature between 600 °C and 700 °C. Moreover, the maximum conversion of the sorbent was found to be independent of the CO_2 concentration and increased with temperature. Based on these findings, Fang *et al.*[135] proposed the following semi-empirical equation for the carbonation rate. It accounts for the effect of the total pressure on the rate of sorbent carbonation.

$$\frac{dX_N}{dt} = k_r \left(1 - \frac{X_N}{X_{max,N}}\right)^m \left(C_{CO_2} - C_{CO_2,eq}\right)^{0.083\frac{P}{P_0}} \quad (74)$$

In this model, the exponent m was equal to 2/3 for the kinetic-controlled region and 4/3 for the diffusion-controlled region of the carbonation reaction. The corresponding kinetic rate constants (k_r) were found to be 0.0025 m^3 mol^{-1} s^{-1} and 0.0021 m^3 mol^{-1} s^{-1} for kinetic- and diffusion-controlled regions, respectively.

Again, Fang *et al.*[135] proposed using the two-zone K–L model[179] to represent carbonator hydrodynamics. The model is similar to the one adapted by Abanades *et al.*,[136] with a minor change to account for the solids present in the bubbles. Assuming the volume fraction of solids dispersed in the bubbles (y_b) to be between 10^{-2} and 10^{-3}, the mass balance for the bubble phase is:

$$-\delta u_b{}^* \frac{dC_{CO_2,b}}{dz} = \delta K_{be}\left(C_{CO_2,b} - C_{CO_2,e}\right) + \delta y_b f_a K_r \left(C_{CO_2,b} - C_{CO_2,eq}\right) \quad (75)$$

The carbonation rate constant in the units suitable for the K–L model and the active fraction of CaO in the carbonation process were expressed as:

$$K_r = k_c \left(1 - \frac{X_N}{X_{max,N}}\right)^m \frac{\rho_{CaO}}{M_{CaO}} \quad (76)$$

$$f_a = X_{max,N} - X_N \quad (77)$$

Finally, the overall conversion of CO_2 in the reactor was estimated as the average concentration in the emulsion and the bubble phase.

$$X_{CO_2,exit} = 1 - \frac{\delta u_b{}^* C_{CO_2,b,exit} + (1 - \delta) u_{mf} C_{CO_2,e,exit}}{u_0 C_{CO_2,in}} \quad (78)$$

Although the model by Shimizu *et al.*[28] provided a good representation of the CO_2 capture level in the carbonator, several improvements could be made to enhance prediction accuracy. In the model developed by Abanades *et al.*,[136] a semi-empirical correlation was used to determine sorbent deactivation with the number of carbonation–calcination cycles, which substituted the fixed conversion value after four cycles used by Shimizu *et al.*[28] Moreover, the overall kinetic rate constant defined by the model by Abanades *et al.*[136] accounted for both the chemical reaction rate and the mass transfer rate, resulting in a further improvement in prediction accuracy. A further improvement in the semi-predictive carbonator model was achieved by Fang *et al.*[135] whose model is capable of predicting process performance separately in the chemically- and diffusion-controlled regions of the carbonation reaction. Unfortunately, these semi-predictive models do not account for sorbent sulphation and ash accumulation in the system and this may cause under-estimation of the solids looping rates and, thus the heat requirement in the calciner.

4.3.3 Semi-predictive model with three-zone K–L hydrodynamics. Romano[84] has developed a model for a CFB carbonator by combining the improved three-zone K–L model[182,183] with the maximum conversion expression proposed by Grasa and Abanades[143] and the carbonation kinetics developed by Grasa *et al.*[171] The model developed by Romano[84] is the first one that accounts for the impact of sulphation on average sorbent conversion. This is achieved through estimation of the decay constant and the residual sorbent conversion by fitting eqn (4) to the experimental data from Grasa *et al.*[153]

In the carbonator model, the uniform riser temperature, particle size distribution and superficial velocity were assumed, along with no gas-side mass transfer resistance and perfect solid mixing. The model considered two statistical distributions. The first determines the carbonation–calcination cycle number that a given particle has already experienced using the correlations provided by Abanades[145] and Rodríguez *et al.*[11] These, in combination of the maximum sorbent conversion correlation by Grasa and Abanades[143] with fitting parameters adjusted to consider sulphation, allow determining the maximum average sorbent conversion. The second characterises the fraction of particles of a given residence time in the carbonator, for which the average residence time is defined as in the model by Alonso *et al.*[30] The active solid inventory is

defined in eqn (80) to account for sulphation and ash accumulation effects.

$$f_t = \frac{1}{\tau}\exp\left(-\frac{t}{\tau}\right) \quad (79)$$

$$N_{Ca} = \frac{W_s}{M_s}\left(1 - x_{ash} - x_{CaSO_4}\right) \quad (80)$$

The actual average conversion of the sorbent for a given CO_2 concentration (C_{CO_2}*) and the average carbonation level are determined as:

$$X_{ave} = \sum_{N_{age}=1}^{\infty} r_{N_{age}} \int_0^{\infty} f_t X\left(t, N, C_{CO_2}{}^*\right) dt \quad (81)$$

$$f_{carb} = \frac{X_{ave}}{X_{max,ave}} \quad (82)$$

Using the same approach, the average kinetic constant in suitable units for the K–L model is computed as:

$$K_{ri,ave} = \frac{\rho_s}{M_s} \sum_{N_{age}=1}^{\infty} r_{N_{age}} \int_0^{\infty} f_t k_s S_N \left[1 - X\left(t, N, C_{CO_2}{}^*\right)\right]^{\frac{2}{3}} dt \quad (83)$$

The CO_2 capture level in the carbonator model is then separately calculated from the carbonator mass balance and the K–L model:

$$E_{carb} = \frac{F_R X_{ave}}{F_{CO_2}} = \frac{F_{CO_2} - V_{g,out} C_{CO_2,out}}{F_{CO_2}} \quad (84)$$

Since both the actual average conversion determined using eqn (81) and the outlet CO_2 concentration computed using the K–L model with the average kinetic constant estimated in eqn (83) depend on C_{CO_2}*, the model is solved in an iterative process by varying C_{CO_2}* until eqn (84) is satisfied. This approach was found to reliably predict the performance of the carbonator reactor for the INCAR-CSIC and IFK test units.

The model developed recently by Romano[84] is the most advanced carbonator semi-predictive model available currently as it considers the effect of reactor hydrodynamics on the CO_2 capture level, reaction kinetics, the influence of sulphation on sorbent conversion and ash accumulation. Although it does not consider the diffusion region of the carbonation process, this region is usually neglected in industrial applications, to allow for a compact design of the CFB reactor.[84,145]

4.4 Calciner reactor modelling

4.4.1 Semi-predictive model with simple hydrodynamics. Martínez *et al.*[134] have proposed a model to predict the performance of the calcination process that is based on the steady-state overall mass balance of the calciner.

$$F_{CO_2,calc} = N_{Ca} \cdot r_{calc} = (F_{Ca} + F_0)(X_{carb,ave} - X_{calc}) \quad (85)$$

The average $CaCO_3$ content in the total flow entering the calciner ($X_{carb,ave}$) is determined based on solid flow from the carbonator (F_{ca}) and fresh limestone make-up (F_0). The kinetic rate of the calcination reaction was developed in the earlier work by Martínez *et al.*[184] It was based on the grain model and is similar to the calciner model by Fang *et al.*[135]

$$\frac{d(X_{carb} - X_{calc})}{dt} = k_{calc}\left(1 - \frac{X_{carb} - X_{calc}}{X_{carb}}\right)^{\frac{2}{3}}\left(C_{CO_2,eq} - C_{CO_2}\right) \quad (86)$$

The time required for complete calcination can be determined by integrating eqn (86).

$$t_{calc}{}^* = \frac{3 \cdot X_{carb}}{k_{calc}\left(C_{CO_2,eq} - C_{CO_2}\right)} \quad (87)$$

Martínez *et al.*[184] determined that the calcination rate is constant and independent of the $CaCO_3$ content in the particle. Therefore, the average calcination rate was expressed as:

$$r_{calc} = \begin{cases} \dfrac{X_{carb,ave}}{t_{calc}{}^*} = \dfrac{k_{calc}\left(C_{CO_2,eq} - C_{CO_2}\right)}{3} & \text{for } t < t_{calc}{}^* \\ 0 & \text{for } t \geq t_{calc}{}^* \end{cases} \quad (88)$$

Based on the assumption that the solid phase in the calciner is perfectly mixed and considering the average particle residence time in the calciner, the fraction of particles that has a residence time lower than the time required for complete calcination can be estimated as:

$$f_a = 1 - \exp\left(-\frac{t_{calc}{}^*}{\tau}\right) \quad (89)$$

$$\tau = \frac{N_{Ca}}{F_{Ca} + F_0} \quad (90)$$

Using these definitions, the amount of $CaCO_3$ that disappeared from the solid phase and the amount of CO_2 released in the calciner are given as:

$$(F_{Ca} + F_0)\left(X_{carb,ave} - X_{calc}\right) = (F_{Ca} + F_0) X_{carb,ave} \frac{f_a}{\ln\left[\frac{1}{1 - f_a}\right]} \quad (91)$$

$$N_{Ca} \cdot r_{calc} = N_{Ca} \cdot f_a \cdot \frac{k_{calc}\left(C_{CO_2,eq} - C_{CO_2}\right)}{3} \quad (92)$$

Finally, the efficiency of the calciner (E_{calc}) can be estimated as:

$$E_{calc} = \frac{X_{carb} - X_{calc}}{X_{carb}} = \frac{f_a}{\ln\left[\frac{1}{1 - f_a}\right]} \quad (93)$$

To solve the model an approach similar to the one proposed by Romano[84] needs to be applied. Namely, the value of the C_{CO_2} concentration for which eqn (85) will be satisfied needs to be found in an iterative process.

The calciner semi-predictive model proposed by Martínez *et al.*,[134] has the same level of complexity as the carbonator semi-predictive model by Alonso *et al.*[30] Therefore, these models should be used together to represent CaL performance. The model has the same disadvantages that it does not consider sorbent sulphation and ash accumulation in the system.

4.4.2 Semi-predictive model with two-zone K–L hydrodynamics. As for the carbonator model, Fang *et al.*[135] used experimental data generated by Li *et al.*[181] to develop an apparent kinetic model for the calcination reaction.

$$\frac{dX_{calc}}{dt} = k_{calc}(1 - X_{calc})^{\frac{2}{3}}\left(C_{CO_{2,eq}} - C_{CO_2}\right) \quad (94)$$

The TGA conducted under 90% CO_2 revealed that conversion during the calcination process is inhibited by both temperature and CO_2 concentration. Therefore, the calcination rate constant (k_{calc}) was given in the Arrhenius equation form with the pre-exponential factor ($k_{0,calc}$) of 23 797 and the activation energy (E_a) of 150 kJ mol^{-1}.

Unlike other calciner models, the model proposed by Fang *et al.*[135] accounted for the reactor hydrodynamics using the same K–L model[179] as presented for the carbonator model. In this model, the calcination rate constant and the fraction of $CaCO_3$ that was not regenerated in the calcination stage are represented as:

$$k_r = k_{calc}(1 - X_{calc})^{\frac{2}{3}}\frac{\rho_{CaCO_3}}{M_{CaCO_3}} \quad (95)$$

$$f_a = (1 - X_{calc})X_{max} \quad (96)$$

The semi-predictive model for the calciner proposed by Fang *et al.*[135] provides an enhanced prediction of process performance over the model by Martínez *et al.*,[134] as it considers the detailed hydrodynamics of the reactor. Moreover, the model takes both the chemically- and diffusion-controlled regions into account. However, no correlation was made with sorbent sulphation and ash accumulation in the system, which appears to be the common issue in the process models reviewed here.

4.4.3 Predictive model with CFD hydrodynamics. Ylätalo *et al.*[150] have adapted the CFB3D model code developed by Myöhänen *et al.*[185] to model a three-dimensional oxy-fired calciner reactor (Fig. 19). The calcination reaction rate is expressed using the kinetic constant provided by Silcox *et al.*[186] and the CO_2 equilibrium pressure by Barin.[187]

$$r_{calc} = 1.22 \cdot \exp\left(-\frac{4026}{T}\right) S_m M_{CaCO_3}\left(p_{CO_{2,eq}} - p_{CO_2}\right) \quad (97)$$

The model included detailed modelling of sulphation in the calciner using the correlations developed by Myöhänen *et al.*[185] that account for the specific reaction surface area ($S_{m,i}$) of component i.

$$r_{sulf} = 0.001\exp\left(-\frac{2400}{T}\right)\exp\left(-8X_{CaSO_4}\right)C_{SO_2}C_{O_2}S_{m,CaO}M_{CaO} \quad (98)$$

$$r_{dir,sulf} = 0.01\exp\left(-\frac{3031}{T}\right)C_{SO_2}^{0.9}C_{CO_2}^{-0.75}C_{SO_2}^{0.001}S_{m,CaCO_3}M_{CaCO_3} \quad (99)$$

$$r_{de\text{-}sulf} = 0.005\exp\left(-\frac{10\,000}{T}\right)C_{CO}S_{m,CaSO_4}M_{CaSO_4} \quad (100)$$

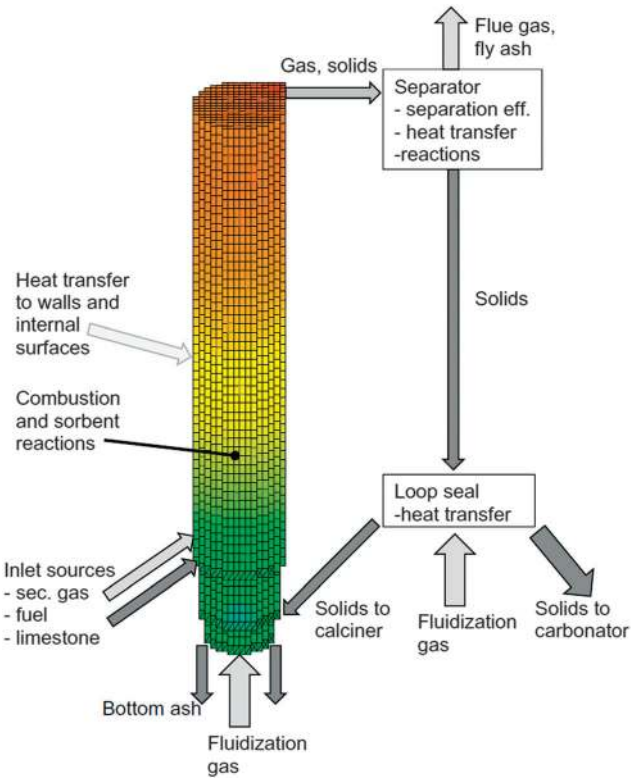

Fig. 19 Three-dimensional CFB calciner model frame (reprinted with permission from Ylätalo *et al.*[150] Copyright 2015 Elsevier).

In contrast to the calciner models presented previously, the CFD model proposed by Ylätalo *et al.*[150] provides detailed information on how sulphation and sorbent properties could affect the calciner performance. Although more demanding computationally, such models will deliver more reliable predictions of calciner operating conditions as they are capable of predicting the temperature and the solids distribution across the reactor. Not only could the CFD models be used to reliably predict and/or optimise performance of the CFB reactor, they can be integrated into the process-wide simulation. Recently, Atsonios *et al.*[188] have proposed to use the CFD model to generate information on CFB hydrodynamics (carbonator and calciner) and CO_2 distribution in the bed (calciner), which is then fed to the carbonator and the calciner kinetic models in the process simulation.

4.5 Summary

The review of the carbonator reactor models undertaken in this section revealed that there are several approaches available in the open literature. However, some of the assumptions or formulations behind these models impose important limitations that may affect the accuracy of their predictions.

The review findings show that five main complexity levels can be distinguished (Fig. 20). Models in the first level are based on first principles, energy and material conservation laws. At an early stage of concept development, which could include uncertainties related to process operating conditions

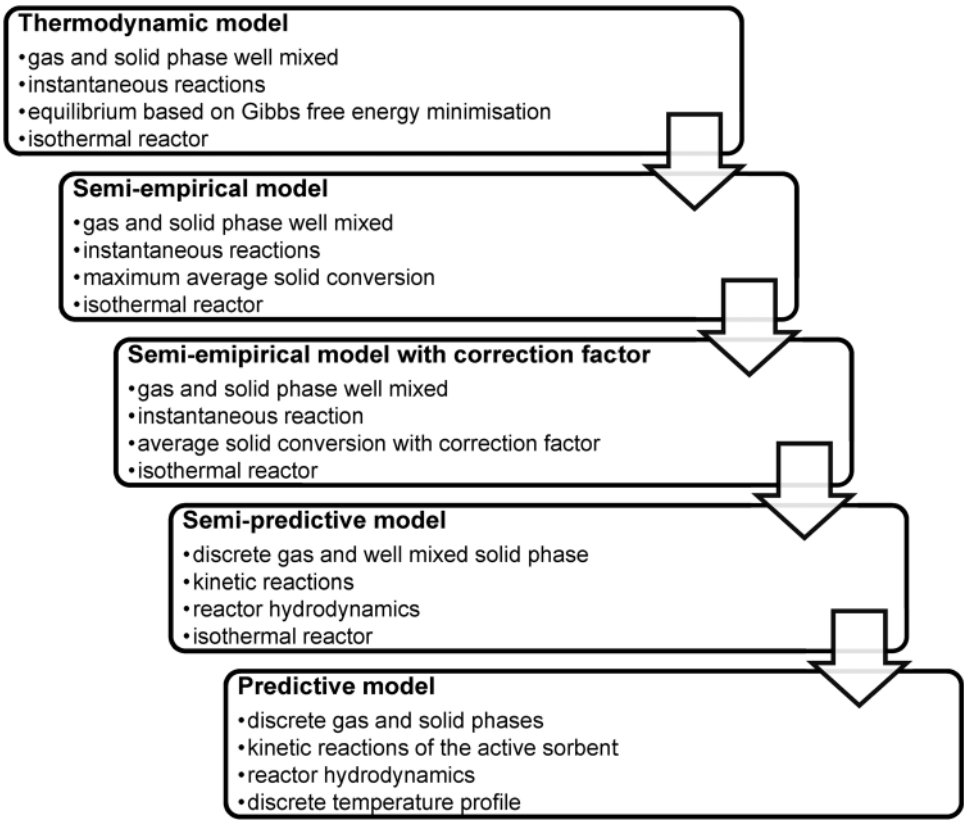

Fig. 20 Different levels of calcium looping model complexity.

and/or sorbent properties, thermodynamic models would perform well and could be used to estimate performance limited by equilibrium. The greatest limitation of such models is lack of correlation to the physical size of the reactor and the assumption of instantaneous reactions. Additionally, in most cases the equilibrium composition in the reactor, hence the sorbent conversion, is based on minimisation of Gibbs' free energy at specified operating conditions and does not depend on what happens upstream of the unit.

The last limitation of the thermodynamic models is partially eliminated in the semi-empirical models, which allow determination of the maximum average sorbent conversion depending on the solid looping rate and fresh sorbent make-up rate, as well as carbonator and calciner performance.[11,39,139] These models, however, assume that the sorbent achieves its maximum average conversion under certain operating conditions, predicting actual reactor performance close to equilibrium performance. Although the results from experimental trials using the 1.7 MW_{th} pilot plant at INCAR-CSIC showed that this assumption is valid for systems operating with high sorbent conversions, which require high fresh sorbent make-up rates, systems operating with low average conversions achieve around 60–90% of equilibrium performance (Fig. 21).

To improve model accuracy, actual average sorbent conversion is determined by applying a correction factor to the maximum average sorbent conversion in the third level models. This factor can be either assumed,[133,146] as presented in Section 5, or calculated based on the actual and average residence times of the sorbent in the reactor.[30,134] The latter approach greatly enhances model prediction as the determined correction factor accounts for the solid inventory and the reaction kinetics in the reactor.

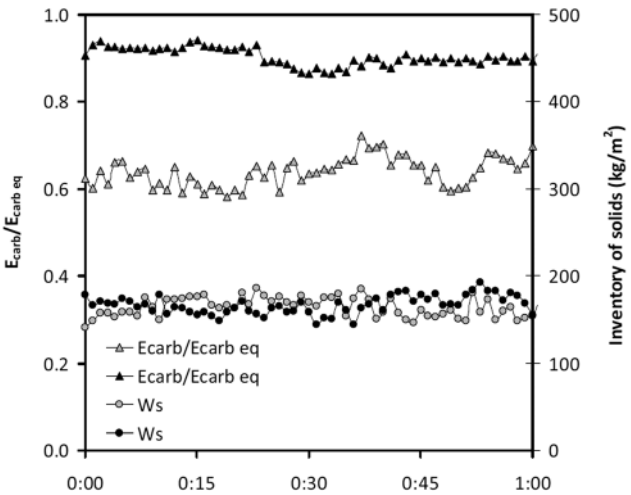

Fig. 21 Comparison of the actual and the equilibrium performance of 1.7 MW_{th} pilot plant at INCAR-CSIC operating at carbonator temperature of 660–690 °C with X_{ave} = 0.11 (grey) and X_{ave} = 0.21 (black) (reprinted with permission from Arias *et al.*[96] Copyright 2015 Elsevier).

The fourth level is achieved through a detailed consideration of reaction kinetics and hydrodynamics in determining the

performance of the reactor. Most of the semi-predictive models developed to predict the performance of the calciner[135] and the carbonator[28,84,135,136] used the hydrodynamic formulations developed by Kunii and Levenspiel,[178,179,182,183] which offer an analytical solution. This approach improves the prediction as the gas concentration depends on the operating conditions and location in the reactor, as well as the sorbent properties. A number of parameters in the K–L model need to be specified, but their values have not been substantiated experimentally and could affect the accuracy of the model.

This, and other assumptions such as isothermal operation and well-mixed solid phase, can be eliminated by applying the predictive models that combine industrial CFD codes with experimentally-determined reaction kinetics to evaluate the reactor[150,189] or the whole CaL plant[188] performance. Such models are the most complex and, therefore, computationally demanding. Although predictive models give the closest representation of the CaL process, they are not applicable at the early stage of concept design because any change in the process design would be followed by a long simulation period required to assess the impact of that change.

In addition to presenting the current approaches for modelling of the CaL processes and identifying their limitations, this review has identified that neither sorbent sulphation nor ash accumulation are widely considered in the models currently developed. The only models accounting for sorbent sulphation were the carbonator model by Romano[84] and the calciner model by Ylätalo *et al.*[150] described in Sections 4.3.3 and 4.4.3, respectively. Although it was claimed by Abanades *et al.*[136] that sorbent sulphation will have a minor effect on carbonation, the experimental analysis by Grasa *et al.*[153] suggests that even a change in the sulphation level of 0.5% in each cycle affects the sorbent decay curve (Fig. 22).

Despite the fact that ash presence in the system would increase the inert solid looping rate and the bed inventory required to achieve a given CO_2 capture efficiency, the effect of ash accumulation in the system was only included in the model by Romano.[84] Moreover, none of the reviewed models account for sorbent attrition and fragmentation, which was identified as another challenge of the CaL process.[13] Therefore, in addition to the sulphation effect on sorbent performance and ash accumulation, loss of sorbent due to attrition and fragmentation should also be considered in the future modelling attempts. This can be done, for example, by implementing the semi-empirical model for sorbent attrition developed by Fennell *et al.*[190] or by adapting the semi-detailed model developed for coal fragmentation by Senneca *et al.*[191]

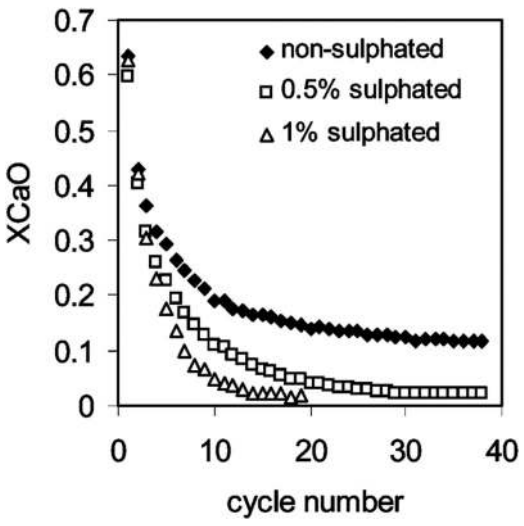

Fig. 22 Decay in the carbonation conversion with the number of carbonation–calcination cycles under different sulphation conversions (reprinted with permission from Grasa *et al.*[153] Copyright 2015 American Chemical Society).

5 Integration of calcium looping to power plants

A key reason for development of computational models for CO_2 capture processes is the ease with which they can be used to analyse retrofit scenarios of existing power plants, or to develop novel concepts for cleaner power generation systems. Models can be a cost-efficient complement to experimental trials of a particular system design under various operating conditions. The greatest advantage of using computational models is the ease of conducting a process-wide analysis for determining optimal overall process performance by indicating the possible integration points.

Since 1999, when the CaL integration was proposed as a viable option for CO_2 capture from CFPPs,[28] a number of studies have investigated different aspects of process integration aiming at improvement of the overall process performance. These included enhancement of process integration through heat exchange network analyses and reduction of CaL process energy requirements through implementation of alternative configurations. The applicability of the CaL process for CO_2 capture from combined cycle power plants was also investigated.

The greatest disadvantage of conventional CO_2 capture systems is a relatively high projected efficiency penalty leading to increased fuel consumption and cost. This section reviews process integration and conceptual studies to quantify efficiency penalties in CFPPs and combined cycle power plants. In addition, the modelling approach for both the power cycle and the CaL process are identified and limitations are analysed to provide a guide for further modelling attempts.

5.1 Conventional coal-fired power plants

5.1.1 Feasibility study for calcium looping for conventional power generation systems. A conceptual study by Shimizu *et al.*[28] analysed the impact of CaL plant integration on a supercritical CFPP. High-pressure steam generated in air-combustion of bituminous coal was used to generate electricity in the primary steam cycle, which operates with gross thermal efficiency of 46.6%$_{HHV}$. Flue gas was treated in the CaL plant with the carbonator operating at 650 °C and the calciner operating at 950 °C with 100% efficiency. The performance of the carbonation process was predicted using the carbonator model described in Section 4.3.2.

With a Ca : C ratio of 8.29, which is slightly smaller than values reported in the pilot-plant tests, and average conversion of 11%, CO_2 capture of 83% was reached in the carbonator, leading to an overall CO_2 capture level of 90.4%. The waste heat in the CaL plant was recovered to produce superheated and reheated steam at subcritical conditions of 172.25 bar/566 °C and 30.4 bar/538 °C, respectively. The gross thermal efficiency of the secondary steam cycle was assumed to be 42.6%$_{HHV}$. With the gross and net power outputs of the integrated system of 1000 MW_{el} and 817 MW_{el}, respectively, the net efficiency was estimated to be 33.4%$_{HHV}$. This was 1.4% points higher than for an oxy-fired combustor with a primary steam cycle of the same gross power output and thus indicated feasibility of the CaL process for reducing CO_2 emissions from the CFPPs.

Unfortunately, Shimizu *et al.*[28] provided no benchmark to the reference CFPP without CO_2 capture plant, which would provide insight into how the retrofit affected the overall performance of the system. Also, sorbent decay was ignored as only four carbonation–calcination cycles were considered in determining sorbent conversion. Furthermore, the performance of both steam cycles was assumed rather than estimated using thermodynamic calculation or process simulation. Although this assumption could be valid for a CFPP operating at a fixed load, it does not allow prediction of part-load operation without knowledge of the gross efficiency correlation. Additionally, by assuming the gross thermal efficiency, the analysis did not account for the power consumption of the CFPP auxiliary equipment, with only ASU and CO_2 compression unit (CCU) considered in estimation of the net thermal efficiency. The power requirements for the CFPP and the CaL plant auxiliary equipment need to be considered to improve the prediction reliability and avoid over-estimating the net thermal efficiency of the integrated system.

5.1.2 Heat integration with the primary and secondary steam cycle. High-temperature operation of the CaL process allows recovering high-grade heat to produce an additional amount of steam. Therefore, there are two options for integrating the CaL process with the existing CFPPs: steam can be utilised either in the primary steam cycle with the assumption that the steam generation rate in the boiler is reduced and the gross power output of the integrated system kept constant, or in the secondary steam cycle leading to higher gross power output. Yang *et al.*[16] investigated both integration options. In the first case, the CaL plant was integrated with the primary steam cycle of an existing 600 MW_{el} CFPP operating with net thermal efficiency of 40.6%$_{LHV}$. Performance of a carbonator operated at 650 °C was represented using the correlation by Abanades *et al.*,[145] with a maximum conversion of 20% to reach 85% CO_2 capture level at Ca : C ratio of 5. It needs to be highlighted that compared to the Ca : C values reported in the pilot-plant tests reviewed in Section 3, the assumed Ca : C ratio is 1.5–3 times lower. This would cause underestimation of the solid looping rate and thus, heat requirement in the calciner. In this study, the calciner was operated at 900 °C and heat for sorbent regeneration was provided through oxy-combustion of coal. The parasitic load stemmed only from the ASU power requirement as no CCU was considered.

Yang *et al.*[16] first proposed using heat in the CaL system to substitute the feedwater heating train in the primary steam cycle. Although this is a valid approach for integrated systems, which has been often proposed for integration of amine-based CO_2 capture plants,[60,73,192–194] its applicability to existing CFPPs could be limited by the swallowing capacity of the steam turbines and/or the electric generator. Moreover, the suggestion by Yang *et al.*[16] that these extractions reduce the thermal efficiency of CFPPs is invalid from the thermodynamic point of view, as they increase the average temperature of heat addition in the boiler leading to an increase in thermal efficiency.[195] Yet, the indicated power output increase of 148.8 MW_{el} and increase in the net thermal efficiency from 19.4%$_{LHV}$ to 25.3%$_{LHV}$, which stems from a higher degree of waste heat utilisation in the integrated system leading to minimisation of steam extractions, could not be achievable in reality due to operational limitations of the existing system. In another integration option, part of the boiler heat load was replaced by heat load from the CaL plant. The boiler in the CaL plant can provide 43.1% of the heat required by the system to operate with gross power output of 600 MW_{el} and net thermal efficiency of 34.1%$_{LHV}$. However, a further study on how such off-design operation conditions would affect the boiler performance needs to be conducted. Furthermore, in evaluating other integration options, the highest net thermal efficiency of 36.8%$_{LHV}$ and gross power output of 1000 MW_{el} were reached when the waste heat from the CaL plant was utilised to generate high-pressure steam to drive the secondary steam cycle. This result revealed that implementation of a secondary steam cycle and its integration with the CaL plant provides superior performance compared to the other CFPP integration options. This is also beneficial in terms of long-term revenue and meeting market demand. However, the estimated minimum net efficiency penalty of 3.8% points (excluding power requirement for CO_2 compression) may not be a representative result, due to low Ca : C ratio assumed in the carbonator.

In addition to evaluating different integration options, the effect of CaL integration to CFPPs operating with different steam conditions was investigated. Martínez *et al.*[83] analysed integration of a CaL plant to an existing 350 MW_{el} subcritical CFPP with net efficiency of 36%$_{LHV}$. The flue gas leaving the boiler, which contained 14.5%$_{vol}$ CO_2, was desulphurised and then entered the CaL plant at typical stack conditions (1.16 bar/180 °C). Performance of the carbonator, which was operated at 650 °C, was represented using the model proposed by Alonso *et al.*[30] described in Section 4.3.1 with the kinetic expression proposed by Grasa *et al.*[196] The sorbent was regenerated in the calciner operating at 950 °C and complete calcination was assumed. The temperature in the calciner was maintained through oxy-combustion of South African coal. Even though this coal contains a relatively small amount of sulphur and the flue gas was desulphurised, an additional amount of $CaCO_3$ (F_{Ca}/F_S = 3) was provided with the make-up stream to account for sorbent sulphation losses. Moreover, part of the captured CO_2 was recycled to maintain the O_2 concentration in the oxidizing gas at 25%$_{mol}$.

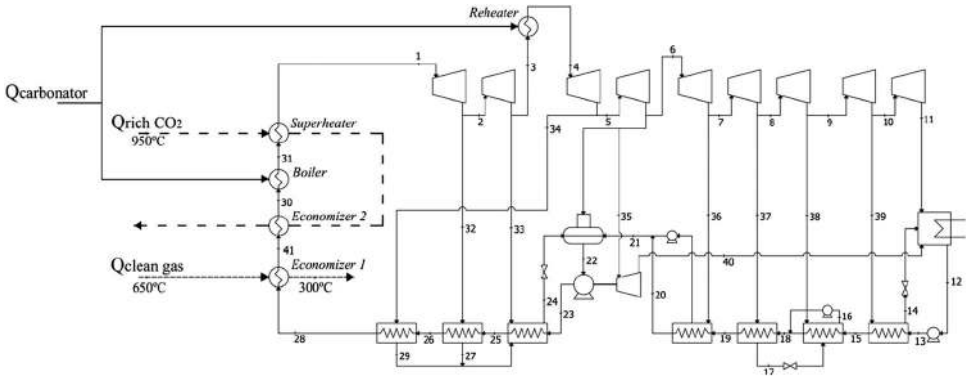

Fig. 23 Reference integration configuration for the CaL plant and supercritical steam cycle (reprinted with permission from Martínez *et al.*[83] Copyright 2015 John Wiley and Sons).

Heat in the carbonator, the clean gas stream and the CO_2 stream was used to generate steam to run the secondary steam cycle (Fig. 23), the gross thermal efficiency of which was assumed to be 45%$_{LHV}$. After deducting the auxiliary power consumption of the plant, the net thermal efficiency was 36%$_{LHV}$. By adjusting the solid circulation rate, the CO_2 capture level in the carbonator was maintained at 70–90%, leading to maximum net thermal efficiency of 33.1%$_{LHV}$–33.4%$_{LHV}$. Although an increase in the CO_2 capture level required higher solid circulation rates, the increase in steam generation exceeded the increased heat requirement in the calciner leading to a rise in net thermal efficiency. The make-up rate was found to be a critical parameter as its increase led to reduction in net thermal efficiency, since more heat was required for fresh sorbent preheating. However, operation at low make-up rates would result in low conversion of the sorbent and thus high circulation rates requiring a larger reactor. Nevertheless, the viability of a CaL plant for subcritical CFPPs, for which the projected efficiency penalties ranged between 8.3% and 10.3% points, has been confirmed. Interestingly, if part of the spent sorbent was utilised in the cement plant as raw material, the amount of energy required for sorbent calcination was not accounted for in the net thermal efficiency calculation, leading to efficiency penalties between 7.5% and 9% points. The study clearly showed that this retrofit would be beneficial for the existing fleet of subcritical power plants, increasing their life span and environmental performance without a drastic net thermal efficiency drop, as is the case for conventional CO_2 capture plants. Nevertheless, performance of the steam cycle, ASU and CCU is determined based on assumed performance indicators that may not be valid for part-load operation. Also, Martínez *et al.*[37] benchmarked the performance of the integrated system against a hypothetical system rather than an existing power plant, which results in misleading conclusions regarding the projected efficiency penalty imposed on the retrofitted system. The performance of an integrated system should be benchmarked against the performance of an existing system to identify the net effect of the CaL plant integration.

Romeo *et al.*[86] have investigated the integration of a secondary supercritical steam cycle (280 bar/600 °C/600 °C) with a CaL plant retrofitted to an existing 450 MW_{el} supercritical CFPP. In the CaL plant design, the temperatures in the carbonator and the calciner were kept at 650 °C and 875 °C, respectively. The performance of the system was represented by assuming 5% purge leading to average sorbent conversion of about 20%. Heat for sorbent recovery was added through combustion of low-sulphur high-rank coal in pure O_2-stream produced in the ASU with specific power of 220 kW h per t-O_2. Romeo *et al.*[86] claimed that no CO_2 recirculation was needed to control the temperature in the calciner because of the large solid inflow at 650 °C and the endothermic character of the calcination reaction. Despite the fact that the pure O_2 stream will be diluted by CO_2 liberated in the calcination reaction, the local temperature of coal particles can be higher than the average bed temperature due to their combustion in a high-O_2-concentration environment.[197,198] Such high temperatures can lead to local hot spots in the calciner on contact of the coal and sorbent particles and cause enhanced sintering and, thus deactivation of the sorbent.[199]

Analysing the CaL process, Romeo *et al.*[86] have proposed an integration configuration comprising five heat integration zones, in which waste heat from the carbonator, CO_2 stream, clean gas stream and purge stream were utilised to generate live and reheated steam, as well as to preheat the feedwater. The secondary supercritical steam cycle driven by heat recovered in the CaL plant generated an additional 193.6 MW_{el} of net power output with net efficiency of 26.7%$_{LHV}$. Although this increased the net power output of the integrated system by 45.3%, the net thermal efficiency dropped by 7.9% points, from 44.9%$_{LHV}$ for the reference CFPP to 37.0%$_{LHV}$ for the integrated system.

Further improvement of the integrated system efficiency can be reached through development of integration schemes characterised with higher heat utilisation levels using a systematic HEN analysis, which is commonly applied in different industries. Such analysis has been used by Lara *et al.*[200,201] to design the heat recovery system for waste heat recovery from the CaL plant, which captures CO_2 from a 500 MW_{el} CFPP with net thermal efficiency of 38.2%$_{LHV}$, to generate steam to drive the secondary steam cycle (290 bar/600 °C/620 °C). Unfortunately, no information was provided on the assumptions made to assess the performance of the carbonator and the calciner.

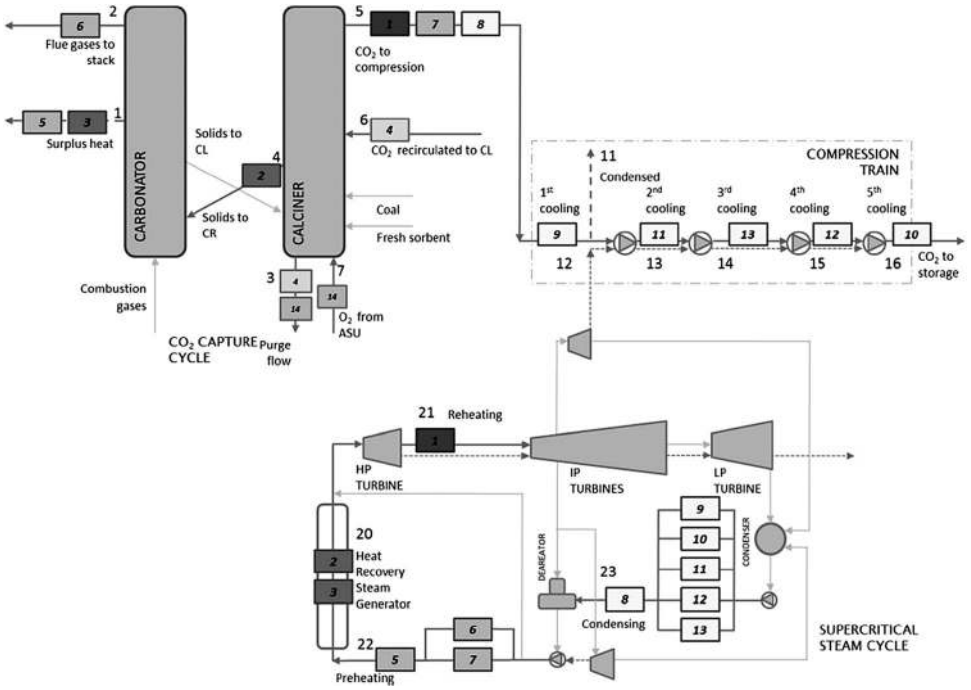

Fig. 24 Economically favourable heat exchanger network design for CaL integration (reprinted with permission from Lara *et al.*[200] Copyright 2015 Elsevier).

Among different HEN configurations proposed, the economically favoured configuration was reached when the streams were matched in such a way that they were exhausted in a single heat exchanger (Fig. 24). This configuration resulted in a net thermal efficiency increase of 0.2% points[201] and 1.2% points.[200]

In contrast to most previous studies, Vorrias *et al.*[132] have investigated integration of a CaL plant to a lignite-fired power plant (235.4 bar/540 °C/540 °C) that delivers 330 MW_{el} of gross power output with net thermal efficiency of 39.1%$_{LHV}$. In this study the conventional CaL plant configuration, which comprises the carbonator and the calciner reactors interconnected with solid lines and operating at 650 °C and 900 °C, respectively, was used. Having assumed that the carbonation reaction reached chemical equilibrium, sorbent conversion in the carbonator was represented using the maximum average conversion model by Abanades *et al.*[39] without the correction factor. The performance of the calciner was represented using the chemical and phase equilibrium through the Gibbs' free energy minimization at a given temperature. Also, the heat for sorbent regeneration is provided through oxy-combustion of lignite in an oxidizing medium containing 80%$_{vol}$ O_2. Although Vorrias *et al.*[132] claimed that this concentration was sufficient to avoid hot spots in the calciner that would increase the sorbent sintering rate, experimental and other modelling trials[33,98,100,104,133] suggested that the O_2 concentration should be below 50%$_{vol}$ to avoid hot-spots in the reactor and thus excessive degradation of the sorbent performance.

Further, to utilise high-grade heat to generate additional steam to run the secondary supercritical steam cycle (235.4 bar/540 °C/540 °C), Vorrias *et al.*[132] proposed to integrate two systems for increased heat utilisation in the CaL plant. The first is a solid recirculation heat exchanger which is proposed to be a set of concentric L-valves as illustrated in Fig. 25a. It is assumed that the system performs as a co-current heat exchanger with a temperature approach of 10 °C. However, the performance of such a system at a large scale has not yet been demonstrated. Moreover, as lignite consists of a considerable amount of moisture (36.8%$_{wt}$), oxy-combustion performance would be affected. Therefore, the second system, a BFB lignite dryer (Fig. 25b) which uses recompressed water vapour as a fluidising medium, was proposed to reduce the moisture content in lignite to 12%$_{wt}$, comparable to the average moisture content of hard coal.[202]

Analysis of the overall process performance revealed that the net thermal efficiency of the integrated system reached 34.1%$_{LHV}$ if both the solid–solid heat exchanger and the BFB lignite dryer were implemented. This falls to 34.0%$_{LHV}$ and 32.5%$_{LHV}$, respectively, if only the first or second system is implemented. Nevertheless, the net projected efficiency penalty imposed on integration of the CaL plant reached the lowest value of 5.0% points, which is considerably lower than in previous studies. It is not known if such improvement results from implementing the proposed systems or using no correction factor to determine the actual average sorbent conversion and high O_2 concentration in the oxidising medium. The net projected efficiency penalty due to CaL plant integration was found to be 2.9% points lower than for a corresponding MEA plant, but only 0.9% points lower for an oxy-fuel lignite-fired power plant.

5.1.3 Alternative configurations for efficiency improvement. Although most studies of the CaL process focus on the conventional process configuration proposed by Shimizu,[28] other configurations, which aim to improve the overall process efficiency mainly through reduction of the O_2 requirement, were proposed by Abanades *et al.*[39] and Martínez *et al.*[133]

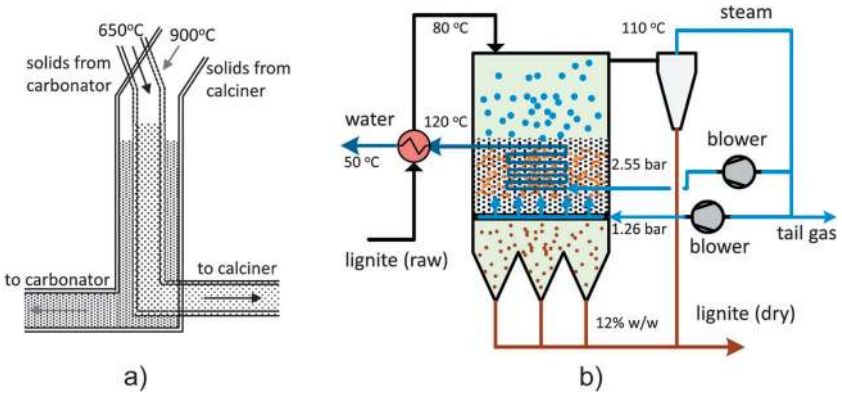

Fig. 25 Design of (a) solid–solid heat exchanger and (b) lignite bubbling fluidised bed dryer (reprinted with permission from Vorrias *et al.*[132] Copyright 2015 Elsevier).

In the first study proposing alternative configurations for efficiency improvement, Abanades *et al.*[39] investigated integration of a 100 MW_{el} supercritical CFPP with an assumed net thermal efficiency of 46%$_{LHV}$. In the basic configuration, the flue gas was treated in the carbonator operated at 650 °C, the performance of which is modelled using eqn (8) and (9). A complete sorbent regeneration was conducted at 950 °C using oxy-combustion of coal. In addition, the overall CO_2 capture level was assumed to be 90% and the captured CO_2 was compressed to 100 bar prior to being transported. Considering the power requirement to run the CCU and the ASU, the efficiency of the integrated system dropped by 7.2% points, to 38.8%.

As the efficiency penalty in the CaL process stems mainly from the O_2 production for oxy-fuel combustion in the calciner, Abanades *et al.*[39] have proposed an alternative calciner design in which the heat for the sorbent regeneration is supplied through the metallic walls from an external source (Fig. 26). Their study assumed that the heat source is a fluidised bed combustor fuelled with an air and fuel mixture that operates at 1050 °C. Steam is used as a fluidising medium in the calciner operated at 850 °C, leading to a CO_2 partial pressure of 0.4 bar. Although this configuration would be characterised by higher thermal efficiency and no requirement for O_2 production, it would require materials that have not yet been tested in practice. Also, a close integration of the combustor and the calciner is required, as a considerable heat transfer area of 800 m^2 is required. Despite the engineering challenges, this configuration was reported to have a net thermal efficiency of 39.4%, resulting in a projected efficiency penalty of 6.6% points. This is 1.6% points less than for the basic configuration.

To avoid application of untested materials, Abanades *et al.*[39] proposed that the heat requirement of the calcination reaction could be satisfied using a solid heat carrier (Fig. 27). In this configuration, CO_2 partial pressure of 0.4 bar, which is required to lower the calcination temperature to 850 °C, is achieved through utilisation of a vacuum. The process involves a common

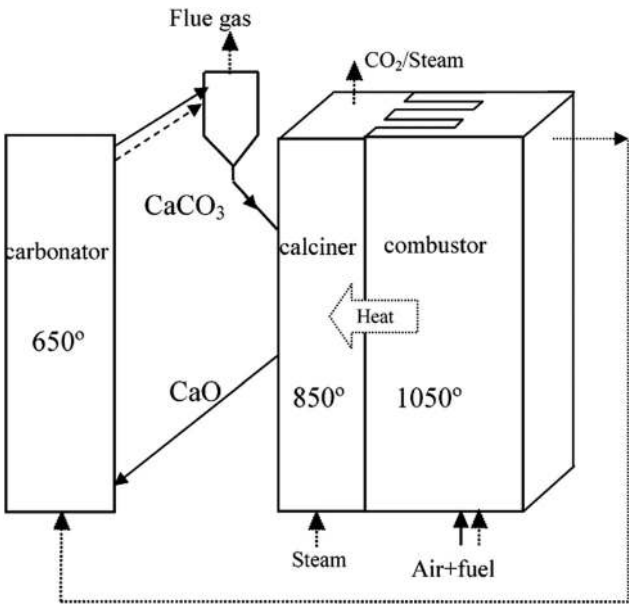

Fig. 26 Heat transfer-integrated calciner and combustor (reprinted with permission from Abanades *et al.*[39] Copyright 2015 American Chemical Society).

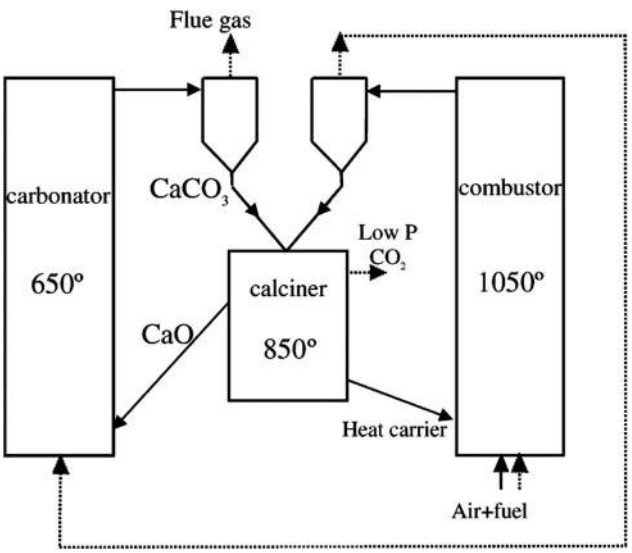

Fig. 27 Indirect heat transfer from combustor to the calciner (reprinted with permission from Abanades *et al.*[39] Copyright 2015 American Chemical Society).

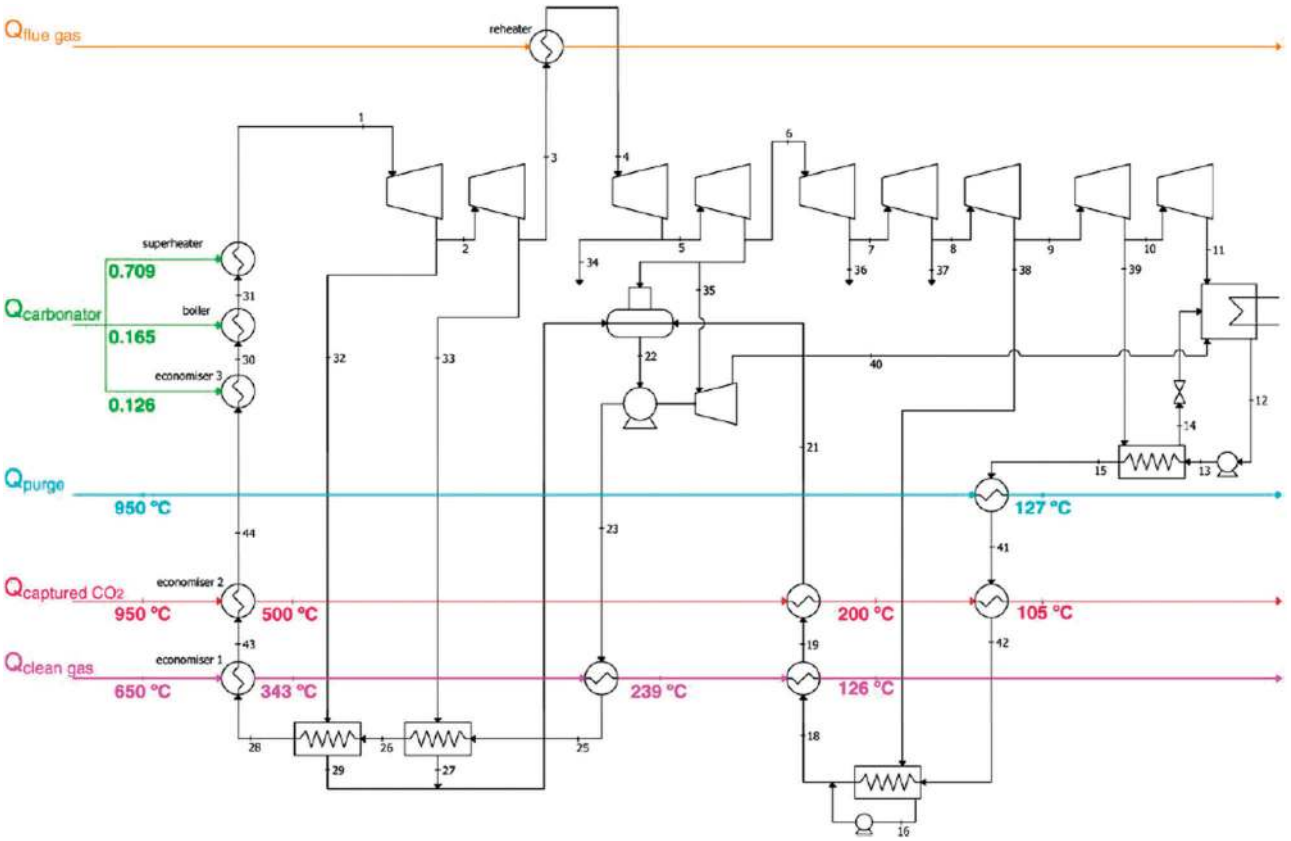

Fig. 28 Heat integration of the three-fluidised-bed combustion system with CaL CO_2 capture with the supercritical steam cycle (reprinted with permission from Martínez *et al.*[148] Copyright 2015 Elsevier).

CFB combustor that is fired with an air and fuel mixture. The solid bed material, which is a dense material, such as Al_2O_3 or deteriorated CaO, is heated in the combustor, separated from the combustion gas stream and finally fed to the calciner. However, as this configuration assumes that the heat carrier particles would be mixed with the CO_2 sorbent in the calciner, it is still not clear whether a continuous separation of these particles based on differences in their densities would be possible at the required scale. Nevertheless, this configuration offers net thermal efficiency of 40.0%$_{LHV}$, which is 2.2% points over the basic CaL configuration.

This configuration was also investigated by Martínez *et al.*[148] who studied its integration with the supercritical steam cycle (600 °C/280 bar). The coal combustion took place at 1030 °C, with 15%$_{vol}$ of excess air that entered the combustor at 400 °C. The energy input to the system through the coal combustion was assumed to be 1 GW_{th}. The flue gas, which contained 15.7%$_{vol}$ CO_2, was used to reheat the steam in the steam cycle and to preheat the combustion air, and eventually entered the carbonator at 380 °C. The carbonator, which operated at 650 °C, was modelled using the carbonator model developed by Alonso *et al.*[30] with the kinetic model for the multiple reaction cycles by Grasa *et al.*[196] Under given operating conditions, the CO_2 capture efficiency in the carbonator was estimated to be 89%. Again, a complete calcination process took place in the calciner operated at 950 °C, which corresponds to partial pressure of 1.93 bar. Heat for the sorbent regeneration came from the solid stream heated in the combustor. The pressure of the separated CO_2 was increased to 150 bar in the CCU comprising the five-stage compressor and the pump, and then it was cooled to 40 °C.

Martínez *et al.*[148] have identified five possible heat sources in the analysed CaL plant, which were heat released in the carbonator and heat carried with the clean gas, purge, flue gas and CO_2 process streams. Having integrated these sources as illustrated in Fig. 28 and considering the power requirement for CO_2 compression, the net power output of 378 MW_{el}, corresponding to net thermal efficiency of 37.8%, was obtained. This was 4.3% points higher than a comparable oxy-fired CFPP.

More recently, Martínez *et al.*[133] have proposed several process configurations that aim to reduce the efficiency penalty in a CaL plant integrated to a 500 MW_{el} CFPP of gross thermal efficiency of 44.4%$_{LHV}$. The temperature in the carbonator and calciner were set at 650 °C and 930 °C. The performance of the carbonator was represented by the maximum average conversion of the sorbent determined using the expression proposed by Abanades[145] and Grasa *et al.*,[171] and a correction factor of 0.8 to estimate the actual average conversion. Complete calcination was assumed in the calciner. As heat for sorbent regeneration was provided through oxy-combustion of coal, O_2 was produced in the ASU, which was characterised with specific power consumption of 220 kW h per t-O_2. Recirculated CO_2 amounted to 40% of the inlet gas to control the temperature in the calciner.

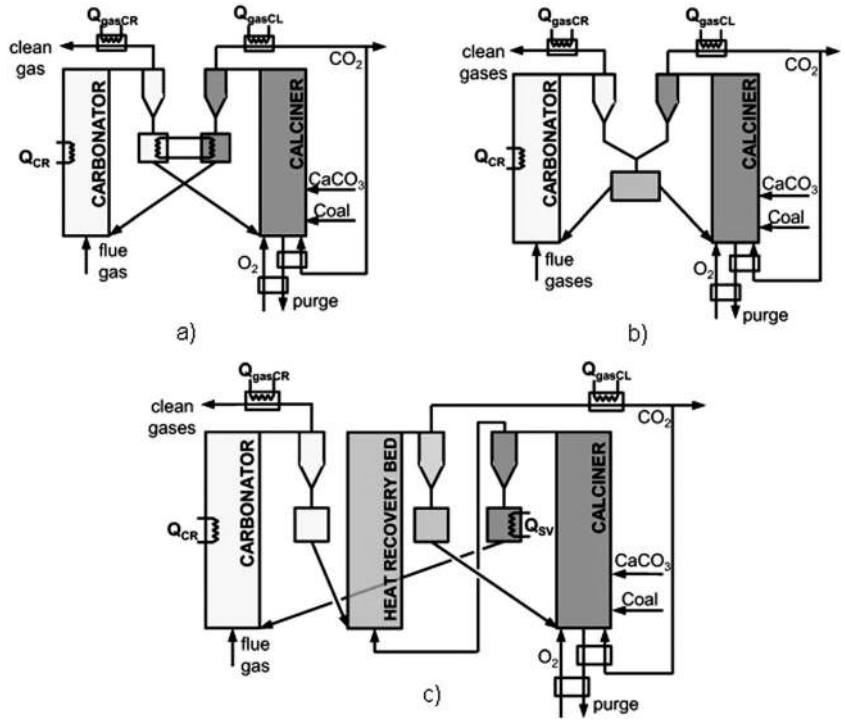

Fig. 29 Alternative calcium looping process configurations including: (a) seal valve indirect heat exchanger, (b) mixing seal valve and (c) heat recovery fluidised bed (adapted with permission from Martínez *et al.*[133] Copyright 2015 Elsevier).

The first configuration (Fig. 29a) assumes that heat is transferred from the solids leaving the calciner to the solids leaving the carbonator by means of an indirect heat exchanger integrated with the seal valves of the reactors. It is assumed that the solids leave both seal valves at the same temperature. However, this is not achievable in practice as there is no developed technology to carry out this process. To overcome this engineering challenge, Martínez *et al.*[133] proposed using a single mixing seal valve for both reactors (Fig. 29b). Although in this configuration solids can directly exchange heat, the fraction of the active CaO entering the carbonator is reduced due to solid mixing. In the last configuration, the sensible heat of the CO_2 stream leaving the calciner is recovered to preheat the solid particles from the carbonator in an additional heat recovery fluidised bed (Fig. 29c). Although the flue gas acts as a fluidising medium and mixes with the partially carbonated sorbent particles, no carbonation reaction could occur in the heat recovery bed. This is because the fast carbonation reaction cannot proceed, as the active CaO was trapped in the core of each solid particle, the surface of which has been covered with the $CaCO_3$ layer formed in the carbonator.[203] Although in this configuration the heat required by the calcination process is satisfied through oxy-fuel combustion, it is expected to increase the thermal efficiency of the CaL process by 1.4% points with a subsequent reduction in fuel consumption of 9%.

Another configuration proposed by Martínez *et al.*[204] utilises a multi-step cyclonic preheater, which is similar to the ones used in the cement industry (Fig. 30). In this additional piece of equipment heat available in the CO_2 stream leaving the calciner is utilised to preheat solids leaving the carbonator to around 725 °C prior to entering the calciner. The temperature in the carbonator and calciner were set at 650 °C and 950 °C. The performance of the carbonator and the calciner were represented by the Charitos *et al.*[149] (Section 4.3.1) and Martínez *et al.*[134] (Section 4.4.1) models, respectively. Although implementation of the cyclonic preheater has not changed the energetic efficiency of the integrated system, it reduced the energy requirement of the calciner. This was shown in reduction of the coal consumption by up to 13.3% and the oxygen consumption by 13.6%.

Finally, following the successful demonstration of the sub-pilot facility described in Section 3.5, Wang *et al.*[26,32] have investigated a CFPP retrofit with the CaL plant involving a sorbent regeneration stage through hydration (Fig. 31). Compared to the conventional CaL process, the proposed CCR process comprises an additional reactor which aims to improve conversion of the sorbent.

The performance of the calciner and hydrator reactors was computed based on the assumption that the systems reach equilibrium state at 1000 °C and 500 °C, respectively. In the conventional CaL process, a high calcination temperature would cause an excessive sintering of the sorbent leading to a reduction in the sorbent carrying capacity.[13] This is not the case in the CCR process as the sorbent is reactivated on contact with steam in the hydrator. Probably the lack of CO_2 recirculation to control the O_2 concentration in the calciner was also due to the sorbent regeneration potential of the CCR process. Furthermore, in the experimental campaign using the sub-pilot CCR plant the CO_2 capture level of 90% in the carbonator was achieved at a Ca : C of 1.3. In the carbonator model used by Wang *et al.*,[26,32] a Ca : C ratio of 1.4 was used to determine the

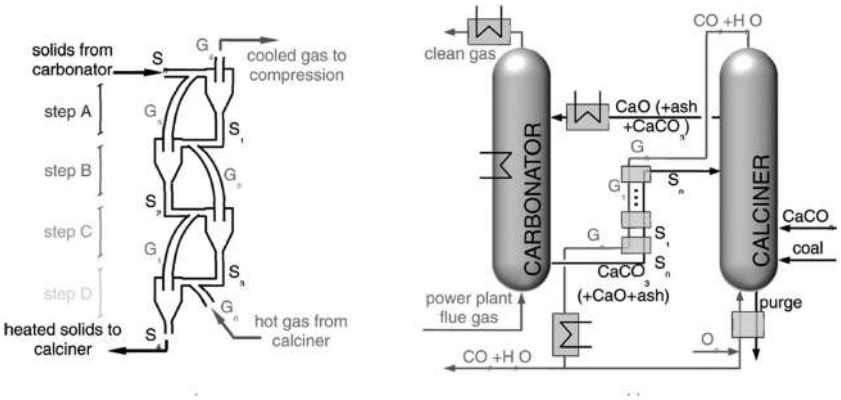

Fig. 30 Improvement of the calcium looping process performance through implementation of the cyclonic preheater (reprinted with permission from Martínez *et al.*[204] Copyright 2015 American Chemical Society).

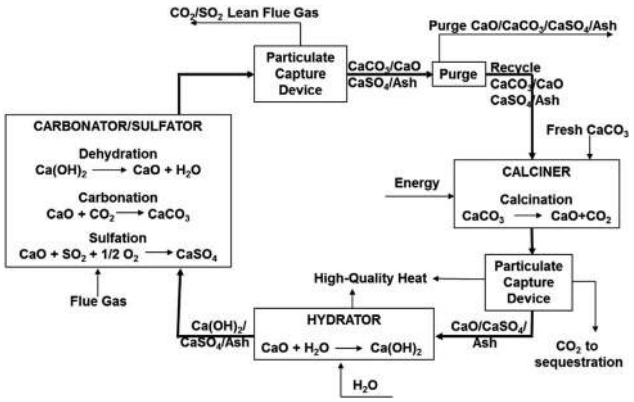

Fig. 31 Conceptual design of hydrated calcium looping process (reprinted with permission from Wang *et al.*[32] Copyright 2015 Elsevier).

solid looping rate required to capture 90% of CO_2 and 100% of SO_2 at 625 °C.

Wang *et al.*[32] have analysed integration of the CCR process into the 561 MW_{el} subcritical CFPP operating with an assumed net thermal efficiency of 33.5%$_{HHV}$. As mentioned above, although this approach works relatively well at full-load operation, any deviation from this point would reduce the prediction accuracy. Waste heat from the CCR process was used to generate high-quality steam that is sent to the primary cycles and replaced part of the steam generated in the power boiler. This means that the existing boiler would need to operate in part-load mode. Analysing the integration impact on the overall process efficiency, they have found that a maximum net efficiency of 26.9%$_{HHV}$ was reached if the calciner was indirectly heated using the flue gas from the combustion process. On the other hand, when the calciner was directly heated through oxy-combustion of coal or natural gas, the net efficiency decreased to 26.5%$_{HHV}$ and 26.1%$_{HHV}$, respectively. Such values for net thermal efficiency are considerably lower than in previous integration analyses reviewed. The main reason behind this is low net thermal efficiency of the reference power plant. The maximum projected efficiency penalty was estimated to be 7.4% points, which is considerably less than the 9–12% points estimated for amine-based or oxy-combustion systems. Furthermore, Wang *et al.*[26] have shown that the projected efficiency penalty for the CCR process is 22.2% lower than for a traditional CaL process. As the latter process operates on higher average conversions, this reduction can be associated with reduction of the solid looping rates between the reactors, which leads to a decrease in the heat requirement in the calciner.

5.1.4 Comparison between the average conversion and semi-predictive calcium looping model. A review of the integration and process improvement studies revealed that different models have been used to represent the carbonator performance, with the average conversion and semi-predictive models being most commonly applied. On the other hand the calciner performance has been represented using an equilibrium-based model in all studies reviewed. Therefore, it is important to highlight the impact of the carbonator model selection on the prediction of the integrated process performance.

Ströhle *et al.*[147] and Lasheras *et al.*[31] have analysed integration of a CaL plant to a 1000 MW_{el} ultra-supercritical CFPP (285 bar/600 °C/620 °C), which had a net thermal efficiency of 45.6%, with the aim of optimising overall process performance They assumed that a conventional CaL plant configuration was retrofitted to the existing FGD plant, thus the sulphation effect was kept to a minimum. Waste heat from the CaL plant was used to generate additional steam for the secondary steam cycle with an assumed net thermal efficiency of 49.98%. The performance of the calciner, operated at 900 °C, was determined using a Gibbs reactor and the heat for sorbent regeneration was provided through oxy-combustion of coal (w_{ASU} = 184 kW h per t-O_2). The carbonator was operated at 650 °C with an assumed pressure drop of 100–200 mbar and SO_2 conversion of 99% due to the large Ca/S ratio.

Ströhle *et al.*[147] have compared two commonly applied approaches for carbonator modelling, the maximum average conversion of sorbent model by Abanades *et al.*[39] and the 1D carbonator model by Abanades *et al.*[136] and evaluated the differences between these approaches in terms of overall process performance. Assuming a CO_2 capture level in the carbonator of 80%, application of the maximum average conversion model led to underestimation of the O_2 input to the calciner,

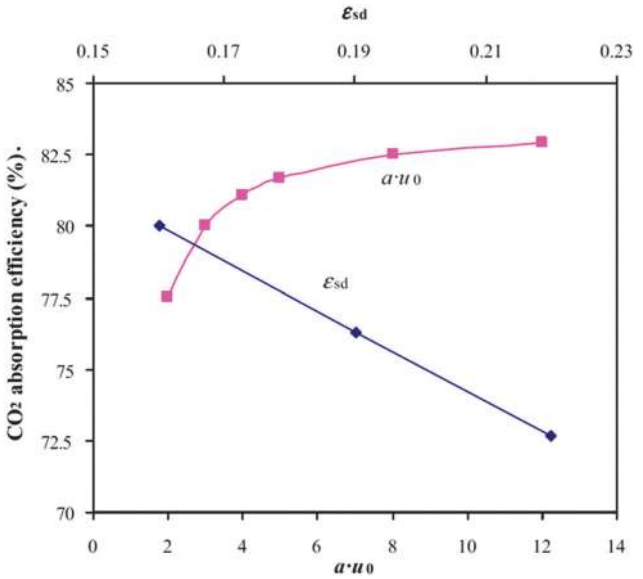

Fig. 32 Effect of KL CFB model uncertainty on the CO_2 capture level in the carbonator (reprinted with permission from Lasheras *et al.*[31] Copyright 2015 Elsevier).

solid looping rates and heat available for steam generation. However, in contrast to studies by Martínez *et al.*[133] and Berstad *et al.*,[146] no correction was made to the maximum average conversion to determine the actual average conversion of the sorbent. Nevertheless, net thermal efficiencies were estimated to be 42.9% and 42.4% for the maximum average conversion and the predictive 1D carbonator model, respectively. It can be concluded, therefore, that application of the maximum average conversion model with a reasonable correction factor would give a reasonable prediction of the overall process performance.

In a study by Lasheras *et al.*,[31] the effect of the uncertainty in the K–L CFB model, which requires specification of the decay constant (a) and the solid fraction in the dense region (ε_d), on the overall process performance was assessed. The analysis revealed that variation in the key input parameters led to 10% variation of the CO_2 capture level in the carbonator (Fig. 32). This indicates that further experimental studies are required to identify the K–L model parameters.

5.2 Combined cycle power plants

5.2.1 Feasibility of calcium looping process for natural gas-fired power plants. Conversely to previous studies that analysed integration of a CaL plant to a CFPP, Berstad *et al.*[146] have analysed the applicability of this CO_2 capture technology to decarbonise a natural gas combined-cycle power plant (NGCC). The reference NGCC delivers 416.4 MW_{el} with net thermal efficiency of 52.6%$_{HHV}$. To account for the gas pressure losses in the carbonator, the gas turbine discharge pressure was increased by 0.02 bar, resulting in a discharge temperature of 611 °C. Such a temperature makes it more feasible to retrofit the CaL plant right after the gas turbine island (Fig. 33).

CO_2 capture from NGCCs is more difficult than from CFPPs, as the CO_2 concentration in the flue gas is approximately 4%$_{vol}$. Therefore, to achieve a CO_2 capture level between 85% and 86% in the carbonator, its operating temperature needs to be 600 °C. To represent the performance of the carbonator, the maximum average conversion model proposed by Rodríguez *et al.*[11,40] was used. As the actual carbonation conversion (X_{carb}) is usually lower than the maximum value, a correction factor of 0.75, expressed as the X_{carb}/X_{ave} ratio, was adapted to enhance the accuracy of the model prediction. Such a conservative assumption is in agreement with the experimental results as presented in Section 3. To reach the actual carbonation conversion of 0.2, a F_0/F_{CaO} ratio of 0.06 was used. The sorbent is regenerated in the calciner, which is modelled as an equilibrium reactor with a calcination efficiency of 100%. A temperature of 950 °C is maintained in the calciner by means of oxy-combustion of

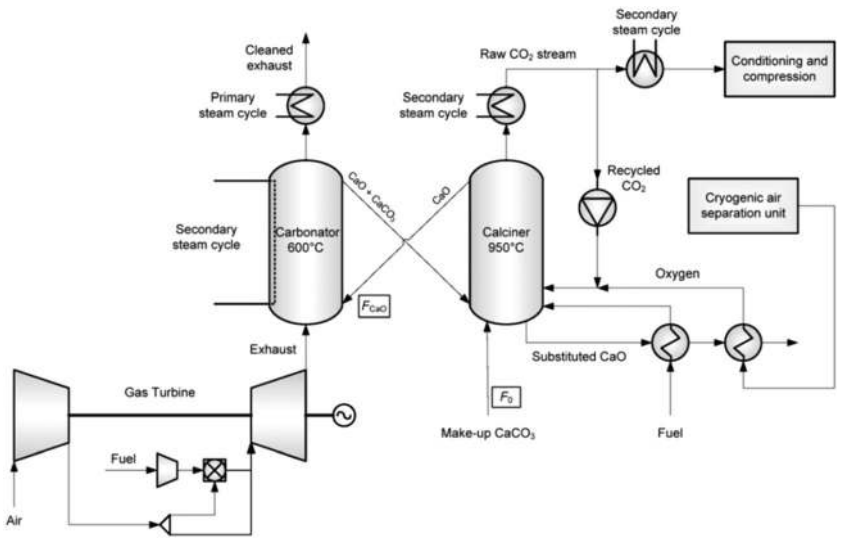

Fig. 33 Conceptual design of integration of calcium looping plant to natural gas combined cycle power plant (reprinted with permission from Berstad *et al.*[146] Copyright 2015 Elsevier).

natural gas. The $95\%_{mol}$-purity O_2 stream is produced in the cryogenic ASU and mixed with the recycled CO_2 to maintain $25\%_{mol}$ O_2 concentration in the oxidising gas. The pressure drop in the calciner is accounted for through an increase of the recycled CO_2 pressure of 0.03 bar. The remaining CO_2 is directed to the CCU, which is modelled as four compression stages and one pumping stage with intercooling to 28 °C, where it is compressed to 150 bar before being transported.

The waste heat from the CaL plant was utilised to generate an additional amount of steam that was then used to drive the secondary steam cycle. As the solids transported from the calciner to the carbonator carry a considerable amount of energy, the effect of the heat recuperation between the solid streams on the energy requirement in the calciner was investigated. Overall, three options for steam conditions (120 bar/560 °C/560 °C, 120 bar/610 °C/610 °C and 202 bar/610 °C/610 °C) were analysed for two CaL process configurations (with and without solid–solid heat recuperation). The study revealed that in the best case scenario, where solid–solid heat recuperation was implemented and the HP steam was generated at 610 °C and 202 bar, the projected efficiency penalty amounted to 9.1% points. This was found to be 1.3% points higher than for the reference NGCC with a conventional MEA CO_2 capture plant. Therefore, a CaL plant may not be a preferable option for NGCCs, which can be attributed to low CO_2 concentration in flue gas that results in lower driving force for the carbonation reaction. In turn, to reach the desired CO_2 capture level, the carbonator operating temperature needed to be lowered to 600 °C. The primary steam cycle location upstream of the CaL plant contributed to the efficiency penalty as less flue gas was fed to the primary waste heat steam generator. A possible solution for both issues was presented by Biliyok and Yeung[205] who showed that exhaust gas recirculation and/or supplementary firing could increase the flue gas temperature, flow rate and CO_2 concentration. However, feasibility of this solution is doubtful as it would further increase the capital cost by 20%, while reducing the levelised cost of electricity by only 6%.

5.2.2 High-reliability and high-efficiency coal-gasification power generation systems. The need for high-efficiency and environmentally friendly fossil-fuel power generation systems led to development of IGCC as an alternative to CFPPs. Kunze *et al.*[131] considered the reference 510 MW_{el} IGCC plant having net thermal efficiency of $39.4\%_{LHV}$, in which coal is gasified in the O_2-rich environment. Produced syngas is then cleaned to remove impurities, such as metals, sulphur and nitrogen compounds, and CO is converted to CO_2 in the water–gas shift reaction, which is then removed through a pre-combustion system using acid gas removal (AGR) based on an amine (MDEA) process. Finally, the purified syngas, which at this stage consists mostly of H_2, is combusted in a gas turbine coupled with an electric generator. The waste heat from the discharge gas is used to generate high-pressure steam at 170 bar, which then generates electricity in the bottoming steam cycle.

Kunze *et al.*[131] have proposed substituting a pre-combustion AGR system with a post-combustion CaL plant (Fig. 34). The carbonator was modelled as a stoichiometric reactor with conversion of 20% and operating temperature of 650 °C. The

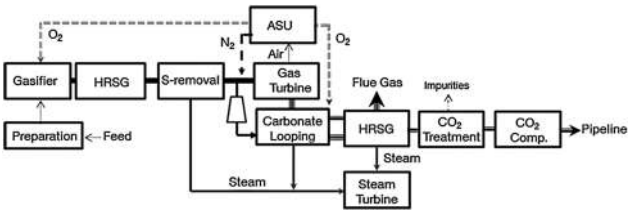

Fig. 34 Conceptual design of integration of calcium looping plant to IGCC (reprinted with permission from Kunze *et al.*[131] Copyright 2015 Elsevier).

desired CO_2 capture level in the carbonator of 90% was assured through adjusting the solids looping rate in the system. In contrast to the other studies, the calciner, which operated at 950 °C, was modelled as a stoichiometric reactor with conversion of 95% to account for sorbent sintering. The heat requirement for sorbent regeneration was met through direct oxy-combustion of syngas in the calciner. It was proposed that O_2 was produced using the oxygen transfer membrane, which separates O_2 from the high-pressure air diverted from the gas turbine compressor at temperatures of 850–900 °C, and then mixed with recycled CO_2 to control the calcination temperature. The remaining CO_2 was sent to purification and compression to 110 bar.

The waste heat available in the CaL plant was utilised to generate high-pressure steam (250 bar/630 °C/650 °C) that was fed to a bottoming dual-pressure supercritical steam cycle. This substitution of a subcritical bottoming steam cycle in the conventional IGCC plant led to improvement in net thermal efficiency of 3.8% points, to $43.2\%_{LHV}$ and a 9.5% increase in the net thermal power, to 462 MW_{el}. Such performance is in the range for the supercritical CFPPs without a CO_2 capture plant.[206,207] For this reason, the IGCC plants with CaL could be a feasible option for production of clean power from coal, with an increased reliability due to the lack of complicated chemical plant as in the conventional systems.

Alternative process configuration for a H_2-fuelled IGCC power plant that comprises a DFB system has been proposed by Wang *et al.*[130] (Fig. 35). The performance of each reactor in the system was based on the assumption that chemical and phase equilibrium is reached. The gasifier reactor is composed of the BFB gasifier, in which allothermal steam gasification of coal takes place at 700 °C, integrated with a carbonator riser operated at 600 °C. As the gasifier is assumed to operate with 50% conversion of coal, the unreacted char and sorbent are fed to the calciner, which operates at 900 °C. The heat required to sustain the calcination reaction stems from the oxy-combustion of char. The H_2-rich gas is used to fuel an F-class gas turbine, in which the compressor operates at a pressure ratio of 17 and expander temperature of 1350 °C.

The waste heat available in the integrated system is utilised to sustain the gasification reaction by diverting part of the regenerated sorbent to the gasifier and to generate the steam for the bottoming subcritical steam cycle (125 bar/565 °C/565 °C). The net thermal efficiency of the proposed process was $42.7\%_{LHV}$, while a CO_2 capture level of 95% was reached.

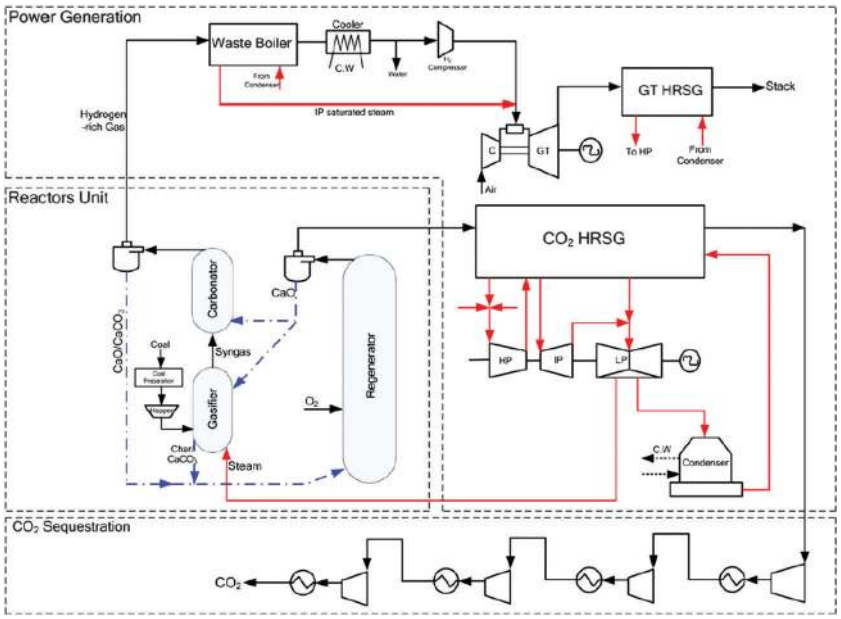

Fig. 35 Conceptual design of integration of calcium looping plant to IGCC (reprinted with permission from Wang *et al.*[130] Copyright 2015 Elsevier).

The efficiency was considerably higher than for a supercritical CFPP retrofitted with an ammonia-based CO_2 capture plant (net thermal efficiency of 27.9%$_{HHV}$).[208] This is also 5.7% points higher than for a CFPP retrofitted with the CaL plant analysed by Romeo *et al.*[86] (Section 5.1.2).

It is also important to benchmark the process performance improvements through substitution of the dual-stage Selexol process, which is commonly considered in the IGCC power plants, with the CaL plant. Connell *et al.*[129] have evaluated such performance improvement in an IGCC power plant, which comprises two F-class gas turbines (Case 2 in Black *et al.*[209]). In the considered CaL configuration, which was based on the double-looping CCR process developed and successfully demonstrated by Wang *et al.*,[26,32] each reactor was assumed to reach chemical and phase equilibrium at a given operating temperature. In contrast to previous studies, the carbonator was operated at 33 bar, which required a temperature of 700 °C to allow $Ca(OH)_2$ dissociation and hence the water/gas shift reaction. To increase the average sorbent conversion, and hence operate the system at Ca : C ratio of 1.3 that was identified in the pilot-plant testing to allow reaching more than 90% CO_2 capture, the sorbent is hydrated at 2 bar and 493 °C. The reason for the hydrator being operated at an elevated pressure was to increase its operating temperature and allow for more waste heat recovery in the system. An operating temperature of more than 875 °C in the calciner is maintained through oxy-combustion of coal. The conceptual IGCC design assumes that the heat from the CaL plant is utilised to generate steam for the bottoming steam cycle (Fig. 36).

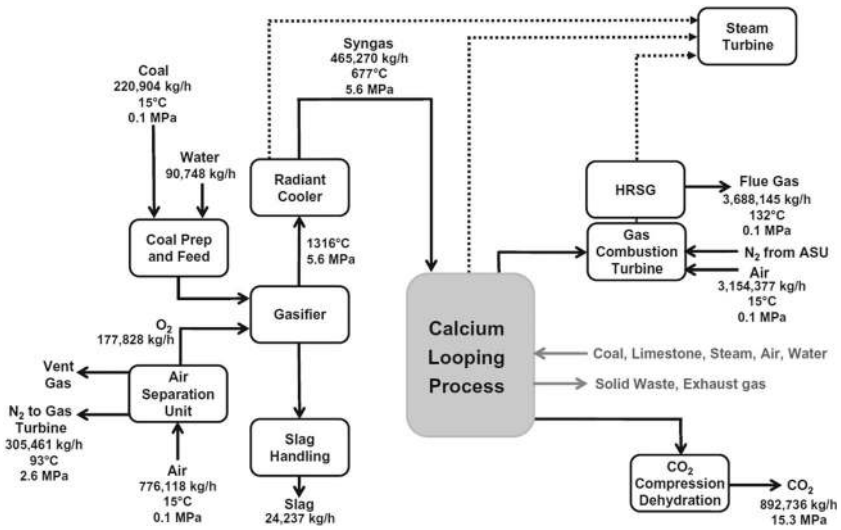

Fig. 36 Conceptual design of integration of calcium looping plant to IGCC (reprinted with permission from Connell *et al.*[129] Copyright 2015 Elsevier).

Having compared the performance of the IGCC with the CCR process and the conventional IGCC with dual stage Selexol process, Connell *et al.*[129] have found that net thermal efficiency increased by 0.4% points, from 32.7%$_{HHV}$ to 33.1%$_{HHV}$, with the coal oxy-combustion accounting for 41% of the total heat input to the process. This performance was 6.5% points higher than for a comparable subcritical CFPP retrofitted with an MEA scrubbing system.[209] More importantly, the net power output of the system increased by 71.7%, from 543.2 MW_{el} to 932.9 MW_{el}.

In the IGCC power plant, the CaL process can be used as either post-combustion, with the standard AGR process used for syngas treatment, or pre-combustion technology. Cormos and Cormos[128] have investigated the difference between these approaches for a 561.15 MW_{el} IGCC power plant of 44.36%$_{LHV}$ net thermal efficiency. The performance of all reactors in the system was determined based on thermodynamic equilibrium, as no significant differences were found when the kinetics of the calcination and carbonation processes were considered. In the investigated CaL plant, the carbonator and the calciner were operated at 650–700 °C and 900–950 °C, respectively. The temperature in the calciner was maintained through oxy-combustion of coal. It was also assumed that the CaL plant was fully heat-integrated with the rest of the plant.

In the first configuration, the CaL plant was proposed to be retrofitted after the power block (Fig. 37a), which would provide a flexible integrated system. Conversely, the second configuration assumes that the carbonator was located after the AGR plant (Fig. 37b). Steam is supplied directly to the calciner to facilitate the water/gas shift reaction allowing the H_2-rich stream to be fed to the power block.

Analysis of the overall plant performance indicators revealed that on integration of the CaL plant the net thermal efficiency dropped by 10.1% points for the post-combustion configuration and by 7.3% points for the pre-combustion configuration. With utilisation of the waste heat to produce high-pressure steam, which was then used to produce power in the bottoming steam cycle, the net power output increased by 14.6% and 19.4% for the post-combustion and pre-combustion configurations, respectively. Although such results show that the former configuration is more promising in terms of overall process performance, its higher integration degree would affect plant flexibility. Moreover, Cormos and Cormos[128] have concluded that the net efficiency penalty of the post-combustion configuration is comparable with the one associated with conventional post-combustion scrubbing technologies. Hence application of CaL as a post-combustion CO_2 capture plant will not bring any benefit in terms of process performance. However, the pre-combustion configuration was found to result in a net efficiency penalty 1–2% points lower than conventional pre-combustion scrubbing technologies.

5.2.3 Zero-emissions coal-based power generation systems. Due to high-temperature operation of the CaL process, it can serve as a base for development of novel highly-efficient and low-emission power generation systems. Two alternative coal-gasification combined cycle power plants, which utilise the CaL process as both a pre-combustion CO_2 capture technology and heat source, have been investigated by Romano and Lozza.[127,210] Both zero-emissions coal mixed technology (ZECOMIX) (Fig. 38) and zero-emissions coal mixed technology with air gas turbine (ZECOMAG) (Fig. 39) can be divided into four sections – chemical island, oxygen island, CO_2 island and power island – and they only differ in the power island configuration.

In the chemical island, where each reactor was assumed to operate under equilibrium conditions, coal slurry is gasified under an H_2 atmosphere in a hydrogasifier producing syngas that is then shifted to the H_2-rich stream in the carbonator. A small amount of O_2 is utilised to sustain the operating temperature at 700–1000 °C, depending on the operating pressure ranging between 30 bar and 70 bar. The overall chemical

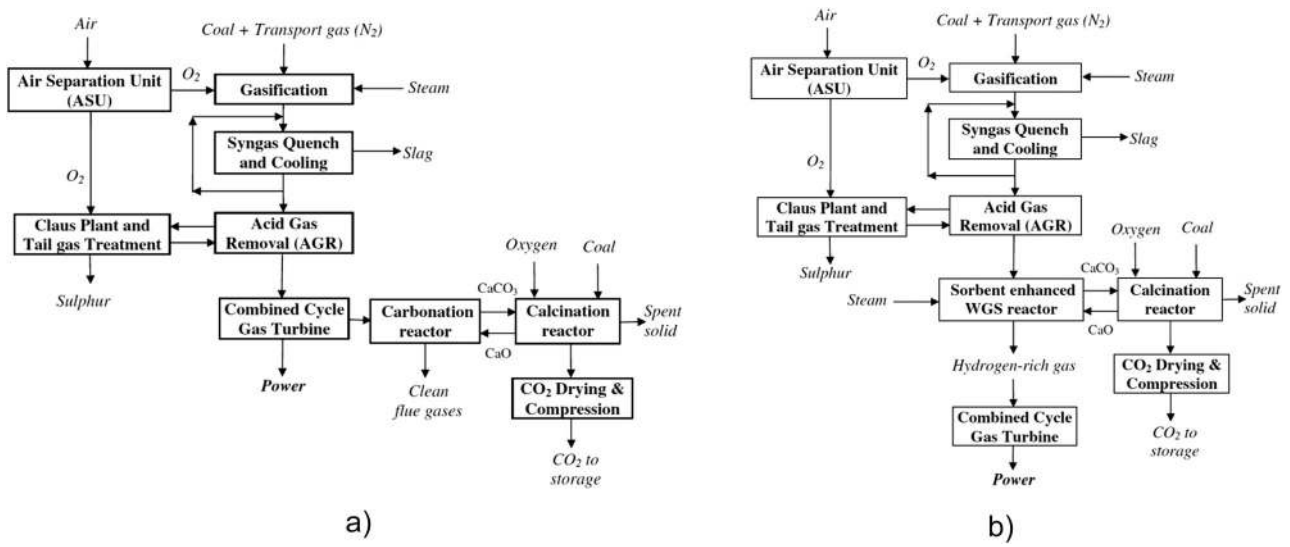

Fig. 37 Conceptual design of integration of (a) post-combustion and (b) pre-combustion calcium looping plant to IGCC (adapted with permission from Cormos and Comros.[128] Copyright 2015 Elsevier).

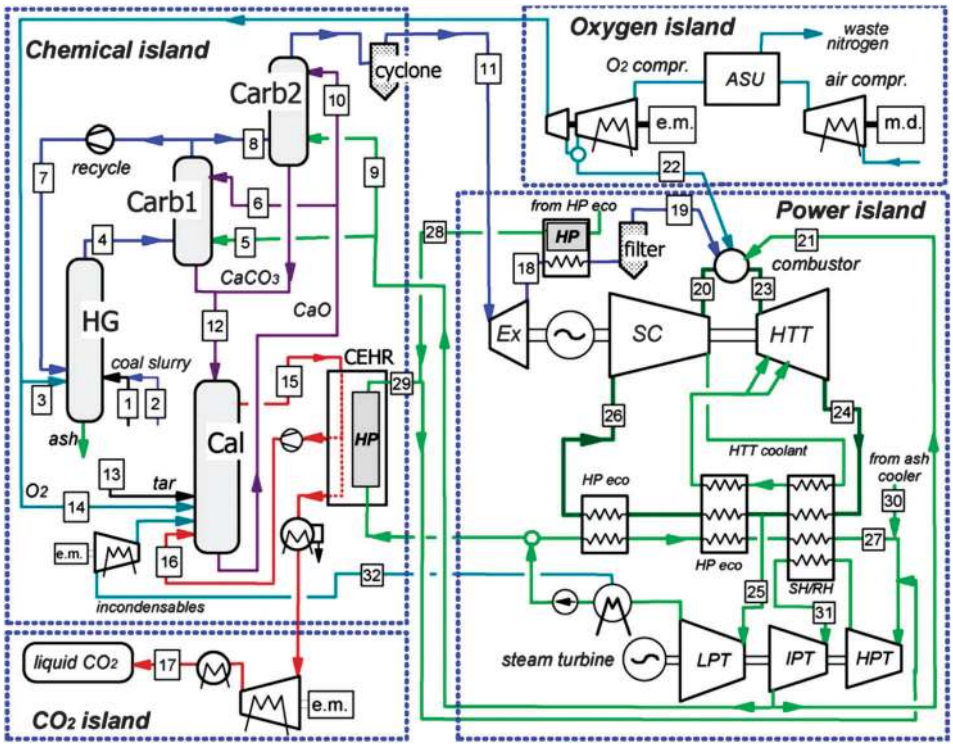

Fig. 38 Conceptual design of Zero-Emissions COal MIXed technology (reprinted with permission from Romano and Lozza.[210] Copyright 2015 Elsevier).

reaction taking place in the hydrogasifier and the carbonator is presented in eqn (101). This reaction was found to be exothermal, as the heat released on the exothermal CO_2 removal from the syngas was enough to sustain the steam

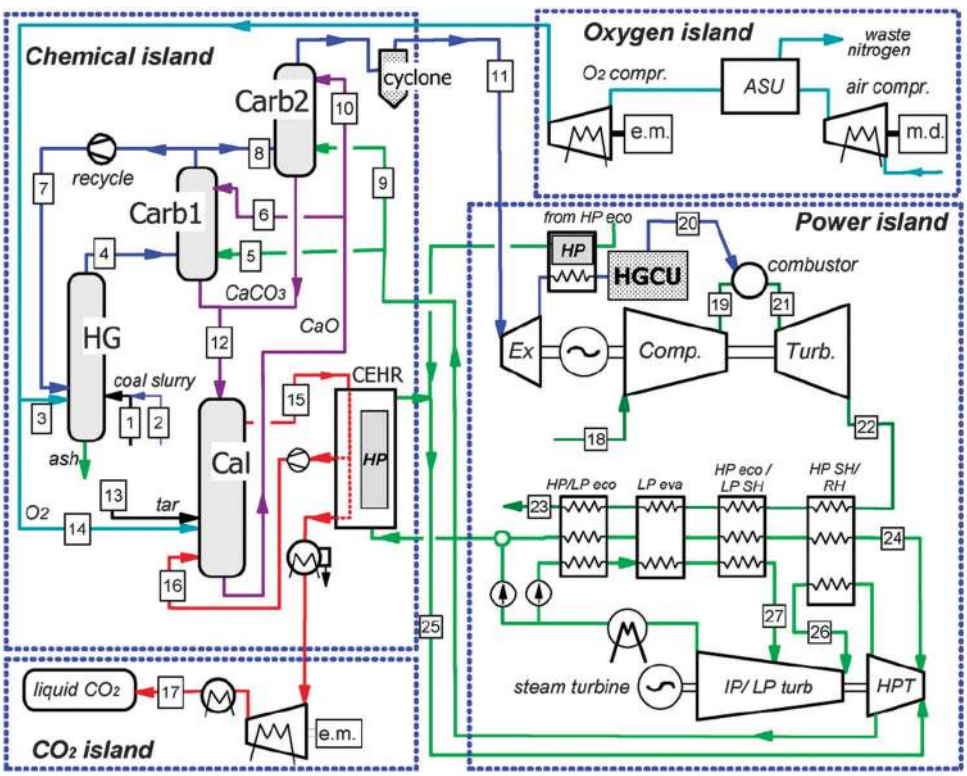

Fig. 39 Conceptual design of Zero-Emissions COal Mixed technology with Air Gas turbine (reprinted with permission from Romano and Lozza.[127] Copyright 2015 Elsevier).

reforming reaction. Part of the H_2-rich stream is recycled from the carbonator to the hydrogasifier.

$$CH_4 + 2H_2O + CaO \rightarrow 4H_2 + CaCO_3 \qquad \Delta H_r^\circ = -14.5 \text{ kJ mol}^{-1} \quad (101)$$

It was assumed that the carbonator operates with an average conversion of 50% that was substantiated with the expected progress in sorbent treatment, production and reactivation.[210] Sorbent regeneration was assumed to be conducted at an elevated pressure and temperatures ranging between 920 °C and 1250 °C, regardless of sorbent sintering and degradation. Such high temperatures were achieved through oxy-combustion of the refinery residuals with 90% oxygen excess, as usage of the produced syngas would reduce the net thermal efficiency of the process, while usage of coal at such a high temperature would result in ash melting.

The power island of ZECOMIX technology comprises a semi-closed Joule cycle, in which heat from the syngas oxy-combustion and the combustion gases are mixed with compressed steam to control the combustor outlet temperature. Such a mixture is expanded in a high-temperature steam turbine and then used for supercritical steam generation in the bottoming steam cycle. The incondensable species, such as CO_2 and O_2, are removed from the condenser and from the deaerator with part of the steam sent to the calciner. This approach allows the ASU load to be minimised as unreacted O_2 is recycled to the calciner. Conversely, ZECOMAG technology has a more conventional power island, in which the syngas is burned with air in an open gas turbine cycle, and the discharged flue gas is used to generate supercritical steam in the dual-pressure heat recovery steam generator for the steam cycle.[127] Despite its more conventional configuration, ZECOMAG cannot be considered as a zero-emissions technology as the gas turbine flue gas, which consists of CO_2, NO_x and SO_x, is exhausted to the environment.

Analysis of the overall process performance revealed that ZECOMIX and ZECOMAG yield similar maximum net thermal efficiencies of 46.69%$_{LHV}$ and 46.74%$_{LHV}$, respectively. The analysis also revealed that the net efficiency of ZECOMIX was degraded by 0.59% points on increase of the steam compressor pressure from 25 bar to 48.5 bar, and by 2.32% points on reduction of the calciner temperature to 920 °C. In addition, reduction of the average sorbent conversion in the carbonator from 66.7% to 20.0% was found to reduce the net thermal efficiency of ZECOMIX by 3% points and of ZECOMAG by 2.5%. This indicates that sorbent performance is critical in terms of the overall process efficiency. Finally, the net power output of 667.5 MW_{el} for ZECOMIX when the steam compressor is operated with a pressure ratio of 25, was found to be 25.2% higher than for ZECOMAG with the gas turbine compressor operated with a pressure ratio of 20. The maximum net power output achievable by ZECOMIX was found to be 1242.2 MW_{el} if the steam compressor inlet pressure was increased from 1.02 bar to 1.9 bar.

5.3 Summary

5.3.1 Integration impact on the overall process performance. Depending on the power plant type, the net projected efficiency penalty imposed by post-combustion CaL plant integration was 2.6[37]–7.9%[86] points for a CFPP and 9.1–11.4%[146] points for a combined cycle power plant.

A very low net projected efficiency penalty of 2.6% points was estimated by Martínez *et al.*[37] in investigating a subcritical CFPP retrofit with a CaL plant and supercritical secondary steam cycle. This shows that implementation of CaL plants into subcritical units, the majority of the current CFPP fleet, would result in a minor net efficiency penalty compared to conventional CO_2 capture technologies. Nevertheless, the mean net projected efficiency penalty for a CFPP was 6–7% points with 2.5–3% points associated with the CaL plant itself and the remainder caused by the CCU. Yang *et al.*[16] have estimated an extremely low net thermal efficiency of 21.2% for a CaL plant integrated into a CFPP without any heat recovery system. This implies that as high-grade heat is available in the CaL plant, it needs to be recovered efficiently to reach high overall performance.

The studies by Berstad *et al.*[146] and Cormos and Cormos[128] revealed that integration of a CaL plant as a post-combustion technology into the NGCC and the IGCC power plant would result in a net efficiency penalty comparable to conventional CO_2 capture systems. This could be associated with low partial pressure of CO_2 in the flue gas, and thus lower driving force for the carbonation reaction. However, in studies where a CaL plant was used as a substitute for a complex gas processing plant integrated as a pre-combustion CO_2 capture technology into an IGCC system, the net thermal efficiency increased by 0.4[129]–3.8%[131] points, and reached 43.2%$_{LHV}$.[131] The study by Romano and Lozza[127,210] revealed that development of new coal-based power generation systems based on the CaL process, which are characterised by net thermal efficiencies of 46.69%$_{LHV}$ for CO_2 capture higher than 95%, is feasible. Such values for net thermal efficiency, which are in the range of supercritical and ultra-supercritical CFPPs without CO_2 capture plants, and increased process reliability due to the lack of complicated chemical plant indicate that gasification-based power plants with pre-combustion CaL could become a cost-efficient and environmentally-friendly technology for coal-based power generation, and could allow further coal utilisation.

It is important to highlight that all of the reviewed studies use different initial sets of assumptions regarding the reference power plant. Moreover, the reference net thermal efficiencies of the CFPPs gathered in Table 7 vary between 32.7–44.6%$_{HHV}$ (studies using higher heating value basis), and 36.0–46.0%$_{LHV}$ (studies using lower heating value basis). However, as mentioned in the introduction, the average net thermal efficiency of the existing global fleet has been identified to be 33%$_{LHV}$, which corresponds to 30–31%$_{HHV}$ depending on fuel composition.[211] As the sub-critical units, which operate with low net thermal efficiencies and yet account for around 75% of the global CFPP capacity,[6] can be expected to be still in operation in the near future, the further analyses of the CaL process integration should focus on a portfolio of steam conditions to assure prediction accuracy and realism. This implies that baseline reference models for CaL process integration need to be established, which can be done, for example, by replicating

Table 7 Summary of the process integration studies

Reference	Power plant type	Gross power output (MW_{el})	Reference net thermal efficiency ($\%_{LHV}$)	Net thermal efficiency of integrated system ($\%_{LHV}$)	Efficiency penalty (% points)
Shimizu *et al.*[28]	SC-CFPP[a]	1000	N/A	33.4[d]	N/A
Yang *et al.*[16]	SC-CFPP[a]	600	40.6	25.3–36.8	3.8–15.3
Abanades *et al.*[39]	USC-CFPP[a]	100	46	38.8–40.0	6–7.2
Martínez *et al.*[83]	SubC-CFPP[a]	350	36	30.3–33.4	2.6–5.7
Martínez *et al.*[148]	SC-CFPP[a]	433.7	N/A	37.8	N/A
Martínez *et al.*[133]	CFPP[b]	500	44.35		N/A
Romeo *et al.*[86]	SC-CFPP[a]	450	44.93	37.0	7.93
Lara *et al.*[200]	SC-CFPP[a]	500	38.2	33.0	5.2
Lara *et al.*[201]	SC-CFPP[a]	500	38.2	34.0	6.2
Ströhle *et al.*[147]	USC-CFPP[a]	1100	45.6	42.4–42.8	2.8–3.2
Lasheras[31]	USC-CFPP[a]	1000	45.6	42.7	2.9
Wang *et al.*[32]	USC-CFPP[a]	561	44.6[d]	37.2–38.0[d]	6.6–7.4
Wang *et al.*[26]	SubC-CFPP[a]	500[e]	35.8[d]	N/A	N/A
Wang *et al.*[26]	SC-CFPP[a]	500[e]	39.0[d]	N/A	N/A
Vorrias *et al.*[132]	SC-LFPP[c]	330	42.5	37.5	5.0
Berstad *et al.*[146]	NGCC	418.8	52.6[d]	41.2–43.5[d]	9.1–11.4
Kunze *et al.*[131]	IGCC	510	39.4	43.2	−3.8
Wang *et al.*[130]	IGCC	N/A	N/A	42.7	N/A
Connel *et al.*[129]	IGCC	734	32.7[d]	33.1[d]	−0.4
Cormos and Cormos[128]	IGCC	561.2	44.4	34.2–37.0	7.4–10.2
Romano and Lozza[210]	ZECOMIX	N/A	N/A	44.4–46.7	N/A
Romano and Lozza[127]	ZECOMAG	N/A	N/A	46.7	N/A

[a] SC – supercritical; USC – ultra-supercritical; SubC – Subcritical. [b] Steam conditions not specified. [c] Supercritical lignite-fired power plant. [d] HHV basis. [e] Net power output.

CFPP (subcritical and supercritical), NGCC and IGCC models from the revised NETL report[209] and developing ultra-supercritical CFPP model based on the European Benchmarking Task Force documents.[212,213] Table 7 reveals that not only are the reference CFPPs based on different steam conditions, from sub-critical to ultra-supercritical, but also their gross power outputs and net thermal efficiencies vary considerably. The performance of the reference IGCC plants vary significantly as well. As this makes a comparison of results across different analyses impossible, a set of baseline reference models, which should include models for CFPP, NGCC and IGCC plants with consideration of different steam conditions, needs to be established. Such baseline reference models would allow for a reliable comparison of further process developments using process simulations.

5.3.2 Modelling approaches, assumptions and limitations. This review identified limitations in the approaches for modelling CaL plants and their integration into the power plants (Table 8). Firstly, it was found that in several studies the net or gross thermal efficiency of the secondary steam cycle,[26,28,31,32,37,39,83,147] as well as specific power consumptions of ASU[26,28,31,32,83,86,128,130,133,146,147,200,201] and CCU[26,28,32,83] were assumed rather than estimated using thermodynamic or process models. Although this approach could be valid for a particular system operating at a fixed load, any deviation from the operating point, such as part-load operation, would reduce the accuracy of the prediction. Moreover, such approach applied to represent the performance of the secondary steam cycle, ASU and CCU, restricts applicability of a detailed design of the HEN of the entire process.

Secondly, the studies reviewed assumed that total calcination is achieved in the calciner, with the exception of the study by Kunze *et al.*[131] who assumed 95% conversion in the calciner to account for less favourable calcination conditions. Thirdly, all the studies utilised thermodynamic models to represent the calcination process, mostly achieving chemical equilibrium through Gibbs' free energy minimisation. Most of the studies analysing the combined cycle power plants used thermodynamic models also for the carbonator, with the exception of Berstad *et al.*,[146] while more complex models, such as average conversion models[16,39,132,133,147] and 1D carbonator models based on K–L hydrodynamics[28,31,147] were used in analysing the CFPPs. Interestingly, the study by Ströhe *et al.*,[147] in which both models have been compared, revealed that, although application of the maximum average conversion model without the correction factor resulted in underestimation of several process parameters, the overall process performance of a CFPP with a CaL process was the same for both models. Furthermore, the sensitivity study performed by Lasheras *et al.*[31] revealed that the uncertainty in the K–L model can affect CaL plant performance by up to 10%. As this can have a significant effect on estimation of overall process performance, further experimental tests are necessary to identify the required parameters.

It is worth pointing out that the lower operating temperature (600 °C) of the carbonator in the CaL linked with the NGCC compared to studies reviewed in Section 5.1 (650 °C), which assessed integration of the CFPP and the CaL process, results in slower carbonation reaction, hence larger units are required. Moreover, low CO_2 partial pressure in the NGCC flue gas makes the carbonation process more difficult, and thus the maximum CO_2 capture level of only 86% in the carbonator was achieved. Although the carbonator temperature could be further lowered, favouring chemical equilibrium at the expense of reaction kinetics, the desired high-pressure steam temperature of 550–560 °C[146] would not be achievable.

Table 8 Summary of modelling approaches and assumptions in investigating calcium looping integration to power plants

	Carbonator assumptions		Calciner assumptions		Modelling approach for other system components		
Reference	Model	Operating conditions	Model	Operating conditions	ASU	CCU	Secondary steam cycle
Shimizu *et al.*[28]	Semi-predictive model with KL hydrodynamics	T = 650 °C Ca : C = 8.29 E_{carb} = 83%	Equilibrium	T = 950 °C X_{calc} = 100%	Assumed w_{ASU} = 25.9 MJ per kmol-O_2	Assumed w_{CCU} = 24.5 MJ kmol^{-1}-CO_2	Assumed η_g = 42.6%$_{HHV}$
Yang *et al.*[16]	Average conversion w/o correction	T = 650 °C Ca : C = 5 E_{carb} = 85%	Equilibrium	T = 900 °C	Assumed w_{ASU} = 220 kW h per t-O_2	Not considered	Thermodynamic model
Abanades *et al.*[39]	Average conversion w/o correction	T = 650 °C E_{carb} = 75.2%	Equilibrium	T = 950 °C X_{calc} = 100%	Estimated using process model	Estimated using process model	N/A
Martínez *et al.*[83]	Semi-predictive model with simple hydrodynamics	T = 650 °C E_{carb} = 70–90% u_0 = 6 m s^{-1}	Equilibrium	T = 950 °C λ_{O_2} = 1.05 X_{calc} = 100% $y_{O_2,fluidising\ gas}$ = 25%$_{vol}$	Assumed w_{ASU} = 160 kW h per t-O_2	Assumed w_{CCU} = 100 kW h/t-CO_2	Assumed η_g = 45%
Martínez *et al.*[148]	Semi-predictive model with simple hydrodynamics	T = 650 °C E_{carb} = 89%	Equilibrium	T = 950 °C E_{calc} = 100%	Not specified	Estimated using adiabatic compression model with η_a = 75%	Thermodynamic model
Martínez *et al.*[133]	Average conversion with correction	T = 650 °C X_{carb}/X_{ave} = 0.8 E_{carb} = 90%	Equilibrium	T = 930 °C X_{calc} = 100%	Assumed w_{ASU} = 220 kW h per t-O_2	N/A	N/A
Romeo *et al.*[86]	Average conversion w/o correction	T = 650 °C X_{carb} = 20% E_{carb} = 85%	Equilibrium	T = 875–950 °C X_{calc} = 100% $y_{O_2,fluidising\ gas}$ = 95%$_{vol}$	Assumed w_{ASU} = 220 kW h per t-O_2	N/A	Thermodynamic model
Lara *et al.*[200,201]	Average conversion w/o correction	T = 650 °C Ca : C = 5	Equilibrium	T = 950 °C F_0/F_R = 0.025	Assumed w_{ASU} = 220 kW h per t-O_2	Estimated using isentropic compression model with η_i = 80%	Thermodynamic model
Ströhle *et al.*,[147] Lasheras *et al.*[31]	Average conversion w/o correction and Semi-predictive mode with K–L hydrodynamics	T = 650 °C E_{carb} = 80% E_{SO_2} = 99%	Equilibrium	T = 900 °C λ_{O_2} = 1.10 X_{coal} = 0.995	Assumed w_{ASU} = 184.8 kW h per t-O_2	N/A	Assumed η_g = 50.3%$_{LHV}$
Wang *et al.*[26,32]	Equilibrium	T = 625 °C Ca : C = 1.4 E_{carb} = 90% E_{SO_2} = 100%	Equilibrium	T = 1000 °C $y_{O_2,fluidising\ gas}$ = 95%$_{vol}$	Assumed w_{ASU} = 200 kW h per t-O_2	Assumed w_{ASU} = 119 kW h/t-CO_2	Assumed η_g = 42%$_{HHV}$
Vorrias *et al.*[132]	Average conversion w/o correction	T = 650 °C Ca : C = 7 E_{carb} = 90%	Equilibrium	T = 950 °C F_0/F_{CO_2} = 0.1 $y_{O_2,fluidising\ gas}$ = 80%$_{vol}$	Estimated using process model	Estimated using process model	Thermodynamic model
Berstad *et al.*[146]	Average conversion with correction	T = 600 °C X_{carb}/X_{ave} = 0.75 E_{carb} = 85–86%	Equilibrium	T = 950 °C F_0/F_R = 0.06 λ_{O_2} = 1.03 X_{calc} = 100% $y_{O2,fluidising\ gas}$ = 25%$_{vol}$	Assumed w_{ASU} = 200 kW h per t-O_2	Estimated using polytrophic compression model with η_p = 75–80%	Thermodynamic model
Kunze *et al.*[131]	Average conversion w/o correction	T = 650 °C X_{carb} = 0.2 E_{carb} = 90%	Equilibrium	T = 950 °C X_{calc} = 95%	Assumed w_{ASU} = 28 kW h per t-O_2	Assumed w_{ASU} = 83 kW h/t-CO_2	N/A
Wang *et al.*[130]	Equilibrium	T = 600 °C	Equilibrium	T = 900 °C	Assumed w_{ASU} = 245 kW h per t-O_2	Estimated using isentropic compression model with η_i = 75%	Thermodynamic model
Connel *et al.*[129]	Equilibrium	T = 700 °C E_{carb} > 90%	Equilibrium	T > 875 °C	N/A	N/A	N/A
Cormos and Cormos[128]	Equilibrium	T = 650–700 °C	Equilibrium	T = 900–950 °C	Assumed w_{ASU} = 225 kW h per t-O_2	Estimated using process model	Thermodynamic model
Romano and Lozza[127,210]	Equilibrium	T = 875–882 °C X_{carb} = 0.5	Equilibrium	T = 1250	Estimated	Estimated using isentropic compression model with η_i = 89.5%	Thermodynamic model

Finally, although the operating temperatures of the carbonator and the calciner were found to be similar in all studies reviewed, selection of several important parameters seem to be inconsistent (Table 8). Namely, some studies assume that the O_2 in the calciner fluidising gas is diluted with recycled CO_2, and its concentration varies from 25%$_{vol}$[83,146] to 80%$_{vol}$.[132] In addition, several studies claimed that no CO_2 recycle is required and 95%$_{vol}$-purity O_2 can be directly fed to the calciner.[26,32,86] Current pilot-plant testing activities were conducted with the O_2 concentration below 50%$_{vol}$.[33,98,100,104] Therefore, to limit the sorbent deterioration, further integration studies should include the CO_2 recycle to control the temperature in the calciner. Another important parameter is Ca : C ratio that has been assumed to be between 5–8.29 to reach the CO_2 capture levels in the carbonator up to 90% using non-pretreated sorbent. It needs to be highlighted that the pilot-plant tests reviewed in Section 3 claimed that to reach such reduction in the CO_2 emissions in the carbonator, the Ca : C ratio should be higher than 8–11.6.[98,103,107] For this reason, in the studies where low Ca : C ratios were used to reach high CO_2 capture level in the carbonator, prediction of the process performance may be overly optimistic due to under-estimated solids looping rate, and thus heat requirement in the calciner. Moreover, the excess O_2 and the relative limestone make-up rate, which is represented using F_0/F_R ratio, were found to vary between 1.03–1.10 and 0.025–0.06, respectively. This implies the need for establishing baseline design parameters for the CaL process that would allow comparing process performance across analyses.

6 The future of calcium looping in power generation systems

In light of increasing environmental concerns, the power sector seems to be the first in line to be completely decarbonised by 2050. High reliance on coal, however, makes this a challenging task requiring implementation of CO_2 capture technologies in the existing coal-based power generation fleet. Unfortunately, conventional technologies, which utilise chemical sorbents and oxy-fuel combustion, result in a considerable drop in system efficiency, leading to an increase in the cost of electricity. The CaL process is regarded as a feasible alternative to conventional technologies because not only is it characterised by lower loss in power plant efficiency, but it is also capable of increasing the power output of the system.

CaL process viability and performance have been widely investigated in bench- and pilot-scale facilities the size of which varies between 1 kW_{th} and 1.7 MW_{th}. The test campaigns reported in the open literature provide valuable insight into the process operation that can be used for process model development. Nevertheless, this review has shown that the available data were not detailed enough for any test facility to be useful for detailed process model validation. This is caused by, for example, the uncertainty associated with the solid looping rate measurements. To allow detailed process model validation, however, more detailed data should be reported for future tests.

The CaL experimental trials have revealed that the actual CO_2 capture level can be close to that determined by equilibrium provided sufficient solids inventory of moderate conversion and looping rate are maintained. However, deterioration of the sorbent performance, triggered mainly by sintering and sulphation, requires relatively high make-up rates to reach the desired level of average sorbent conversion, which affects the economic performance of the system. Therefore, the further developments of the sorbent performance enhancement measures and/or novel sorbents experiencing lower performance deterioration need to be pursued in the near to mid-term timescale.

To date, the predictions of process performance have been modelled with different levels of complexity. Five levels can be distinguished, which differ in application of the kinetic or equilibrium reactions, considering the concentration changes in the gas and solid phases and implementation of FB hydrodynamics. Importantly, the effect of sulphation on the sorbent activity and inert solids accumulation in the system were rarely included in the models available in the literature. Therefore, to improve the accuracy and reliability of the overall process performance prediction, future models should account for sorbent sulphation and ash accumulation.

Application of the CaL plant to typical coal-based power generation systems was found to impose lower efficiency penalties (6–7% points), compared to conventional CO_2 capture systems, proving the technology viability. Moreover, novel power generation systems that are based on the CaL process have been proposed, and reach net thermal efficiencies close to those of ultrasupercritical CFPPs without CO_2 capture. This implies that the CaL plant can serve as a base system for development of state-of-the-art power generation systems that could be implemented on a large scale in place of current technologies. Nevertheless, it is highlighted that the analyses performed to date used not only different CaL modelling approaches, but more importantly they employed different reference power plants and sets of CaL operating conditions. As this restricts the accuracy of process performance comparison across these analyses, the baseline reference models for the power plant and CaL plant need to be developed. In the near term, such baseline models would allow a reliable comparison of the process performances of the further analyses of the CaL process improvements.

List of abbreviations

AGR	Acid gas removal
ASU	Air separation unit
BFB	Bubbling fluidised bed
CaL	Calcium looping
CaRS-CO_2	Calcium-based reaction separation for CO_2
CCR	Carbonation–calcination reaction process
CCS	Carbon capture and storage
CCU	CO_2 compression unit
CFB	Circulating fluidised bed
CFD	Computational fluid dynamics

CFPP	Coal-fired power plant
DFB	Dual fluidised bed
EB	Entrained bed
FGD	Flue gas desulphurisation unit
HEN	Heat exchanger networks
IFK	The Institute of Combustion and Power Plant Technology (Institut für Feuerungs-und Kraftwerkstechnik)
IGCC	Integrated-gasification combined cycle power plant
INCAR-CSIC	The Instituto Nacional del Carbón – Consejo Superior de Investigaciones Científicas
ITRI	The Industrial Technology Research Institute
K–L	Kunii and Levenspiel model
MB	Moving bed
MDEA	Methyldiethanolamine
MEA	Monoethanolamine
NGCC	Natural gas combined cycle power plant
OSCAR	The Ohio State carbonation ash reactivation process
PZ	Piperazine
RK	Rotary kiln
SER	Sorption-enhanced reforming process
SME	Sorption-enhanced methane steam reforming
TGA	Thermo-gravimetric analyser
ZECOMAG	Zero-emissions coal mixed technology with air gas turbine
ZECOMIX	Zero-emissions coal mixed technology

Nomenclature

Latin symbols

A	Bed cross-section area, m^2
a_1	Fitting parameter in Li and Cai[133] correlation, —
a_2	Fitting parameter in Li and Cai[133] correlation, —
c_0	Freundlich isotherm characteristic, —
C_i	Concentration of species i, kmol m^{-3}
D	Diffusivity coefficient, m^2 s^{-1}
d_b	Bubble diameter, m s^{-1}
E	Activation energy, J $kmol^{-1}$
E_{carb}	CO_2 capture level in the carbonator, —
E_{calc}	Efficiency of the calciner, —
f	Extent of calcination or carbonation, —
F_0	$CaCO_3$ makeup rate, kmol s^{-1}
f_1	Fitting parameter in Li and Cai[133] correlation, —
f_2	Fitting parameter in Li and Cai[133] correlation, —
f_a	Active fraction of particles, —
F_{CO_2}	CO_2 flow rate in the flue gas, kmol s^{-1}
F_H	Sorbent rate diverted to the hydrator, kmol s^{-1}
F_R	CaO looping rate, kmol s^{-1}
h	$CaCO_3$ layer thickness, nm
H_D	Height of the dense phase, m
k	Kinetic rate constant or sorbent deactivation constant or proportionality constant, 1 s^{-1}, m^3 mol^{-1} s^{-1}, m^4 mol^{-1} s^{-1}, —
K_{be}	Bubble and emulsion interchange coefficient, —
k_g	Mass transfer coefficient, m s^{-1}
N	Number of calcination–carbonation cycle, —
n	Sorbent sintering exponent or number of active sites in Langmuir–Hinshelwood mechanism, —
N_{Ca}	Mole inventory of CaO in the bed, kmol
M_i	Molar mass of species i, kg $kmol^{-1}$
P_{CO_2}	Partial pressure of CO_2, atm
r	Reaction rate, kmol m^{-3} s^{-1}, 1 s^{-1}
R	Particle radius, m
r_0	Mole fraction of particles that has never been calcined or initial grain radius, — or m
$r_{C/S}$	Molar ratio of carbon and sulphur in the fuel, —
Re	Reynolds number, —
R_g	Gas constant, J $kmol^{-1}$ K^{-1}
r_N	Mass fraction of particles that has undergone N carbonation–calcination cycles, —
r_i	Un-reacted radius of CaO grain, M
S	Particle surface area, m^2 m^{-3}
Sc	Schmidt number, —
Sh	Sherwood number, —
T	Temperature, K
t^*	Actual residence time, s
u_0	Superficial gas velocity, m s^{-1}
u_b	Bubble rise velocity, m s^{-1}
u_b^*	Rising bubble gas velocity, m s^{-1}
v_{CO_2}	Volume fraction of CO_2 in the gas phase, —
$V_{M,i}$	Molar volume of species i, m^3 $kmol^{-1}$
W_{CaO}	Mass inventory of CaO in the bed, kg
X	Sorbent conversion, —
y_{comb}	mass ratio between fuel going to the main combustor and total fuel into the plant, —

Greek symbols

δ	Volume of bubbles per unit bed volume, —
ε	Porosity of sorbent particle or solid fraction in the reactor, —
θ	Fraction of the active sites, —
ρ_i	Mass density of species i, kg m^{-3}
τ	Average residence time, s
φ_e	Effectivity factor, —
Φ_s	Particle sphericity, —
Ψ	Sorbent pore structural parameter, —

Superscripts

H	Hydrated sorbent

Subscripts

0	Initial conditions
ave,max	Refer to maximum average sorbent conversion
b	Refer to bubble zone
calc	Variable related to calciner operating conditions or stream leaving calciner
carb	Variable related to carbonator operating conditions or stream leaving carbonator
e	Refer to emulsion zone

eq	Equilibrium conditions
mf	Refer to minimum fluidising conditions
max	Refer to maximum sorbent conversion
r	Refer to residual sorbent conversion
s	Refer to intrinsic kinetic constant

References

1 European Commission, *Communication from the Commission to the European Parliament, the Council, the European Economic and Social Committee and the Committee of the Regions, International climate policy post-Copenhagen: Acting now to reinvigorate global action on climate change*, COM(2010) 86, Commission of the European Communities, Brussels, Belgium, 2010.

2 European Commission, *Communication from the Commission to the European Parliament, the Council, the European Economic and Social Committee and the Committee of the Regions, A policy framework for climate and energy in the period from 2020 to 2030*, European Commission, COM(2014) 15, Brussels, Belgium, 2014.

3 European Council, *European Council 23/24 October 2014 – Conclusions, EUCO gv 169/14 CO EUR 13 CONCL 5*, European Commission, Brussels, Belgium, 2014.

4 European Commission, *Communication from the Commission to the European Parliament, the Council, the European Economic and Social Committee of the Regions - Energy Roadmap 2050*, COM(2011) 885/2, European Commission, Brussels, Belgium, 2011.

5 UNEP, *The Emissions Gap Report 2012*, United Nations Environment Programme (UNEP), Nairobi, Kenya, 2012.

6 IEA, *Tracking Clean Energy Progress 2013. IEA Input to the Clean Energy Ministerial*, IEA Publications, Paris, France, 2013.

7 IEA, *Power generation from coal: Measuring and reporting efficiency performance and CO_2 emissions,* IEA Publications, Paris, France, 2010.

8 EIA, *International Energy Outlook 2011, DOE/EIA-0484(2011)*, U.S. Energy Information Administration, Washington, USA, 2011.

9 IEA, *Technology Roadmap: Carbon capture and storage*, IEA Publications, Paris, France, 2013.

10 K. Stéphenne, Start-up of world's first commercial post-combustion coal fired ccs project: Contribution of Shell CANSOLV to Saskpower Boundary Dam ICCS project, in *12thInternational Conference on Greenhouse Gas Control Technologies*, ed. T. Dixon, S. Twinning and H. Herzog, GHGT, Austin, TX, USA, 2014, vol. 63, p. 6106.

11 N. Rodríguez, M. Alonso and J. C. Abanades, Average activity of CaO particles in a calcium looping system, *Chem. Eng. J.*, 2010, **156**(2), 388–394.

12 A. S. Bhown and B. C. Freeman, Analysis and status of post-combustion carbon dioxide capture technologies, *Environ. Sci. Technol.*, 2011, **45**(20), 8624–8632.

13 J. Blamey, E. Anthony, J. Wang and P. Fennell, The calcium looping cycle for large-scale CO_2 capture, *Prog. Energy Combust. Sci.*, 2010, **36**(2), 260–279.

14 C. C. Dean, J. Blamey, N. H. Florin, M. J. Al-Jeboori and P. S. Fennell, The calcium looping cycle for CO_2 capture from power generation, cement manufacture and hydrogen production, *Chem. Eng. Res. Des.*, 2011, **89**, 836–855.

15 M. E. Boot-Handford, J. C. Abanades, E. J. Anthony, M. J. Blunt, S. Brandani, N. Mac Dowell, J. R. Fernandez, M. C. Ferrari, R. Gross, J. P. Hallett, R. S. Haszeldine, P. Heptonstall, A. Lyngfelt, Z. Makuch, E. Mangano, R. T. J. Porter, M. Pourkashanian, G. T. Rochelle, N. Shah, J. G. Yao and P. S. Fennell, Carbon capture and storage update, *Energy Environ. Sci.*, 2014, **7**, 130–189.

16 Y. Yang, R. Zhai, L. Duan, M. Kavosh, K. Patchigolla and J. Oakey, Integration and evaluation of a power plant with a CaO-based CO_2 capture system, *Int. J. Greenhouse Gas Control*, 2010, **4**(4), 603–612.

17 G. Xu, H. G. Jin, Y. P. Yang, Y. J. Xu, H. Lin and L. Duan, A comprehensive techno-economic analysis method for power generation systems with CO2 capture, *Int. J. Energy Res.*, 2010, **34**(4), 321–332.

18 K. Goto, K. Yogo and T. Higashii, A review of efficiency penalty in a coal-fired power plant with post-combustion CO_2 capture, *Appl. Energy*, 2013, **111**, 710–720.

19 B. R. Stanmore and P. Gilot, Review—calcination and carbonation of limestone during thermal cycling for CO_2 sequestration, *Fuel Process. Technol.*, 2005, **86**(16), 1707–1743.

20 D. P. Harrison, Sorption-Enhanced Hydrogen Production: A Review, *Ind. Eng. Chem. Res.*, 2008, **47**(17), 6486–6501.

21 N. H. Florin and A. T. Harris, Enhanced hydrogen production from biomass with in situ carbon dioxide capture using calcium oxide sorbents, *Chem. Eng. Sci.*, 2008, **63**(2), 287–316.

22 E. J. Anthony, Ca looping technology: Current status, developments and future directions, *Greenhouse Gases: Sci. Technol.*, 2011, **1**(1), 36–47.

23 W. Liu, H. An, C. Qin, J. Yin, G. Wang, B. Feng and M. Xu, Performance enhancement of calcium oxide sorbents for cyclic CO_2 capture-a review, *Energy Fuels*, 2012, **26**(5), 2751–2767.

24 A. M. Kierzkowska, R. Pacciani and C. R. Müller, CaO-based CO_2 sorbents: From fundamentals to the development of new, highly effective materials, *ChemSusChem*, 2013, **6**(7), 1130–1148.

25 M.C. Romano, I. Martínez, R. Muroillo, B. Arstad, R. Blom, D.C. Ozcan, H. Ahn and S. Brandani, Process simulation of Ca-looping processes: Review and guidelines, 2013, 11th International Conference on Greenhouse Gas Control Technologies, GHGT 2012, 37, 18-22 November 2012, Kyoto, Japan, 142.

26 W. Wang, S. Ramkumar and L. Fan, Energy penalty of CO_2 capture for the Carbonation–Calcination Reaction (CCR) Process: Parametric effects and comparisons with alternative processes, *Fuel*, 2013, **104**, 561–574.

27 T. Hirama, H. Hosoda, K. Kitano and T. Shimizu, *Method of separating carbon dioxide from carbon dioxide containing gas and combustion apparatus having function to separate carbon dioxide from the combustion gas*, *UK Pat.*, 2291051A, 1996.

28 T. Shimizu, T. Hirama, H. Hosoda, K. Kitano, M. Inagaki and K. Tejima, A Twin Fluid-Bed Reactor for Removal of CO_2 from Combustion Processes, *Chem. Eng. Res. Des.*, 1999, **77**(1), 62–68.

29 R. W. Hughes, D. Y. Lu, E. J. Anthony and A. Macchi, Design, process simulation and construction of an atmospheric dual fluidized bed combustion system for in situ CO2 capture using high-temperature sorbents, *Fuel Process. Technol.*, 2005, **86**(14–15), 1523–1531.

30 M. Alonso, N. Rodríguez, G. Grasa and J. C. Abanades, Modelling of a fluidized bed carbonator reactor to capture CO_2 from a combustion flue gas, *Chem. Eng. Sci.*, 2009, **64**(5), 883–891.

31 A. Lasheras, J. Ströhle, A. Galloy and B. Epple, Carbonate looping process simulation using a 1D fluidized bed model for the carbonator, *Int. J. Greenhouse Gas Control*, 2011, **5**(4), 686–693.

32 W. Wang, S. Ramkumar, D. Wong and L. Fan, Simulations and process analysis of the carbonation–calcination reaction process with intermediate hydration, *Fuel*, 2012, **92**(1), 94–106.

33 D. Y. Lu, R. W. Hughes and E. J. Anthony, Ca-based sorbent looping combustion for CO2 capture in pilot-scale dual fluidized beds, *Fuel Process. Technol.*, 2008, **89**(12), 1386–1395.

34 J. M. Valverde, A model on the CaO multicyclic conversion in the Ca-looping process, *Chem. Eng. J.*, 2013, **228**, 1195–1206.

35 J. Yin, C. Qui, B. Feng, L. Ge, C. Luo, W. Liu and H. An, Calcium Looping for CO_2 Capture at a Constant High Temperature, *Energy Fuels*, 2014, **28**(1), 307–318.

36 E. H. Baker, The calcium oxide-carbon dioxide system in the pressure range 1-300 atmospheres, *J. Chem. Soc.*, 1962, 464–470.

37 I. Martínez, R. Murillo, G. Grasa and J. C. Abanades, Integration of a Ca-looping system for CO_2 capture in an existing power plant, *Energy Procedia*, 2011, **4**, 1699–1706.

38 J. Valverde, P. E. Sanchez-Jimenez, A. Perejon and L. A. Perez-Maqueda, CO_2 multicyclic capture of pretreated/doped CaO in the Ca-looping process. Theory and experiments, *Phys. Chem. Chem. Phys.*, 2013, **15**, 11775–11793.

39 J. C. Abanades, E. J. Anthony, J. Wang and J. E. Oakey, Fluidized Bed Combustion Systems Integrating CO_2 Capture with CaO, *Environ. Sci. Technol.*, 2005, **39**(8), 2861–2866.

40 N. Rodriguez, M. Alonso, G. Grasa and J. C. Abanades, Heat requirements in a calciner of $CaCO_3$ integrated in a CO_2 capture system using CaO, *Chem. Eng. J.*, 2008, **138**(1–3), 148–154.

41 V. Manovic and E. J. Anthony, Improvement of CaO-based sorbent performance for CO_2 looping cycles, *J. Therm. Sci.*, 2009, **13**(1), 89–104.

42 C. J. Abanades and D. Alvarez, Conversion limits in the reaction of CO_2 with lime, *Energy Fuels*, 2003, **17**, 308–315.

43 R. H. Borgwardt, Calcium oxide sintering in atmospheres containing water and carbon dioxide, *Ind. Eng. Chem. Res.*, 1989, **28**(4), 493–500.

44 L. Zhen-Shan and C. Ning-Sheng, Process analysis of CO_2 capture from flue gas using carbonation–calcination cycles, *Environmental and Energy Engineering*, 2008, **54**(7), 1912–1925.

45 F. García-Labiano, A. Rufas, L. F. De Diego, M. D. L. Obras-Loscertales, P. Gayán, A. Abad and J. Adánez, Calcium-based sorbents behaviour during sulphation at oxy-fuel fluidised bed combustion conditions, *Fuel*, 2011, **90**(10), 3100–3108.

46 M. C. Duke, B. Ladewig, S. Smart, V. Rudolph and J. C. D. Da Costa, Assessment of post-combustion carbon capture technologies for power generation, *Front. Chem. Eng. China*, 2010, **4**(2), 184–195.

47 M. Maroto-Valer, *Developments and Innovation in Carbon Dioxide (CO_2) Capture and Storage Technology, Volume 1 - Carbon Dioxide (CO_2) Capture, Transport and Industrial Applications,* Woodhead Publishing, Cambridge, UK, 2010.

48 S. A. Rackley, *Carbon Capture and Storage*, Elsevier, Burlington, USA, 2010.

49 B. Zhao and Y. Su, Process effect of microalgal-carbon dioxide fixation and biomass production: A review, *Renewable Sustainable Energy Rev.*, 2014, **31**, 121–132.

50 H. S. Kheshgi, H. Thomann, N. A. Bhore, R. B. Hirsch, M. E. Parker and G. F. Teletzke, Perspectives on CCS cost and economics, *SPE Economics and Management*, 2012, **4**(1), 24–31.

51 M. Renner, Carbon prices and CCS investment: A comparative study between the European Union and China, *Energy Policy*, 2014, **75**, 327–340.

52 CSIRO, *Assessing Post-Combustion Capture for Coal-fired Power Stations in Asia-Pacific Partnership Countries, EP116217*, CSIRO Advanced Coal Technology, Newcastle, NW, USA, 2012.

53 A. B. Rao and E. S. Rubin, A Technical, Economic and Environmental Assessment of Amine-Based CO_2 Capture Technology for Power Plant Greenhouse Gas Control, *Environ. Sci. Technol.*, 2002, **36**(20), 4467–4475.

54 R. R. Bottoms, *Process for separating acidic gases*, *U.S. Pat.*, 1783901, 1930, available online at: http://bit.ly/1GIWnoS, accessed 30/05/2015.

55 L. Kohl and R. B. Nielsen, *Gas purification*, 5th edn, Gulf Publishing Company, Huston, Texas, USA, 1997.

56 L. E. Öi, CO_2 removal by absorption: Challenges in modelling, *Math. Comp. Model. Dyn.*, 2010, **16**(6), 511–533.

57 J. C. M. Pires, F. G. Martins, M. C. M. Alvim-Ferraz and M. Simões, Recent developments on carbon capture and storage: an overview, *Chem. Eng. Res. Des.*, 2011, **89**(9), 1446–1460.

58 E. S. Rubin, H. Mantripragada, A. Marks, P. Versteeg and J. Kitchin, The outlook for improved carbon capture technology, *Prog. Energy Combust. Sci.*, 2012, **38**(5), 630–671.

59 P. Folger, *Carbon Capture: A Technology Assessment, R41325*, Congressional Research Service, 2013available online at: http://bit.ly/1esPfhA, accessed 30/05/2015.

60 D. P. Hanak, C. Biliyok, H. Yeung and R. Białecki, Heat integration and exergy analysis for a high ash supercritical coal-fired power plant integrated with a post-combustion carbon capture process, *Fuel*, 2014, **134**, 126–139.

61 H. M. Kvamsdal, M. C. Romano, L. van der Ham, D. Bonalumi, P. van Os and E. Goetheer, Energetic evaluation of a power plant integrated with a piperazine-based

CO_2 capture process, *Int. J. Greenhouse Gas Control*, 2014, **28**(1), 343–355.

62 D. H. Van Wagener, U. Liebenthal, J. M. Plaza, A. Kather and G. T. Rochelle, Maximizing coal-fired power plant efficiency with integration of amine-based CO_2 capture in greenfield and retrofit scenarios, *Energy*, 2014, **72**, 824–831.

63 R. Strube and G. Manfrida, CO_2 capture in coal-fired power plants - impact on plant performance, *Int. J. Greenhouse Gas Control*, 2011, **5**(4), 710–726.

64 R. Shao and A. Stangeland, *Amines Used in CO_2 Capture - Health and Environmental Impacts,* The Bellona Foundation, 2009, available at: http://bit.ly/1fpznvO, accessed 30/05/2015.

65 B. Thitakamol, A. Veawab and A. Aroonwilas, Environmental impacts of absorption-based CO_2 capture unit for post-combustion treatment of flue gas from coal-fired power plant, *Int. J. Greenhouse Gas Control*, 2007, **1**(3), 318–342.

66 K. Veltman, B. Singh and E. G. Hertwich, Human and Environmental Impact Assessment of Postcombustion CO_2 Capture Focusing on Emissions from Amine-Based Scrubbing Solvents to Air, *Environ. Sci. Technol.*, 2010, **44**(4), 1496–1502.

67 H. Bai and A. C. Yeh, Removal of CO_2 Greenhouse Gas by Ammonia Scrubbing, *Ind. Eng. Chem. Res.*, 1997, **36**(6), 2490–2493.

68 T. Brown, C. C. Perry and B. Manthey, *Pleasant Prairie carbon capture demonstration project, Progress report*, Alstom, Wisconsin, 2009.

69 V. Telikapalli, F. Kozak, J. Francois, B. Sherrick, J. Black, D. Muraskin, M. Cage, M. Hammond and G. Spitznogle, CCS with the Alstom chilled ammonia process development program–Field pilot results, *Energy Procedia*, 2011, **4**, 273–281.

70 H. Yu, S. Morgan, A. Allport, A. Cottrell, T. Do, J. McGregor, L. Wardhaugh and P. Feron, Results from trialling aqueous NH_3 based post-combustion capture in a pilot plant at Munmorah power station: Absorption, *Chem. Eng. Res. Des.*, 2011, **89**(8), 1204–1215.

71 J. P. Ciferno, P. DiPietro and T. Tarka, *An economic scoping study for CO_2 capture using aqueous ammonia,* National Energy Technology Laboratory, Advanced Resources International, Energetics Incorporated, 2005.

72 E. Gal, *Chilled-ammonia Post Combustion CO_2 Capture System–Laboratory and Economic Evaluation Results, 1012797,* EPRI, Palo Alto, CA, USA, 2006.

73 L. M. Romeo, S. Espatolero and I. Bolea, Designing a supercritical steam cycle to integrate the energy requirements of CO_2 amine scrubbing, *Int. J. Greenhouse Gas Control*, 2008, **2**(4), 563–570.

74 M. Wang, A. Lawal, P. Stephenson, J. Sidders and C. Ramshaw, Post-combustion CO_2 capture with chemical absorption: A state-of-the-art review, *Chem. Eng. Res. Des.*, 2011, **89**(9), 1609–1624.

75 K. P. Resnik, J. T. Yeh and H. W. Pennline, Aqua ammonia process for simultaneous removal of CO_2, SO_2 and NO_x, *Int. J. Environ. Technol. Manage.*, 2004, **4**(1–2), 89–104.

76 F. Shakerian, K. Kim, J. E. Szulejko and J. Park, A comparative review between amines and ammonia as sorptive media for post-combustion CO_2 capture, *Appl. Energy*, 2015, **148**, 10–22.

77 B. Zhao, Y. Su, W. Tao, L. i. Li and Y. Peng, Post-combustion CO_2 capture by aqueous ammonia: A state-of-the-art review, *Int. J. Greenhouse Gas Control*, 2012, **9**, 355–371.

78 M. Zhao, A. I. Minett and A. T. Harris, A review of techno-economic models for the retrofitting of conventional pulverised-coal power plants for post-combustion capture (PCC) of CO_2, *Energy Environ. Sci.*, 2013, **6**(1), 25–40.

79 B. Sutton, Statement from Peabody Energy on the Department Of Energy's decision to suspend FutureGen, *Peabody Energy*, 2015, available online at http://bit.ly/1LsNh3d, 18/03/2015.

80 C. Marshall and M. Quiñones, Clean Coal Power Plant Killed, Again, *Sci. Am.*, 2015, available online at: http://bit.ly/1DAqa2i, 18/03/2015.

81 R. Soundararajan and T. Gundersen, Coal based power plants using oxy-combustion for CO_2 capture: Pressurized coal combustion to reduce capture penalty, *Appl. Therm. Eng.*, 2013, **61**(1), 115–122.

82 R. Soundararajan, T. Gundersen and M. Ditaranto, *Oxy-combustion coal based power plants: Study of operating pressure, oxygen purity and downstream purification parameters*, Italian Association of Chemical Engineering – AIDIC, 2014.

83 I. Martínez, R. Murillo, G. Grasa and J. Carlos Abanades, Integration of a Ca looping system for CO_2 capture in existing power plants, *AIChE J.*, 2011, **57**(9), 2599–2607.

84 M. C. Romano, Modeling the carbonator of a Ca-looping process for CO_2 capture from power plant flue gas, *Chem. Eng. Sci.*, 2012, **69**(1), 257–269.

85 N. Markusson, The politics of FGD deployment in the UK (1980s-2009), *Case study for the project CCS: Realising the potential*, University of Edinburgh, Edinburgh, Scotland, 2012.

86 L. M. Romeo, J. C. Abanades, J. M. Escosa, J. Paño, A. Giménez, A. Sánchez-Biezma and J. C. Ballesteros, Oxyfuel carbonation–calcination cycle for low cost CO_2 capture in existing power plants, *Energy Convers. Manage.*, 2008, **49**(10), 2809–2814.

87 J. C. Abanades, G. Grasa, M. Alonso, N. Rodriguez, E. J. Anthony and L. M. Romeo, Cost structure of a postcombustion CO_2 capture system using CaO, *Environ. Sci. Technol.*, 2007, **41**(15), 5523–5527.

88 C. C. Cormos, Economic evaluations of coal-based combustion and gasification power plants with post-combustion CO_2 capture using calcium looping cycle, *Energy*, 2014, **78**, 665–673.

89 C. C. Cormos, Assessment of chemical absorption/adsorption for post-combustion CO_2 capture from Natural Gas Combined Cycle (NGCC) power plants, *Appl. Therm. Eng.*, 2015, **82**, 120–128.

90 C. Huang, H. Hsu, W. Liu, J. Cheng, W. Chen, T. Wen and W. Chen, Development of post-combustion CO_2 capture with $CaO/CaCO_3$ looping in a bench scale plant, *Energy Procedia*, 2011, **4**, 1268–1275.

91 M. H. Chang, C. M. Huang, W. H. Liu, W. C. Chen, J. Y. Cheng, W. Chen, T. W. Wen, S. Ouyang, C. H. Shen and

H. W. Hsu, Design and Experimental Investigation of Calcium Looping Process for 3-kW_{th} and 1.9-MW_{th} Facilities, *Chem. Eng. Technol.*, 2013, **36**(9), 1525–1532.

92 X. CCSA, Taiwan inaugurates advanced carbon capture plant, *CCSA Weekly Newsletter*, 2013, **212**(2), 4.

93 N. Rodríguez, M. Alonso and J. C. Abanades, Experimental investigation of a circulating fluidized-bed reactor to capture CO_2 with CaO, *AIChE J.*, 2011, **57**(5), 1356–1366.

94 M. Alonso, N. Rodríguez, B. González, G. Grasa, R. Murillo and J. C. Abanades, Carbon dioxide capture from combustion flue gases with a calcium oxide chemical loop. Experimental results and process development, *Int. J. Greenhouse Gas Control*, 2010, **4**(2), 167–173.

95 A. Sánchez-Biezma, J. C. Ballesteros, L. Diaz, E. de Zárraga, F. J. Álvarez, J. López, B. Arias, G. Grasa and J. C. Abanades, Postcombustion CO_2 capture with CaO. Status of the technology and next steps towards large scale demonstration, *Energy Procedia*, 2011, **4**, 852–859.

96 B. Arias, M. E. Diego, J. C. Abanades, M. Lorenzo, L. Diaz, D. Martínez, J. Alvarez and A. Sánchez-Biezma, Demonstration of steady state CO_2 capture in a 1.7MW_{th} calcium looping pilot, *Int. J. Greenhouse Gas Control*, 2013, **18**, 237–245.

97 A. Sánchez-Biezma, J. Paniagua, L. Diaz, M. Lorenzo, J. Alvarez, D. Martínez, B. Arias, M. E. Diego and J. C. Abanades, Testing postcombustion CO_2 capture with CaO in a 1.7 MW_t pilot facility, *Energy Procedia*, 2013, **37**, 1–8.

98 J. Ströhle, M. Junk, J. Kremer, A. Galloy and B. Epple, Carbonate looping experiments in a 1 MWth pilot plant and model validation, *Fuel*, 2014, **127**, 13–22.

99 L. Bates, Screw conveyors, in *Bulk solids handling: equipment selection and operation*, ed. D. McGlinchey, Blackwell Publishing Ltd, UK, 2008, 1st edn, pp. 197–220.

100 N. Rodríguez, M. Alonso, J. C. Abanades, A. Charitos, C. Hawthorne, G. Scheffknecht, D. Y. Lu and E. J. Anthony, Comparison of experimental results from three dual fluidized bed test facilities capturing CO_2 with CaO, *Energy Procedia*, 2011, **4**, 393–401.

101 A. Charitos, C. Hawthorne, A. R. Bidwe, L. Korovesis, A. Schuster and G. Scheffknecht, Hydrodynamic analysis of a 10 kW_{th} Calcium Looping Dual Fluidized Bed for post-combustion CO_2 capture, *Powder Technol.*, 2010, **200**(3), 117–127.

102 H. Dieter, A. R. Bidwe, G. Varela-Duelli, A. Charitos, C. Hawthorne and G. Scheffknecht, Development of the calcium looping CO_2 capture technology from lab to pilot scale at IFK, University of Stuttgart, *Fuel*, 2014, **127**, 23–37.

103 A. Charitos, C. Hawthorne, A. R. Bidwe, S. Sivalingam, A. Schuster, H. Spliethoff and G. Scheffknecht, Parametric investigation of the calcium looping process for CO_2 capture in a 10 kW_{th} dual fluidized bed, *Int. J. Greenhouse Gas Control*, 2010, **4**(5), 776–784.

104 H. Dieter, C. Hawthorne, M. Zieba and G. Scheffknecht, Progress in Calcium Looping Post Combustion CO_2 Capture: Successful Pilot Scale Demonstration, *Energy Procedia*, 2013, **37**, 48–56.

105 C. Hawthorne, H. Dieter, A. Bidwe, A. Schuster, G. Scheffknecht, S. Unterberger and M. Käß, CO_2 capture with CaO in a 200 kW_{th} dual fluidized bed pilot plant, *Energy Procedia*, 2011, **4**, 441–448.

106 H. Dieter, Design concepts, operating experiences and experimental results of the 200 kW_{th} calcium-looping pilot plant, *2nd International Workshop on Oxy-FBC Technology*, 28-29 June, Stuttgart, 2012, available at: http://bit.ly/1aqVqok, 30/05/2015.

107 G. Varela, A. Charitos, M. E. Diego, E. Stavroulakis, H. Dieter and G. Scheffknecht, Investigations at a 10 kW_{th} calcium looping dual fluidized bed facility: Limestone calcination and CO_2 capture under high CO_2 and water vapor atmosphere, *Int. J. Greenhouse Gas Control*, 2015, **33**, 103–112.

108 A. Ghosh-Dastidar and S. Mahuli, *Calcium carbonate sorbent and methods of making and using same*, *US Pat.*, 5779464, 1998.

109 S. Mahuli and R. Agnihotri, *Suspension carbonation process of reaction of partially utilized sorbent*, *US Pat.*, 6309996 B1, 2001.

110 H. Gupta, T. J. Thomas, A. A. Park, M. V. Iyer, P. Gupta, R. Agnihotri, R. A. Jadhav, H. W. Walker, L. K. Weavers, T. Butalia and L. Fan, Pilot-scale demonstration of the OSCAR process for high-temperature multipollutant control of coal combustion flue gas, using carbonated fly ash and mesoporous calcium carbonate, *Ind. Eng. Chem. Res.*, 2007, **46**(14), 5051–5060.

111 L. Fan, H. Gupta and M. V. Iyer, *Separation of carbon dioxide (CO_2) from gas mixtures by calcium based reaction reparation (CaRS-CO_2) process, US Pat., 0233029, 2008.*

112 W. Wang, S. Ramkumar, S. Li, D. Wong, M. Iyer, B. B. Sakadjian, R. M. Statnick and L. Fan, Subpilot demonstration of the carbonation-calcination reaction (CCR) process: High-temperature CO_2 and sulfur capture from coal-fired power plants, *Ind. Eng. Chem. Res.*, 2010, **49**(11), 5094–5101.

113 R. T. Symonds, D. Y. Lu, R. W. Hughes, E. J. Anthony and A. Macchi, CO_2 capture from simulated syngas via cyclic carbonation–calcination for a naturally occurring limestone: Pilot-plant testing, *Ind. Eng. Chem. Res.*, 2009, **48**(18), 8431–8440.

114 A. Cotton, K. N. Finney, K. Patchigolla, R. E. A. Eatwell-Hall, J. E. Oakey, J. Swithenbank and V. Sharifi, Quantification of trace element emissions from low-carbon emission energy sources: (I) Ca-looping cycle for post-combustion CO2 capture and (II) fixed bed, air blown down-draft gasifier, *Chem. Eng. Sci.*, 2014, **107**, 13–29.

115 A. M. Cotton, *Engineering scale-up and environmental effects of the calcium looping cycle for post-combustion CO_2 capture, PhD thesis,* Cranfield University, Cranfield, UK, 2013.

116 M. Kavosh, *Process engineering and development of post-combustion CO_2 separation from fuels using limestone in CaO-looping cycle, PhD thesis,* Cranfield University, Cranfield, 2011.

117 D. Geldart, Types of gas fluidization, *Powder Technol.*, 1973, **7**(5), 285–292.

118 F. Fang, Z. S. Li and N. S. Cai, Continuous CO_2 capture from flue gases using a dual fluidized bed reactor with

calcium-based sorbent, *Ind. Eng. Chem. Res.*, 2009, **48**(24), 11140–11147.

119 I. Aigner, C. Pfeifer and H. Hofbauer, Co-gasification of coal and wood in a dual fluidized bed gasifier, *Fuel*, 2011, **90**(7), 2404–2412.

120 C. Pfeifer, J.C. Schmid, T. Pröll and H. Hofbauer, Next generation biomass gasifier, Proceedings of the 19th European Biomass Conference and Exhibition, June 6-10 2010, Berlin, Germany, 2010.

121 M. Broda, V. Manovic, Q. Imtiaz, A. M. Kierzkowska, E. J. Anthony and C. R. Müller, High-purity hydrogen via the sorption-enhanced steam methane reforming reaction over a synthetic CaO-based sorbent and a Ni catalyst, *Environ. Sci. Technol.*, 2013, **47**(11), 6007–6014.

122 J. R. Hufton, S. Mayorga and S. Sircar, Sorption-enhanced reaction process for hydrogen production, *AIChE J.*, 1999, **45**(2), 248–256.

123 S. Rawadieh and V. G. Gomes, Steam reforming for hydrogen generation with in situ adsorptive separation, *Int. J. Hydrogen Energy*, 2009, **34**(1), 343–355.

124 H. Hofbauer, R. Rauch, K. Bosch, R. Koch and C. Aichernig, Biomass CHP Plant Güssing – A Success Story, in *Pyrolysis and Gasification of Biomass and Waste*, ed. A. V. Bridgwater, CPL Press, Newsbury, UK, 2003, pp. 371–383.

125 S. Koppatz, C. Pfeifer, R. Rauch, H. Hofbauer, T. Marquard-Moellenstedt and M. Specht, H_2 rich product gas by steam gasification of biomass with in situ CO_2 absorption in a dual fluidized bed system of 8 MW fuel input, *Fuel Process. Technol.*, 2009, **90**(7–8), 914–921.

126 F. Kirnbauer, V. Wilk and H. Hofbauer, Performance improvement of dual fluidized bed gasifiers by temperature reduction: The behavior of tar species in the product gas, *Fuel*, 2013, **108**, 534–542.

127 M. C. Romano and G. G. Lozza, Long-term coal gasification-based power with near-zero emissions. Part B: Zecomag and oxy-fuel IGCC cycles, *Int. J. Greenhouse Gas Control*, 2010, **4**(3), 469–477.

128 C. C. Cormos and A. M. Cormos, Assessment of calcium-based chemical looping options for gasification power plants, *Int. J. Hydrogen Energy*, 2013, **38**(5), 2306–2317.

129 D. P. Connell, D. A. Lewandowski, S. Ramkumar, N. Phalak, R. M. Statnick and L. Fan, Process simulation and economic analysis of the Calcium Looping Process (CLP) for hydrogen and electricity production from coal and natural gas, *Fuel*, 2013, **105**, 383–396.

130 D. Wang, S. Chen, C. Xu and W. Xiang, Energy and exergy analysis of a new hydrogen-fueled power plant based on calcium looping process, *Int. J. Hydrogen Energy*, 2013, **38**(13), 5389–5400.

131 C. Kunze, S. De and H. Spliethoff, A novel IGCC plant with membrane oxygen separation and carbon capture by carbonation-calcinations loop, *Int. J. Greenhouse Gas Control*, 2011, **5**(5), 1176–1183.

132 I. Vorrias, K. Atsonios, A. Nikolopoulos, N. Nikolopoulos, P. Grammelis and E. Kakaras, Calcium looping for CO_2 capture from a lignite fired power plant, *Fuel*, 2013, **113**, 826–836.

133 A. Martínez, Y. Lara, P. Lisbona and L. M. Romeo, Energy penalty reduction in the calcium looping cycle, *Int. J. Greenhouse Gas Control*, 2012, **7**, 74–81.

134 I. Martínez, G. Grasa, R. Murillo, B. Arias and J. C. Abanades, Modelling the continuous calcination of $CaCO_3$ in a Ca-looping system, *Chem. Eng. J.*, 2013, **215–216**, 174–181.

135 F. Fang, Z. Li and N. Cai, Experiment and modeling of CO_2 capture from flue gases at high temperature in a fluidized bed reactor with Ca-based sorbents, *Energy Fuels*, 2009, **23**(1), 207–216.

136 C. J. Abanades, E. J. Anthony, D. Y. Lu, C. Salvador and D. Alvarez, Capture of CO_2 from combustion gases in a fluidized bed of CaO, *Environmental and Energy Engineering*, 2004, **50**(7), 1614–1622.

137 B. Arias, G. S. Grasa and J. C. Abanades, Effect of sorbent hydration on the average activity of CaO in a Ca-looping system, *Chem. Eng. J.*, 2010, **163**(3), 324–330.

138 P. Lisbona, A. Martínez, Y. Lara and L. M. Romeo, Integration of carbonate CO_2 capture cycle and coal-fired power plants. A comparative study for different sorbents, *Energy Fuels*, 2010, **24**(1), 728–736.

139 Z. Li, N. Cai and E. Croiset, Process analysis of CO_2 capture from flue gas using carbonation–calcination cycles, *AIChE J.*, 2008, **54**(7), 1912–1925.

140 J. M. Valverde, P. E. Sanchez-Jimenez and L. A. Perez-Maqueda, Ca-looping for postcombustion CO_2 capture: a comparative analysis on the performances of dolomite and limestone, *Appl. Energy*, 2015, **138**, 202–215.

141 J. Wang and E. J. Anthony, A common decay behavior in cyclic processes, *Chem. Eng. Commun.*, 2007, **194**(11), 1409–1420.

142 J. Wang and E. J. Anthony, On the decay behavior of the CO_2 absorption capacity of CaO-based sorbents, *Ind. Eng. Chem. Res.*, 2005, **44**(3), 627–629.

143 G. S. Grasa and J. C. Abanades, CO_2 capture capacity of CaO in long series of carbonation–calcination cycles, *Ind. Eng. Chem. Res.*, 2006, **45**(26), 8846–8851.

144 A. I. Lysikov, A. N. Salanov and A. G. Okunev, Change of CO_2 carrying capacity of CaO in isothermal recarbonation-decomposition cycles, *Ind. Eng. Chem. Res.*, 2007, **46**(13), 4633–4638.

145 J. C. Abanades, The maximum capture efficiency of CO_2 using a carbonation–calcination cycle of $CaO/CaCO_3$, *Chem. Eng. J.*, 2002, **90**(3), 303–306.

146 D. Berstad, R. Anantharaman and K. Jordal, Post-combustion CO_2 capture from a natural gas combined cycle by $CaO/CaCO_3$ looping, *Int. J. Greenhouse Gas Control*, 2012, **11**, 25–33.

147 J. Ströhle, A. Lasheras, A. Galloy and B. Epple, Simulation of the carbonate looping process for post-combustion CO_2 capture from a coal-fired power plant, *Chem. Eng. Technol.*, 2009, **32**(3), 435–442.

148 I. Martínez, R. Murillo, G. Grasa, N. Rodríguez and J. C. Abanades, Conceptual design of a three fluidised beds combustion system capturing CO_2 with CaO, *Int. J. Greenhouse Gas Control*, 2011, **5**(3), 498–504.

149 A. Charitos, N. Rodríguez, C. Hawthorne, M. Alonso, M. Zieba, B. Arias, G. Kopanakis, G. Scheffknecht and J. C. Abanades, Experimental Validation of the Calcium Looping CO_2 Capture Process with Two Circulating Fluidized Bed Carbonator Reactors, *Ind. Eng. Chem. Res.*, 2011, **50**(16), 9685–9695.

150 J. Ylätalo, J. Parkkinen, J. Ritvanen, T. Tynjälä and T. Hyppänen, Modeling of the oxy-combustion calciner in the post-combustion calcium looping process, *Fuel*, 2013, **113**, 770–779.

151 R. H. Borgwardt, Sintering of nascent calcium oxide, *Chem. Eng. Sci.*, 1989, **44**(1), 53–60.

152 P. Sun, J. R. Grace, C. J. Lim and E. J. Anthony, Removal of CO_2 by calcium-based sorbents in the presence of SO2, *Energy Fuels*, 2007, **21**(1), 163–170.

153 G. S. Grasa, M. Alonso and J. C. Abanades, Sulfation of CaO particles in a carbonation–calcination loop to capture CO_2, *Ind. Eng. Chem. Res.*, 2008, **47**(5), 1630–1635.

154 E. J. Anthony and D. L. Granatstein, Sulfation phenomena in fluidized bed combustion systems, *Prog. Energy Combust. Sci.*, 2001, **27**(2), 215–236.

155 A. Lyngfelt and B. Leckner, Sulphur capture in fluidized bed boilers: The effect of reductive decomposition of CaSO4, *Chem. Eng. J.*, 1989, **40**(2), 59–69.

156 R. Baker, The reversibility of the reaction $CaCO_3 \leftarrow CaO + CO_2$, *J. Appl. Chem. Biotechnol.*, 1973, **23**(10), 733–742.

157 C. Salvador, D. Lu, E. J. Anthony and J. C. Abanades, Enhancement of CaO for CO_2 capture in an FBC environment, *Chem. Eng. J.*, 2003, **96**(1–3), 187–195.

158 G. P. Curran, C. E. Fink and E. Gorin, Carbon dioxide-acceptor gasification process: studies of acceptor properties, *Advanced Chemistry Services*, 1967, **69**, 141–165.

159 A. Silaban, M. Narcida and D. P. Harrison, Characteristics of the reversible reaction between $CO_{2(g)}$ and calcined dolomite, *Chem. Eng. Commun.*, 1996, **146**(1), 149–162.

160 M. Aihara, T. Nagai, J. Matsushita, Y. Negishi and H. Ohya, Development of porous solid reactant for thermal-energy storage and temperature upgrade using carbonation/decarbonation reaction, *Appl. Energy*, 2001, **69**(3), 225–238.

161 V. Manovic, E. J. Anthony, G. Grasa and J. C. Abanades, CO_2 looping cycle performance of a high-purity limestone after thermal activation/doping, *Energy Fuels*, 2008, **22**(5), 3258–3264.

162 H. C. Mantripragada and E. S. Rubin, Calcium looping cycle for CO_2 capture - Performance, cost and feasibility analysis, *Energy Procedia*, 2013, **63**, 2199–2206.

163 V. Manovic and E. J. Anthony, Steam reactivation of spent CaO-based sorbent for multiple CO_2 capture cycles, *Environ. Sci. Technol.*, 2007, **41**(4), 1420–1425.

164 P. S. Fennell, J. F. Davidson, J. S. Dennis and A. N. Hayhurst, Regeneration of sintered limestone sorbents for the sequestration of CO_2 from combustion and other systems, *J. Energy Inst.*, 2007, **80**(2), 116–119.

165 R. W. Hughes, D. Lu, E. J. Anthony and Y. Wu, Improved long-term conversion of limestone-derived sorbents for in situ capture of CO_2 in a fluidized bed combustor, *Ind. Eng. Chem. Res.*, 2004, **43**(18), 5529–5539.

166 G. Grasa, R. Murillo, M. Alonso, B. González, N. Rodríguez and J.C. Abanades, Steam reactivation of CaO-based natural sorbents applied to a carbonation–calcination loop for CO2 capture, 4th International Conference on Clean Coal Technologies, Dresden, Germany, 2009. Cited in; B. Arias, G. S. Grasa and J. C. Abanades, Effect of sorbent hydration on the average activity of CaO in a Ca-looping system, *Chem. Eng. J.*, 2010, **163**, 324–330.

167 J. Blamey, V. Manovic, E. J. Anthony, D. R. Dugwell and P. S. Fennell, On steam hydration of CaO-based sorbent cycled for CO_2 capture, *Fuel*, 2015, **150**, 269–277.

168 D. K. Lee, An apparent kinetic model for the carbonation of calcium oxide by carbon dioxide, *Chem. Eng. J.*, 2004, **100**(1–3), 71–77.

169 S. Bhatia and D. Perlmutter, Effect of the product layer on the kinetics of the CO_2-lime reaction, *AIChE J.*, 1983, **29**(1), 79–86.

170 G. Gupta and L. S. Fan, Carbonation-calcination cycle using high reactivity calcium oxide for carbon dioxide separation from flue gas, *Ind. Eng. Chem. Res.*, 2002, **41**, 4035–4042.

171 G. S. Grasa, J. C. Abanades, M. Alonso and B. González, Reactivity of highly cycled particles of CaO in a carbonation–calcination loop, *Chem. Eng. J.*, 2008, **137**(3), 561–567.

172 Y. S. Yu, W. Q. Liu, H. An, F. S. Yang, G. X. Wang, B. Feng, Z. X. Zhang and V. Rudolph, Modeling of the carbonation behavior of a calcium based sorbent for CO_2 capture, *Int. J. Greenhouse Gas Control*, 2012, **10**, 510–519.

173 S. K. Mahuli, R. Agnihotri, R. Jadhav, S. Chauk and L. Fan, Combined calcination, sintering and sulfation model for $CaCO_3$-SO_2 reaction, *AIChE J.*, 1999, **45**(2), 367–381.

174 P. Sun, J. R. Grace, C. J. Lim and E. J. Anthony, Determination of intrinsic rate constants of the CaO-CO_2 reaction, *Chem. Eng. Sci.*, 2008, **63**(1), 47–56.

175 R. H. Borgwardt, Calcination kinetics and surface area of dispersed limestone particles, *AIChE J.*, 1985, **31**(1), 103–111.

176 F. García-Labiano, A. Abad, L. F. de Diego, P. Gayán and J. Adánez, Calcination of calcium-based sorbents at pressure in a broad range of CO_2 concentrations, *Chem. Eng. Sci.*, 2002, **57**(13), 2381–2393.

177 J. S. Dennis and A. N. Hayhurst, The effect of CO_2 on the kinetics and extent of calcination of limestone and dolomite particles in fluidised beds, *Chem. Eng. Sci.*, 1987, **42**(10), 2361–2372.

178 D. Kunii and O. Levenspiel, *Fluidization engineering*, Butterworth-Heinemann, Stoneham, MA, USA, 2nd edn, 1991.

179 D. Kunii and O. Levenspiel, Fluidized reactor models. 1. For bubbling beds of fine, intermediate and large particles. 2. For the lean phase. Freeboard and fast fluidization, *Ind. Eng. Chem. Res.*, 1990, **29**(7), 1226–1234.

180 E. Turnbull and J. F. Davidson, Fluidized combustion of char and volatiles from coal, *AIChE J.*, 1984, **30**(6), 881–889.

181 Z. Li and N. Cai, Modeling of multiple cycles for sorption-enhanced steam methane reforming and sorbent regeneration in fixed bed reactor, *Energy Fuels*, 2007, **21**(5), 2909–2918.

182 D. Kunii and O. Levenspiel, Circulating fluidized-bed reactors, *Chem. Eng. Sci.*, 1997, **52**(15), 2471–2482.

183 D. Kunii and O. Levenspiel, The K-L reactor model for circulating fluidized beds, *Chem. Eng. Sci.*, 2000, **55**(20), 4563–4570.

184 I. Martínez, G. Grasa, R. Murillo, B. Arias and J. C. Abanades, Kinetics of calcination of partially carbonated particles in a Ca-looping system for CO_2 capture, *Energy Fuels*, 2012, **26**(2), 1432–1440.

185 K. Myöhänen and T. Hyppänen, A three-dimensional model frame for modelling combustion and gasification in circulating fluidized bed furnaces, *Int. J. Chem. React. Eng.*, 2011, **9**, A25.

186 G. D. Silcox, J. C. Kramlich and D. W. Pershing, Mathematical model for the flash calcination of dispersed $CaCO_3$ and $Ca(OH)_2$ particles, *Ind. Eng. Chem. Res.*, 1989, **28**(2), 155–160.

187 *Thermochemical data of pure substances, VCH Verlagsgesellshaft mbH*, ed. I. Barin, Federal Republic of Germany, Weumheim, 1989.

188 K. Atsonios, M. Zeneli, A. Nikolopoulos, N. Nikolopoulos, P. Grammelis and E. Kakaras, Calcium looping process simulation based on an advanced thermodynamic model combined with CFD analysis, *Fuel*, 2015, **153**, 371–381.

189 J. Ylätalo, J. Ritvanen, B. Arias, T. Tynjälä and T. Hyppänen, 1-Dimensional modelling and simulation of the calcium looping process, *Int. J. Greenhouse Gas Control*, 2012, **9**, 130–135.

190 P. S. Fennell, R. Pacciani, J. S. Dennis, J. F. Davidson and A. N. Hayhurst, The effects of repeated cycles of calcination and carbonation on a variety of different limestones, as measured in a hot fluidized bed of sand, *Energy Fuels*, 2007, **21**(4), 2072–2081.

191 O. Senneca, M. Urciuolo and R. Chirone, A semidetailed model of primary fragmentation of coal, *Fuel*, 2013, **104**, 253–261.

192 J. R. Gibbins and R. I. Crane, Scope for reductions in the cost of CO_2 capture using flue gas scrubbing with amine solvents, *Proc. Inst. Mech. Eng., Part A*, 2004, **218**(4), 231–239.

193 R. Khalilpour and A. Abbas, HEN optimization for efficient retrofitting of coal-fired power plants with post-combustion carbon capture, *Int. J. Greenhouse Gas Control*, 2011, **5**(2), 189–199.

194 S. Kishimoto, T. Hirata, M. Iijima, T. Ohishi, K. Higaki and R. Mitchell, Current status of MHI's CO_2 recovery technology and optimization of CO_2 recovery plant with a PC fired power plant, *Energy Procedia*, 2009, **1**(1), 1091–1098.

195 Y. A. Cengel and M. A. Boles, *Thermodynamics: an engineering approach*, McGraw-Hill, New York, NY, USA, 6th in SI units edn, 2007.

196 G. Grasa, R. Murillo, M. Alonso and J. C. Abanades, Application of the random pore model to the carbonation cyclic reaction, *AIChE J.*, 2009, **55**(5), 1246–1255.

197 T. Joutsenoja, P. Heino, R. Hernberg and B. Bonn, Pyrometric temperature and size measurements of burning coal particles in a fluidized bed combustion reactor, *Combust. Flame*, 1999, **118**(4), 707–717.

198 V. Manovic, M. Komatina and S. Oka, Modeling the temperature in coal char particle during fluidized bed combustion, *Fuel*, 2008, **87**(6), 905–914.

199 R. T. Symonds, D. Y. Lu, V. Manovic and E. J. Anthony, Pilot-scale study of CO_2 capture by CaO-based sorbents in the presence of steam and SO_2, *Ind. Eng. Chem. Res.*, 2012, **51**(21), 7177–7184.

200 Y. Lara, P. Lisbona, A. Martínez and L. M. Romeo, A systematic approach for high temperature looping cycles integration, *Fuel*, 2014, **127**, 4–12.

201 Y. Lara, P. Lisbona, A. Martínez and L. M. Romeo, Design and analysis of heat exchanger networks for integrated Ca-looping systems, *Appl. Energy*, 2013, **111**, 690–700.

202 ECN, ECN Phyllis classification, 2012, available at: http://bit.ly/1hrh1cu, accessed 30/05/2015.

203 B. Arias, J. C. Abanades and G. S. Grasa, An analysis of the effect of carbonation conditions on CaO deactivation curves, *Chem. Eng. J.*, 2011, **167**(1), 255–261.

204 A. Martínez, Y. Lara, P. Lisbona and L. M. Romeo, Operation of a cyclonic preheater in the ca-looping for CO_2 capture, *Environ. Sci. Technol.*, 2013, **47**(19), 11335–11341.

205 C. Biliyok and H. Yeung, Evaluation of natural gas combined cycle power plant for post-combustion CO_2 capture integration, *Int. J. Greenhouse Gas Control*, 2013, **19**, 396–405.

206 B. G. Miller, *Clean Coal Engineering Technology*, Butterworth-Heinemann, Boston, USA, 2011.

207 IEA, *CO2 Emissions from Fuel Combustion - Highlights*, OECD/IEA, Paris, France, 2012 edn, 2012.

208 P. Versteeg and E. S. Rubin, A technical and economic assessment of ammonia-based post-combustion CO_2 capture at coal-fired power plants, *Int. J. Greenhouse Gas Control*, 2011, **5**(6), 1596–1605.

209 J. Black, *Cost and Performance Baseline for Fossil Energy Plants Volume 1: Bituminous Coal and Natural Gas to Electricity, DOE/2010/1397 Revision 2a*, National Energy Technology Laboratory, 2013.

210 M. C. Romano and G. G. Lozza, Long-term coal gasification-based power plants with near-zero emissions. Part A: Zecomix cycle, *Int. J. Greenhouse Gas Control*, 2010, **4**(3), 459–468.

211 IEA, *Technology Roadmap: High-Efficiency, Low-Emissions Coal-Fired Power Generation*, OECD/IEA, Paris, France, 2012.

212 R. Anantharaman, O. Bolland, N. Booth, E. van Dorst, C. Ekstrom, E. Sanchez Fernandes, F. Franco, E. Macchi, G. Manzolini, D. Nikolic, A. Pfeffer, M. Prins, S. Rezvani and L. Robinson, *CArbon-free Electricity by SEWGS: Advanced materials, Reactor- and process design. D 4.9 European best practice guidelines for assessment of CO_2 capture technologies, 213206 FP7 - ENERGY.2007.5.1.1,* Politecnico di Milano, Alstom UK, 2011.

213 O. Bollard, N. Booth, F. Franco, E. Macchi, G. Manzolini, R. Naqvi, A. Pfeffer, S. Rezvani and M. Abu Zara, *Enabling advanced pre-combustion capture techniques and plants. D 1.4.1 Common Framework Definition Document, 211971 FP7 - ENERGY.2007.5.1.1*, Alstom UK, 2009.